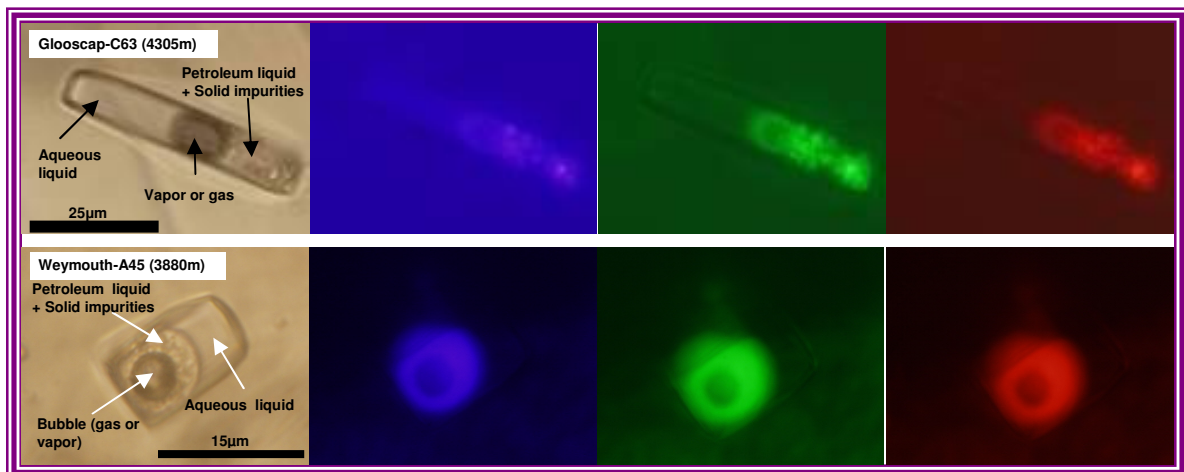


FINAL REPORT
ON
HYDROCARBON FLUID INCLUSION STUDY IN THE ARGO SALT
OF GLOOSCAP-C63 AND WEYMOUTH-A45 WELLS,
OFFSHORE SCOTIAN MARGIN

By
Dr. Yawooz Kettanah
Ph.D. in Economic Geology (Southampton University - UK)
Consultant - Adjunct Professor at the Department of Earth Sciences, Dalhousie University

Submitted to
The Offshore Energy Technical Research Association (OETR A)



23 August 2010

TABLE OF CONTENTS

FINAL REPORT	i
TABLE OF CONTENTS	ii
Table of Figures.....	iii
Table of Tables	vii
Table of Abbreviations	viii
PREFACE.....	1
EXECUTIVE SUMMARY	1
INTRODUCTION.....	3
ARGO SALT	4
BACKGROUND ON FLUID INCLUSIONS	9
GLOOSCAP-C63 WELL	11
Argo salt in Glooscap-C63 well.....	11
Sampling and Sample Treatment	16
Petrographic microscopic studies.....	16
1. Aqueous Fluid Inclusions	16
a. Normal one- and two-phased aqueous fluid inclusions	16
b. Large two-and three-phased accidental aqueous fluid inclusions.....	18
c. Normal three-phased aqueous fluid inclusions	19
d. Necked aqueous fluid inclusions.....	21
2. Secondary Petroleum Fluid Inclusions	23
3. Other Inclusions.....	37
a. Hematite crystal inclusions	37
b. Anhydrite crystal inclusions.....	38
c. Quartz crystal inclusions.....	39
d. Lubricant-like liquid:	40
WEYMOUTH-A45 WELL	41
Well Summary:	41
Argo salt in Weymouth-A45 well.....	43
Sampling and Sample Treatment	43
Petrographic Microscopic Studies.....	45
1. Aqueous Fluid Inclusions (AFI).....	48
2. Secondary Petroleum and Petroleum-Aqueous Fluid Inclusions.....	52
3. Other inclusions	73
a. Hematite crystal inclusions	73
b. Anhydrite crystal inclusions.....	74
c. Quartz crystal inclusions.....	76
d. Lubricant-like liquid.....	77
MICROTHERMOMETRY	78
1. Microthermometry of the fluid inclusions in the salt of Glooscap-C63 well	79
2. Microthermometry of the fluid inclusions in the salt of Weymouth-A45 well..	94
SUMMARY AND DISCUSSION	111
CONCLUSIONS	122
RECOMMENDATIONS.....	124
REFERENCES.....	126
END	128

Table of Figures

Fig. 1: Location map of Weymouth-A45 (continental slope) and Glooscap-C63 (continental shelf) on the Scotian Continental Margin	6
Fig. 2: Representative salt samples of Glooscap-C63 well grading between clean-colorless to light brown-dark brown due to iron staining.	13
Fig. 4: Normal one- and two phased aqueous fluid inclusions assemblages in the Argo salt of Glooscap-C63 well. In most cases the vapor bubbles are large relative to the size of fluid inclusions. They are rectangular or cylindrical in shape.....	17
Fig. 5: Large two- and three-phased large aqueous fluid inclusions. The crystal inside the fluid inclusion of lower images is probably anhydrite indicated by its interference colors in crossed-polarized light (lower right).....	19
Fig. 6: Normal three-phased aqueous fluid inclusion assemblages in H ₂ O-NaCl-KCl system.	20
Fig. 7: Necked aqueous (top) and petroleum (bottom) fluid inclusions in the Argo salt of Glooscap-C63 well. They show necking at the lower image.....	22
Fig. 8: Secondary petroleum fluid inclusions grown along a fracture cross-cutting cleavage planes in the Argo Salt at the Glooscap-C63 well. The lower image shows both primary aqueous fluid inclusions (AFI) and secondary petroleum fluid inclusions (PFI).	25
Fig. 9: Secondary petroleum-aqueous fluid inclusions grown along perpendicular cleavage planes. They show fluorescence in UV, green and red lights.	26
Fig. 10: Various shapes of petroleum-bearing fluid inclusions in Argo Salt at the Glooscap-C63 well.....	27
Fig 11a: One-, two- and three-phased petroleum fluid inclusions.....	28
Fig 11b: Four-phased petroleum fluid inclusions (petroleum liquid with solid impurities + aqueous liquid + gas or vapor bubble).....	29
Fig. 12: Aqueous-Petroleum Fluid Inclusions in Argo Salt in Glooscap-C63 (top two rows) and Weymouth-A45 (lower three rows) wells. Petroleum part is mostly impure in both but show distinct isolated liquid ring with more intense fluorescence in Weymouth and more dispersed and less fluorescent in Glooscap-C63 well samples.	30
Fig. 13a: Representative images of the studied samples showing various petroleum-bearing fluid inclusions in plane polarized light (left), as well as UV light (blue) and visible spectrum green and red lights in the studied Glooscap-C63 salt samples.	31
Fig. 13b: Representative images of the studied samples showing various petroleum-bearing fluid inclusions in plane polarized light (left), as well as UV light (blue) and visible spectrum green and red lights in the studied Glooscap-C63 salt samples.	32
Fig. 13c: Representative images of the studied samples showing various petroleum-bearing fluid inclusions in plane polarized light (left), as well as UV light (blue) and visible spectrum green and red lights in the studied Glooscap-C63 salt samples.	33
Fig. 13d: Representative images of the studied samples showing various petroleum-bearing fluid inclusions in plane polarized light (left), as well as UV light (blue) and visible spectrum green and red lights in the studied Glooscap-C63 salt samples.	34
Fig. 13e: Representative images of the studied samples showing various petroleum-bearing fluid inclusions in plane polarized light (left), as well as UV light (blue) and visible spectrum green and red lights in the studied Glooscap-C63 salt samples.	35

Fig. 13f: Representative images of the studied samples showing various petroleum-bearing fluid inclusions in plane polarized light (left), as well as UV light (blue) and visible spectrum green and red lights in the studied Glooscap-C63 salt samples.	35
Fig. 14: Impurities on the salt chips showing weak fluorescence which could be dead bacteria or algae.	36
Fig. 15: Perfect euhedral hematite inclusions and iron stain in halite of Glooscap-C63 well.....	37
Fig. 16: Tiny anhydrite (light colored) and iron oxides (brown) inclusions left over from dissolved chips as insoluble residue.	38
Fig. 17: Perfect euhedral crystal of quartz as inclusion in salt of Weymouth-A45 well. .	39
Fig. 18: Lubricant-like liquid on the surface of the salt grains and along cleavage planes.	40
Fig. 19: Representative salt samples from Weymouth-A45 (left) and Glooscap-C63 (right) wells showing the obvious color and transparency differences between the two.	44
Fig. 20: Fine grained (10 to >300µm) halite crystals constituting the Argo salt in the Weymouth-A45 well. Larger grains are shown in Fig. 19.	46
Fig. 21: Halite crystals of the Weymouth-A45 well showing perpendicular cleavage planes and assemblages of primary aqueous fluid inclusions (AFIs) between cleavages planes parallel to growth zones as well as a linearly oriented assemblages of secondary petroleum fluid inclusions (PFIs) trapped along a healed fracture zone.	47
Fig. 22: One-phased rectangular-shaped aqueous fluid inclusions assemblages (AFI) of possibly primary origin along side with secondary AFI-PFI and PFI which crosscut the PFI .and show fluorescence in the salt of Weymouth-A45 well.	49
Fig. 23a: One-phased pin-like (a and b), elliptical (c, d and f), hexagonal (g) and lens-shaped (a, d, e, h, I, j) aqueous fluid inclusions in the salt of Weymouth-A45 well.	50
Fig. 23b: One-phased rectangular aqueous fluid inclusions (AFI) in the salt of Weymouth-A45 well. Side by side with petroleum fluid inclusions (PFI).....	51
Fig.24: Petroleum fluid inclusions of various shapes and characters in the Argo salt of Weymouth-A45 well.....	54
Fig. 25a. Petroleum fluid inclusions showing one- and two-phased types.....	55
Fig. 25b. Petroleum fluid inclusions of two- and three-phases types (A = aqueous; P = petroleum)	56
Fig 25c. Petroleum fluid inclusions showing three- and four-phased types	57
Fig. 26: A very long pin-shaped, three-phased aqueous-petroleum-vapor or gas fluid inclusion (A = aqueous; P = petroleum; G = gas or vapor).	58
Fig. 27a: Representative images of petroleum fluid inclusions in the studied samples. The colored images show fluorescence of liquid petroleum in UV, green and red light.....	59
Fig. 27b: Representative images of petroleum fluid inclusions in the studied samples. The colored images show fluorescence of liquid petroleum in UV, green and red light.....	60
Fig. 27c: Representative images of petroleum fluid inclusions in the studied samples. The colored images show fluorescence of liquid petroleum in UV, green and red light.....	61
Fig. 27d: Representative images of petroleum fluid inclusions in the studied samples. The colored images show fluorescence of liquid petroleum in UV, green and red light.....	62
Fig. 27e: Representative images of petroleum fluid inclusions in the studied samples. The colored images show fluorescence of liquid petroleum in UV, green and red light.....	63

Fig. 27f: Representative images of petroleum fluid inclusions in the studied samples. The colored images show fluorescence of liquid petroleum in UV, green and red light.....	64
Fig. 28a: One-phased and two-phased petroleum fluid inclusions showing linear pattern of distribution in the salt of Weymouth-A45 well.	65
Fig. 28b: Two-phased petroleum-aqueous fluid inclusions showing linear pattern of distribution in the salt of Weymouth –A45 well.....	66
Fig.29: Irregular-shaped aqueous-petroleum fluid inclusion showing 5 (top) and 3 (bottom) separate spots (rings) of liquid petroleum within the aqueous liquid.	67
Fig. 30: Mode of occurrence of PFI and AFI-PFI. They either exist alone as assemblages or together in the same sample.....	68
Fig. 31: Petroleum-bearing fluid inclusions showing linear elongate nature (top) and orientation of many small inclusions along dissected fractures (bottom).....	69
Fig. 32: Gas-dominated petroleum-bearing fluid inclusions showing elongate net-like pattern and fluorescence of the minor liquid part only as thin rims around gas bubbles.	70
Fig. 33: One and multi-phased petroleum-bearing fluid inclusion assemblages with no obvious relation to fractures; however they are probably situated parallel to such planes of weaknesses which can not be seen in such images for this reason.....	71
Fig. 34: Oval shaped aqueous fluid inclusions (could be of primary or secondary origin) (AFI) side-by-side with secondary petroleum fluid inclusions oriented along dissecting fractures (PFI).	72
Fig. 35: Euhedral hematite crystals as inclusions in the Weymouth-A45 salt.....	73
Fig. 36: Anhydrite crystal inclusions in Weymouth A-45 salt. The dark images are taken under crossed polars showing the isotropic nature of halite and anisotropic behavior of anhydrite.	75
Fig. 37: Perfect euhedral crystal of quartz as inclusion in salt of Weymouth-A-45 well.	76
Fig. 38: Lubricant-like liquid along cleavage planes and on the surface of the halite crystals in the salt samples of Weymouth-A45 well.....	77
Fig. 39a: Histogram of freezing point temperatures (T_f) versus depth in the fluid inclusions of Glooscap-C63 well. T_f average = -82°C ; median = -81°C ; minimum =.....	86
-119°C ; maximum = -64°C	86
Fig. 39b: Histogram of metastable eutectic temperatures (initial melting - T_{im}) versus depth in the fluid inclusions of Glooscap-C63 well. T_{im} average = -40°C ; median =.....	86
-38°C ; minimum = -51°C ; maximum = -34°C	86
Fig. 39c: Histogram of eutectic temperatures (T_e) versus depth in the fluid inclusions of Glooscap-C63 well. T_e average = -26°C ; median = -25°C ; minimum = -38°C ; maximum = -22°C	87
Fig. 39d: Histogram of peritectic temperatures (final melting – T_m) versus depth in the fluid inclusions of Glooscap-C63 well. T_m average = -2°C ; median = -1.8°C ; minimum = -6.8°C ; maximum = 0°C	87
Fig. 39e: Histogram of homogenization temperatures (T_h) versus depth in the fluid inclusions of Glooscap-C63 well. T_h average = 282°C ; median = 283°C ; minimum = 110°C ; maximum = 380°C	88
Fig. 40a: Microthermometric behavior of a group of aqueous fluid inclusions showing phase changes during cooling-heating processes (sample G4185).....	89
Fig. 40b: Microthermometric behavior of a group of aqueous fluid inclusions showing phase changes during cooling-heating processes (sample G4305).....	90

Fig. 40c: Microthermometric behavior of an aqueous fluid inclusion showing phase changes during cooling-heating processes (sample G4525).....	91
Fig. 40d: Microthermometric behavior of a large accidental aqueous fluid inclusion showing no phase changes during cooling-heating processes other than changes in the bubble size and deformation in the internal structure and external shape until final decrepitation (sample 4300).....	92
Fig. 41: Pure petroleum fluid inclusions (with no aqueous components) of one-phased type (gas of dark black color and liquid of light color associated with aqueous fluid inclusions (sample G4405). Only pure liquid fluid inclusions show fluorescence.....	93
Fig. 42a: Histogram of freezing point temperatures (T_f) versus depth of the PFI-AFI, PFI, and AFI in the salt of Weymouth-A45 well. T_f [median = -77°C ; average = -75°C ; minimum = -84°C ; maximum = -63°C].....	100
Fig. 42b: Histogram of metastable eutectic temperatures (initial melting- T_{im}) versus depth of the PFI-AFI, PFI, and AFI in the salt of Weymouth-A45 well. T_{im} [median = -52°C ; average = -50°C ; minimum = -53°C ; maximum = -38°C]	100
Fig. 42c: Histogram of eutectic temperatures (T_e) versus depth of the AFI-PFI fluid inclusions in the salt of Weymouth-A45 well. T_e [median = -37°C ; average = -36°C ; minimum = -42°C ; maximum = -27°C].....	101
Fig. 42d: Histogram of peritectic temperatures (final melting – T_m) versus depth of the PFI-AFI, PFI, and AFI in the salt of Weymouth-A45 well. T_m [median = -3°C ; average = -3.7°C ; minimum = -6.5°C ; maximum = -2°C].....	101
Fig. 42e: Histogram of homogenization temperatures (T_h) versus depth of the PFI-AFI, PFI, and AFI in the salt of Weymouth-A45 well. T_h [median = 56°C ; average = 62°C ; minimum = 17°C ; maximum = 170°C]	102
Fig. 43a: Two-phased AFI-PFI showing brown coloration as a sign of freezing during microthermometric treatment.....	103
Fig. 43b: Multi-phased AFI-PFI showing no color change during freezing which has produced a bubble during cooling and homogenized by disappearance of the bubble at 22°C . The ring-like petroleum phase did not mix with the aqueous phase inspite of excessive heating and end up with decrepitation $\sim 50^{\circ}\text{C}$. The change of shape and size as a result of deformation during treatment is evident.	104
Fig. 43c: Microthermometric behavior of three-phased AFI-PFI in Wymouth-A45 salt (sample W3880). It is aqueous liquid-dominated with a small spot of oil and a large bubble. $T_f=-80^{\circ}\text{C}$; $T_{im}=-52^{\circ}\text{C}$; $T_e=-39^{\circ}\text{C}$; $T_m=-6^{\circ}\text{C}$; $T_h=+170^{\circ}\text{C}$	105
Fig. 44a: Microthermometric treatment of one-phased liquid petroleum which did not show any color changes or distinct signs during phase changes other than gradual deformation of the bubble during cooling ($\sim -100^{\circ}\text{C} \pm$ few degrees) and regaining its original spherical shape approximately at the same range of temperature during heating. For details enlarged views see Figs. 44-a1 and 44-a2.	106
Fig. 44a-1: Microthermometric treatment of one-phased liquid petroleum which did not show any color changes or distinct signs during phase changes other than gradual deformation of the bubble during cooling ($\sim -100^{\circ}\text{C} \pm$ few degrees) and regaining its original spherical shape approximately at the same range of temperature during heating.	107
Fig. 44a-2: Microthermometric treatment of one-phased liquid petroleum which did not show any color changes or distinct signs during phase changes other than gradual	

deformation of the bubble during cooling ($\sim -100^{\circ}\text{C} \pm \text{few degrees}$) and regaining its original spherical shape approximately at the same range of temperature during heating.	108
Fig. 44b: Microthermometric treatment of two-phased liquid petroleum inclusions (PFI) which neither showed any color changes nor distinct signs during phase changes other than gradual size increase and deformation of the bubble during cooling ($\sim >-75^{\circ}\text{C} \pm \text{few degrees}$) and regaining its original spherical shape approximately at the same range of temperature during heating.	109
Fig. 45: A gas dominated petroleum fluid inclusions initially with no signs of fluorescence (left) turns into liquid-dominated phase at excessive temperature (right) with distinct fluorescence due to condensation of the gas under high temperature and high internal pressure build up within the inclusion. The circular fluorescent spots to the right of the gas inclusion are coming from other fluid inclusions which are out of focus.	110
Fig. 46: Tight folds in the salt of Pugwash Mine diapir as an indication of brittle style deformation: (a) a composite roof view showing a domal structure (b) wall view (c) enlarged view from b. The yellowish-brownish salt is halite; the reddish brown salt is sylvite horizons; the white spots are anhydrite filling cracks in salt.	121

Table of Tables

Table 1: Salt-intersected wells in Scotian Margin and Grand Banks arranged according to their longitude positions (the table was prepared by the writer based on data obtained from the basin database. The salt morphology was kindly interpreted by David Brown of the CNSOPB.	5
Table 2. Basic data about the studied wells: Glooscap-C63 and Weymouth-A45. (http://basin.gsca.nrcan.gc.ca/wells/index_e.php)	7
Table 3: Studied samples from Glooscap-C63 and Weymouth-A45 wells under transmitted polarized and fluorescent microscope (T + F) and microthermometrically (M)	8
Table 4: Formations penetrated by the Glooscap-C63 well (data from the well report; .. the log is kindly provided by Patrick Letouzey of BeicipFranlab)	14
Table 5: Lithostratigraphy of Weymouth A-45 well (Datalog Canada Ltd, 2004; http://basin.gdr.nrcan.gc.ca/wells)	42
Table 6: Microthermometrically studied salt samples from Glooscap-C63 and Weymouth-A45 wells	83
Table 7: Micrometric results for the fluid inclusions in the salt of Glooscap-C63 well. AFI = Aqueous fluid inclusions; PFI = Petroleum fluid inclusions; AFI-PFI = Aqueous + petroleum phases within the same fluid inclusion; AFI* = Large accidental primary fluid inclusions; T_f = Freezing Temperature; T_{im} = Metastable Eutectic (initial melting) temperature; T_e = Eutectic melting temperature; T_m = Peritectic (final melting) temperature; T_h = Temperature of homogenization; n.o.= not observed.	84
Table 8: Micrometric results for the fluid inclusions in the salt of Weymouth-A45 well. AFI= Aqueous fluid inclusions; PFI= Petroleum fluid inclusions; AFI-PFI = Aqueous + petroleum phases within the same fluid inclusion; T_f = Freezing Point Temperature; T_{im} =	

Metastable Eutectic Temperature (initial melting); T_e = Eutectic Melting Temperature; T_m = Peritectic Temperature (final melting); T_h = Homogenization Temperature; n.o. = not observed.*3901 is excluded from statistics due to its much lower T_{im} and T_e	98
Table 9: Median, average, minimum and maximum values for freezing, initial melting, eutectic, final melting and homogenization temperatures for the microthermometrically of the analyzed fluid inclusions in the salt of Weymouth-A45 well	99
Fig. 42a: Histogram of freezing point temperatures (T_f) versus depth of the PFI-AFI, PFI, and AFI in the salt of Weymouth-A45 well. T_f [median = -77°C ; average = -75°C ; minimum = -84°C ; maximum = -63°C].....	100
Table 10: Summary comparison between the properties of rock salt in Glooscap-C3 and Weymouth-A45 wells.	117

Table of Abbreviations

AFI = Aqueous fluid inclusions
PFI = Petroleum fluid inclusions
AFI-PFI = mixed aqueous + petroleum phases
FIA = Fluid Inclusion Assemblages
Petroleum-bearing Fluid Inclusions = PFI and PFI-AFI
T_f = Freezing Point Temperature
T_{im} = Metastable Eutectic Temperature (initial melting)
T_e = Eutectic Melting Temperature
T_m = Peritectic Temperature (final melting)
T_h = Homogenization Temperature
n.o. = not observed

PREFACE

This final report is provided in accordance with the research agreement signed between OETR Association and the writer “Yawooz Kettanah” dated 1 April 2010 regarding hydrocarbon fluid inclusion study of Argo Salt in Glooscap-C63 and Weymouth-A45 wells. The main purpose of the study is to look for petroleum fluid inclusions in salt and in the case of their presence to predict the possible source of petroleum.

EXECUTIVE SUMMARY

The Argo salt intersected in Glooscap-C63 and Weymouth-A45 wells was studied for its petroleum fluid inclusion content in this project. The salt in Glooscap-C63 well is 497 m thick, pillow-shaped, autochthonous and located beneath the Scotian Continental Shelf at a depth of 4045.5-4542.4 m within Mohican Subbasin; while that of Weymouth-A45 well is 1508 m thick, canopy/diapir-shaped, allochthonous and located beneath the Scotian Continental Slope at a depth of 2840.0-4348.0 m within Sable Subbasin. Eighty four salt samples were studied from Glooscap-C63 and Weymouth-A45 well. The studies included both transmitted and fluorescent microscopy for all samples and microthermometry for thirty nine samples. The study results are summarized in Table 10.

The salt of both wells have similarities such as containing crystal inclusions of anhydrite, hematite and rarely quartz as well as lubricant-like liquid; and differences such as the color and transparency as well as differences in their fluid inclusions. Both contain aqueous (AFI), petroleum PFI) and heterogeneously trapped mixed petroleum-aqueous (PFI-AFI) fluid inclusions. PFI are common in both wells and have been observed in almost all samples but they are richer in Weymouth-A45 well. The AFI in Glooscap-C63 well samples are occasionally one-phased (liquid), mostly two-phased (liquid and vapor) of H_2O -NaCl system, and rarely three-phased (liquid-vapor-daughter crystal) of H_2O -NaCl-KCl system. The AFI in the salt of Weymouth-A45 well are mostly one-phased (liquid) and less commonly two-phased (liquid + vapor) and belong to H_2O - CaCl_2 -NaCl and/or H_2O - MgCl_2 -NaCl systems and some others are air-filled. The median of T_f , T_{im} , T_e , T_m and T_h in the AFI and PFI-AFI of Glooscap-C63 well's salt are -81°C , -38°C , -25°C , -1.8°C and 286°C respectively; the corresponding values for Weymouth-A-45 well's

salt are -73°C, -52°C, -37°C, -3°C and 81°C respectively. Although the AFI have the appearance of primary fluid inclusions but they have similar microthermometric characteristics to those of the associated PFI-AFI which mean that they have been reequilibrated under burial conditions indicated by their high homogenization temperatures. The homogenization temperatures are too high for the Glooscap-C63 salt and more reasonable for the Weymouth-A45 salt due to above mentioned reasons. If the homogenization temperature for the fluid inclusions in Weymouth-A45 well is dependable, it means that trapping has taken place at a depth slightly higher than 3 km taking into a consideration an average thermal gradient of 25°C/km. However, due to the weakness and soft nature of halite, their content of fluid inclusions usually stretch naturally under deep burial conditions and also during cooling-heating measurements, and for this reason the microthermometric results might not represent the real trapping conditions and must be treated cautiously. The mixed PFI-AFI are very common in both wells and they exist as 2-, 3-, and 4-phased inclusions (aqueous + petroleum ± solid impurities ± vapor or gas). There is a distinct difference between the PFI-AFI in the two wells. The petroleum phase form a distinct immiscible spot(s) within the aqueous phase in the salt of Weymouth-A45 well but it is usually dispersed with no distinct boundaries in the salt of Glooscap-C63 well; the petroleum phase of both wells usually contain tiny, dust-like solid impurities which could be degenerated petroleum products or some sort of oil-generating bacteria or algae.

The PFI in both wells exist as pure liquid and/or pure gas phases; they did not show the phase changes indicated in the literature for methane fluid inclusions. There are many possible reasons for that such as their stretching during microthermometric treatment (cooling-heating), natural reequilibrium at depth conditions or they may contain some compounds other than methane or a mixture of them. Their median homogenization temperature is 79°C in salt of Glooscap-C63 well and 23°C in the salt of Weymouth-A45 well. Strong fluorescence behavior of petroleum-bearing fluid inclusions in UV and visible light spectrums in both wells suggest that the petroleum consist of complex, high-molecular weight, aromatic or cyclic hydrocarbon compounds higher than methane. Gas Chromatography-Mass Spectrometry (GC-MS) can be used to identify the biomarkers compounds and Raman Spectrometry (RS) to identify the molecular compounds in the

petroleum-bearing fluid inclusions (PFI and PFI-AFI). Using such analytical techniques can reveal the identity of the petroleum in these inclusions and whether it is the same type of petroleum in both studied wells.

The petroleum in the petroleum-bearing fluid inclusions was probably trapped in the Argo salt soon after its generation from the source rocks and probably migrated along faults to approach the salt body and then moved along planes of weaknesses (fractures, cleavages and crystal contacts) to settle within the salt which was behaving in a brittle way in its lateral/vertical movement. The most probable source rocks for the petroleum are the shale/clay-dominated Late Triassic/Early Jurassic Eurydice formation which is widely distributed at depth under the Scotian Margin underlying the Argo salt and other younger formations.

INTRODUCTION

Among the wells drilled so far in the Canadian Atlantic Continental Margin Offshore Scotia and Newfoundland, at least 26 wells have intersected Argo salt deposits (Table 1). The intersected salt bodies are mostly of diapiric morphology (allochthonous) and less of pillow shape (autochthonous). The salt in Glooscap-C63 well is of pillow shape while it is of canopy/diapir shape in Weymouth-A45 well. Both wells are located on the Scotian Margin and fall within the Scotian Basin along the Canadian Atlantic Continental margin (Fig. 1). These two wells were chosen on the basis of their setting, the former being of autochthonous while the latter of allochthonous nature and also because both have intersected considerable salt thickness (Table 2). Cutting samples were collected from both wells (Table 3) because of the lack of core samples. The collected samples were studied for their content of petroleum fluid inclusions (PFI) under both transmitted polarized light and fluorescent light microscope using Advanced Research Olympus BX51 Microscope provided with Olympus DP71 digital camera. Salt samples with suitable fluid inclusions content were also microthermometrically studied using Linkam heating-freezing stage.

ARGO SALT

The basic geological data about Argo salt is given in Williams et al (1985). Argo Salt was first described by McIver (1972) which was redefined as Argo Formation by Jansa and Wade (1975) whose type section was described by Wade (1981). Based on palynological evidences, Early Jurassic age was proposed for the Argo Formation (McIver, 1972 and Bujak and Williams, 1977), while Barss et al (1979) dated the formation as Late Triassic (Rhaetian) to Early Jurassic (early Hettangian). The thickness of Argo Formation is 780 m in its type well but it varies considerably and its depositional thickness possibly exceeded 1830 m stretching from LaHave Platform of the southwestern Scotian Shelf to the East Newfoundland Basin in the northeast as indicated from seismic profiles; intense flow of the salt resulted in its localization in anticlinal and diapiric structures and depriving it from other areas where the salt was not detected (Jansa and Wade, 1975). The Argo Formation in Orpheus Basin is conformably overlying the Eurydice Formation (Upper Triassic-Lower Jurassic) with 93 m of interbedded anhydrite, halite and shale as basal gradational contact (McIver, 1972); the upper contact is either sharp or gradational. According to Jansa and Wade (1975) the Argo salt is part of the Late Triassic-Early Jurassic salt basin which also occurs in the other side of the Atlantic Ocean in Tunisia, Algeria, Morocco, Spain and France.

Eurydice Formation underlies and in places lateral equivalent to Argo Formation is more than 573 m in thickness in its type well within Orpheus Graben and consists predominantly of reddish shales, minor amounts of argillaceous siltstone and rare feldspathic sandstone which were deposited under arid conditions in a desert environment (Williams et al 1985). It is possibly widely extended at the base of the Scotian shelf sediments.

Table 1: Salt-intersected wells in Scotian Margin and Grand Banks arranged according to their longitude positions (the table was prepared by the writer based on data obtained from the basin database. The salt morphology was kindly interpreted by David Brown of the CNSOPB).

Well Name	Location		Total Thickness (m)	Basin	Subbasin	Area	Sample Storage	Salt Interval		Salt Thickness (m)	Salt Formation	Salt Morphology
	Lat.	Long.						Start	End			
Mohican I-100	42.99	62.48	4393.40	Scotian	LaHave Platform	Scotian Shelf	CNSOPB-CSLF*	4365.35	4393.39	28.04	Argo	pillow
Glooscap C-63	43.20	62.17	4551.50	Scotian	Mohican Graben	Scotian Shelf	CNSOPB-CSLF*	4045.50	4542.40	496.90	Argo	pillow
Weymouth A-45	43.07	60.60	6520.00	Scotian	Sable	Scotian Slope	CNSOPB-CSLF*	2840.00	4348.00	1508.00	Argo	canopy
Wenonah J-75	43.58	60.44	3669.79	Scotian	Sable	Scotian Shelf	CNSOPB-CSLF*	3560.76	3669.79	109.03	Argo	diapir
Onondaga E-84	43.72	60.22	3988.30	Scotian	Sable	Scotian Shelf	CNSOPB-CSLF*	3959.66	3988.31	28.65	Argo	detached sheet
Sable Island E-48	43.96	60.12	3602.70	Scotian	Sable	Scotian Shelf	CNSOPB-CSLF*	2985.82	3602.74	616.92	Argo	diapir?
Sable Island O-47	43.95	60.11	4198.62	Scotian	Sable	Scotian Shelf	CNSOPB-CSLF*	3887.42	4198.62	311.20	Argo	diapir?
Eurydice P-36	45.43	60.08	2965.10	Scotian	Orpheus Graben	Scotian Shelf	CNSOPB-CSLF*	795.53	2392.68	1597.15	Argo	pillow?
Abenaki L-57	44.28	59.89	2178.41	Scotian	Abenaki	Scotian Shelf	CNSOPB-CSLF*	2167.13	2178.41	11.28	Argo	detached diapir?
Iroquois J-17	44.44	59.79	2086.40	Scotian	Abenaki	Scotian Shelf	CNSOPB-CSLF*	2044.29	2086.36	42.07	Argo	diapir
Primrose F-41	44.00	59.12	2592.30	Scotian	Sable	Scotian Shelf	CNSOPB-CSLF*	1981.50	2592.32	610.82	Argo	detached diapir?
Primrose N-50	44.00	59.11	1713.60	Scotian	Sable	Scotian Shelf	CNSOPB-CSLF*	1707.49	1713.59	6.10	Argo	detached diapir?
Primrose A-41	44.00	59.10	1859.60	Scotian	Sable	Scotian Shelf	CNSOPB-CSLF*	1845.87	1859.59	13.72	Argo	detached diapir?
Argo F-38	45.46	58.84	3386.30	Scotian	Orpheus	Scotian Shelf	CNSOPB-CSLF*	2305.20	3085.19	779.99	Argo	pillow?
Hercules G-15	45.57	58.79	1081.10	Scotian	Orpheus	Scotian Slope	CNSOPB-CSLF*	1054.61	1081.13	26.52	Argo	diapir
Chippewa -L75	44.58	58.70	2125.07	Scotian	Abenaki	Scotian Shelf	CNSOPB-CSLF*	2099.46	2125.07	25.61	Argo	diapir
Chippewa G-67	44.66	58.66	3669.79	Scotian	Abenaki	Scotian Shelf	CNSOPB-CSLF*	3593.50	3669.79	76.29	Argo	diapir
Jason C-20	45.48	58.54	2482.90	Scotian	Orpheus Graben	Scotian Shelf	CNSOPB-CSLF*	2449.37	2482.90	33.53	Argo	wall
Huron P-96	44.60	58.48	3018.40	Scotian	Abenaki	Scotian Shelf	CNSOPB-CSLF*	2995.88	3018.43	22.55	Argo	diapir
Adventure F-80	45.32	57.94	1999.20	Scotian	Orpheus Graben	Scotian Shelf	CNSOPB-CSLF*	1034.19	1999.18	964.99	Argo	detached diapir?
Hermine E-94	45.39	54.50	3267.50	Scotian	Burn Platform	Grand Banks	CNLOPB-ED**	2455.00	3267.50	812.50	Windsor Group	pillow
Emerillon C-5	45.25	54.39	3276.60	Scotian	South Whale	Grand Banks	CNLOPB-ED**	3118.00	3276.60	158.60	Windsor Group	pillow?
Kittiwake P-11	44.68	53.53	3550.00	Scotian	South Whale	Grand Banks	CNLOPB-ED**	3180.00	3550.00	370.00	Argo	detached diapir?
Tern A-68	44.45	53.15	4188.90	Scotian	South Whale	Grand Banks	CNLOPB-ED**	4077.50	4188.90	111.40	Argo	diapir
Tors Cove D-52	44.19	52.40	1473.40	Scotian	South Whale	Grand Banks	CNLOPB-ED**	1308.00	1473.40	165.40	Argo	diapir?
Osprey H-84	44.72	49.46	3473.80	Carson	Carson	Grand Banks	CNLOPB-ED**	1254.00	3303.50	2049.50	Argo	?
*CNSOPB-CSLF = Canada-Nova Scotia Offshore Petroleum Board Core Storage and Laboratory Facility (CNSOPB-CSLF)												
**CNLOB-ED = Canada-Newfoundland and Labrador Offshore Petroleum Board, Exploration Department (CNLOPB-ED)												

Fig. 1: Location map of Weymouth-A45 (continental slope) and Glooscap-C63 (continental shelf) on the Scotian Continental Margin

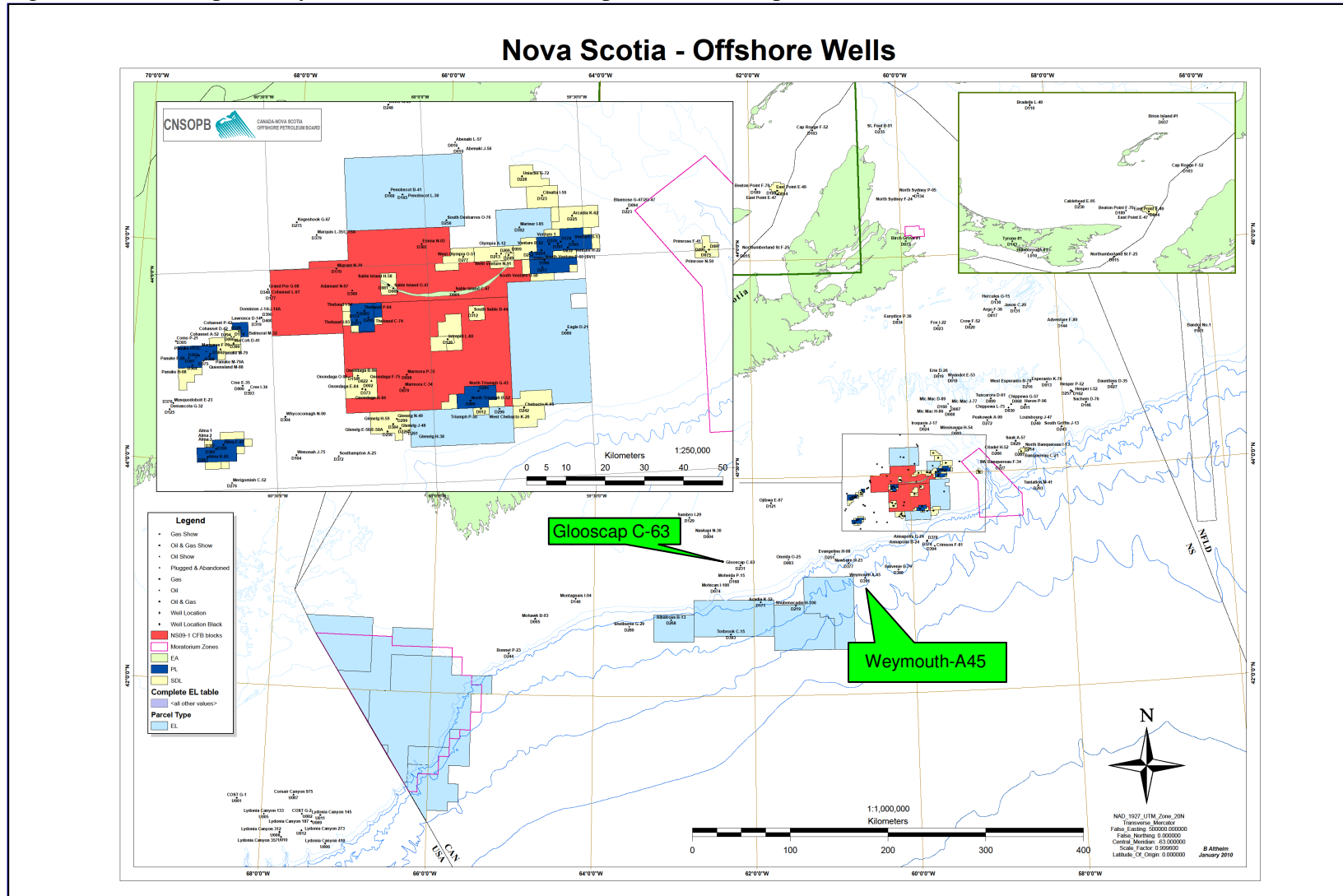


Table 2. Basic data about the studied wells: Glooscap-C63 and Weymouth-A45.
(http://basin.gsca.nrcan.gc.ca/wells/index_e.php)



Well Name	GLOOCAP-C63	WEYMOUTH-A45
Location	43.2 Latitude	43.07 Latitude
	62.17 Longitude	60.6 Longitude
Total Thickness (m)	4551.5	6520
Basin	Scotian	Scotian
Subbasin	Mohican Graben	Sable
Area	Scotian Shelf	Scotian Slope
Sample Storage Place	CNSOPB-CSLF*	CNSOPB-CSLF*
Salt Interval (m)	4045.5 to 4542.4	2840 to 4348
Salt Thickness (m)	496.9	1508
Formation	Argo	Argo
Salt Morphology	Pillow	Canopy/Diapir
Salt Color and Transparency	<p>Transparent, colorless or brown due to iron stain; poor in anhydrite impurities</p> 	<p>Non-transparent, buff colored to brown due to iron staining, rich in anhydrite impurities</p> 

Table 3: Studied samples from Glooscap-C63 and Weymouth-A45 wells under transmitted polarized and fluorescent microscope (T + F) and microthermometrically (M)

GLOOSCAP-C63 well			Weymouth-A45 well		
Sample No = Depth (m)	Studied Samples (x)		Sample No = Depth (m)	Studied Samples(x)	
	T + F	M		T + F	M
4125	x		2950	x	x
4135	x	x	2985	x	
4155	x		3020	x	
4165	x		3055	x	x
4185	x	x	3080	x	
4195	x	x	3110	x	
4205	x	x	3140	x	x
4225	x		3170	x	
4235	x	x	3200	x	x
4240	x		3230	x	
4245	x	x	3260	x	x
4255	x		3290	x	
4265	x		3320	x	
4275	x	x	3350	x	x
4285	x		3380	x	
4295	x		3410	x	x
4300	x	x	3440	x	
4305	x		3470	x	x
4315	x	x	3500	x	
4320+4340	x		3530	x	x
4325	x		3560	x	
4335	x	x	3590	x	
4345	x		3620	x	x
4355	x	x	3645	x	
4365	x		3670	x	
4375	x	x	3700	x	x
4385	x	x	3730	x	
4395	x		3760	x	
4405	x	x	3790	x	x
4410+4440+4460	x		3820	x	x
4415	x	x	3850	x	
4425	x		3880	x	x
4435	x		3910	x	x
4445	x	x	3940	x	x
4455	x		3970	x	
4465	x	x	4000	x	x
4475	x		4030	x	
4485	x	x	4060	x	x
4490+4510+4540	x		4330	x	
4495	x				
4505	x	x			
4515	x				
4525	x	x			
4535	x				
4540	x	x			
Total Number	45	21	Total	39	18

BACKGROUND ON FLUID INCLUSIONS

Fluid Inclusions are the fluids trapped in the crystals during their growth. These fluids could be liquid, vapour, gas, etc., and their composition may be pure water, brines of varying salinity, natural gas, petroleum, silicates, sulphides, carbonate melts and others. Fluid Inclusion Assemblages (FIA) is a group of fluid inclusions which have been trapped at the same time, under approximately the same temperature-pressures and have approximately the same composition (Samson et al., 2003). This means that the FIA represents a “Fluid Event” in the history of the depositional system and they also represent the original fluids available at the site where they were trapped in the mineral/rock (Samson et al., 2003). Therefore recognizing these fluid inclusions under the microscope and analyzing them will reveal the nature of these fluids and also the geological history of the depositional system and the sedimentary basin. Most rocks contain various FIAs and each one of these FIAs represents a unique event in the history of the rock. Therefore FIAs can be chosen by the expert mineralogist to serve the purpose of the study. For example a petroleum geologist will concentrate on the petroleum fluid inclusion (PFI). The presence of petroleum fluid inclusions in the diagenetic cementing minerals or in a healed fracture of a grain or crystal means that oil existed when the cement was forming or during the healing of the fracture. Thus studying the status of PFIs combined with the understanding of the burial history can help deciding the timing of oil migration (Burruss et al. 1985).

Petroleum fluid inclusions are usually know as methane inclusions due to the fact that methane form >80% of natural gases which also contain lesser amounts of other gases (ethane, propane, butane, pentane, nitrogen, hydrogen sulfide, and carbon dioxide (Selley, 1998), however any of these gases can also occur in significant amounts in natural gases. This fact has led Goldstein and Reynolds (1994) to suggest that for most natural gas systems under burial diagenetic conditions, the assumption of methane dominance is probably realistic. Goldstein and Reynolds (1994) suggested that immiscibility is possible in sedimentary environments in the system $\text{H}_2\text{O}-\text{NaCl}-\text{CH}_4$ and accordingly they have divided the fluid inclusions into two categories based on their behavior during freezing: (1) water-dominant with methane, and (2) methane- dominant.

The following paragraphs summarize Goldstein and Reynolds (1994) ideas about petroleum fluid inclusions.

Aqueous fluid inclusions containing high-pressure bubbles of methane or methane-rich gas are expected to form clathrates (solid gas hydrates) during cooling and this can be detected when the bubble suddenly deforms (jerks) above the temperature above that which is necessary for the fluid inclusion to freeze. Two such jerks are expected, one during the formation of clathrate and the other as a result of freezing. Final melting point (T_m) of clathrates depends on the gas and salt content of the fluid inclusion ranging between -20°C to $+25^{\circ}\text{C}$. The methane-dominated fluid inclusions could exist as dark or clear single-phase inclusions while liquid and vapor phases can coexist only at temperatures below the critical temperature of -82.1°C for pure methane which is unlikely for natural gases found in nature (Goldstein and Reynolds, 1994). In dark methane inclusions of low densities (below the critical density), the observer should look for a movement (flicker) along the edge of the inclusion, or look for sharp tails protrude from the body of fluid inclusion where a meniscus could appear demonstrating that the inclusion is gas-dominant but contains a thin rim of liquid around its exterior below the critical temperature. At room temperature the fluid in inclusion is supercritical, but during cooling below critical temperature, liquid and vapor coexist. Below -190°C , methane freezes indicated from the deformation of the bubble. At the triple point temperature of pure methane (-182.5°C), the bubble snaps back to a smooth surface and the inclusion homogenizes at -82.1°C . In methane inclusions of densities higher than the critical density, a bubble will appear during cooling and continue to grow as the liquid contracts. During cooling to the liquid nitrogen temperature (-196°C), the pure liquid methane may freeze below -190°C indicated by instant deformation of the bubble; however this may not be visible if the liquid nitrogen in the stage obscures the image of the inclusion. During heating following freezing event, the observer should look for a snap of the bubble back to its normal shape upon melting of methane which takes place at -182.5°C . Such melting could takes place at higher or lower temperatures if the inclusion contains other volatiles. Continued heating results in shrinking of the gas bubble (if the bulk density of the inclusion is higher than the critical density) or expanding (if the bulk density of the inclusion is lower than the critical density) until one of the phases

disappear at homogenization temperature (T_h). Unlike the aqueous fluid inclusions from the diagenetic conditions, the methane inclusions from the diagenetic conditions may homogenize by disappearance of the vapor phase or of the liquid phase. The above observations can be noticed in large, pure methane-bearing inclusions and are easily detectable in diagenetically formed inclusions because of their small sizes (commonly <7 μ m) and are rarely composed of pure methane. Existence of other gases in methane-rich inclusions alters the low-temperature phase transformations described above. During the freezing process of a gas-dominated fluid inclusion, a freezing event at a temperature higher than the triple point of methane (-182.5°C) is an indication of the coexistence of other components. Furthermore, if the initial melting of a frozen inclusion occurs at a temperature other than the triple point of methane, it means that the inclusion is not pure methane. Another indication of the impurity of methane in inclusion is that if other solid phases melt at higher temperatures after the methane melting. Homogenization of the liquid and vapor phases at higher temperatures than the critical temperature of methane (-82.1°C) also indicates the impurity of methane and the coexistence of other components. Rock salt gain different colors and deform if subjected to heat and irradiation. The colors range from blue-black near the source of radiation to pale blue and purple away from the source (Holloway, 1973). Fluid inclusions migrate towards the radiation source creating bleached areas. Heating and irradiation also create stress on salt crystals resulting in dislocation and gliding along slip planes.

GLOOSCAP-C63 WELL

Argo salt in Glooscap-C63 well

Glooscap-C63 well is located on the Nova Scotia Shelf ~180 km south-southeast of Halifax and 200 km southwest of Sable Island. It was drilled by Husky Oil Operations Ltd and Bow Valley Offshore Drilling Ltd. as an exploratory well in 1983 to evaluate an identified fault-bounded anticlinal structure within the Mohican Basin in the Scotian Shelf to a total depth of 4542.5 m and then plugged and abandoned as a dry well with no indications of hydrocarbons (Well history report, 1983). The targets were early to mid-Jurassic Mohican and Iroquois formations and Triassic Eurydice formation. The

secondary target was the possible stratigraphic closure within the sandstone of the Logan Canyon Formation and possible patch reef development within the Baccaro Member of the Abenaki Formation. Porosity was detected in the coarse clastics of the basal Mohican Formation and also in previously unknown coarse clastics at the base of the Iroquois Formation but with no evidence of hydrocarbons in either of them. Reservoir in the Logan Canyon Formation was wet and patch reef was not found in the Abenaki Formation. The well was not drilled to the prognosed total depth and did not penetrate the Eurydice Formation as planned due to technical problems encountered while drilling through the Argo Formation. The thickness of the Argo salt is ~497 m which was thicker than what was expected. The drilling fluids used for drilling the interval 2653 to 4542 m where the Argo salt was penetrated were fresh water with polymers and lignosulphonate system with barite for weight. The formations penetrated are given in Table 4. The Argo Formation was overlain by basalt and started with a shale horizon from 4045 to 4102 m depth followed by closely interbedded salt and shale/claystone beds throughout the formation. The shale was mostly red-brown and less commonly grey in color, firm to hard, fissile, calcareous to dolomitic and micro-micaceous. The salt is clear, colorless, and transparent and grades to light brown-dark brown due to iron staining (Fig. 2); it is relatively poor in anhydrite crystal inclusions.

The shape of the Argo Formation salt around Glooscap-C63 well is horizontally lying, pillow-shaped (autochthonous) as indicated from seismic profile; significant faulting has taken place on the margin and platform soling on the Argo Formation features (Fig. 3).

Fig. 2: Representative salt samples of Glooscap-C63 well grading between clean-colorless to light brown-dark brown due to iron staining.

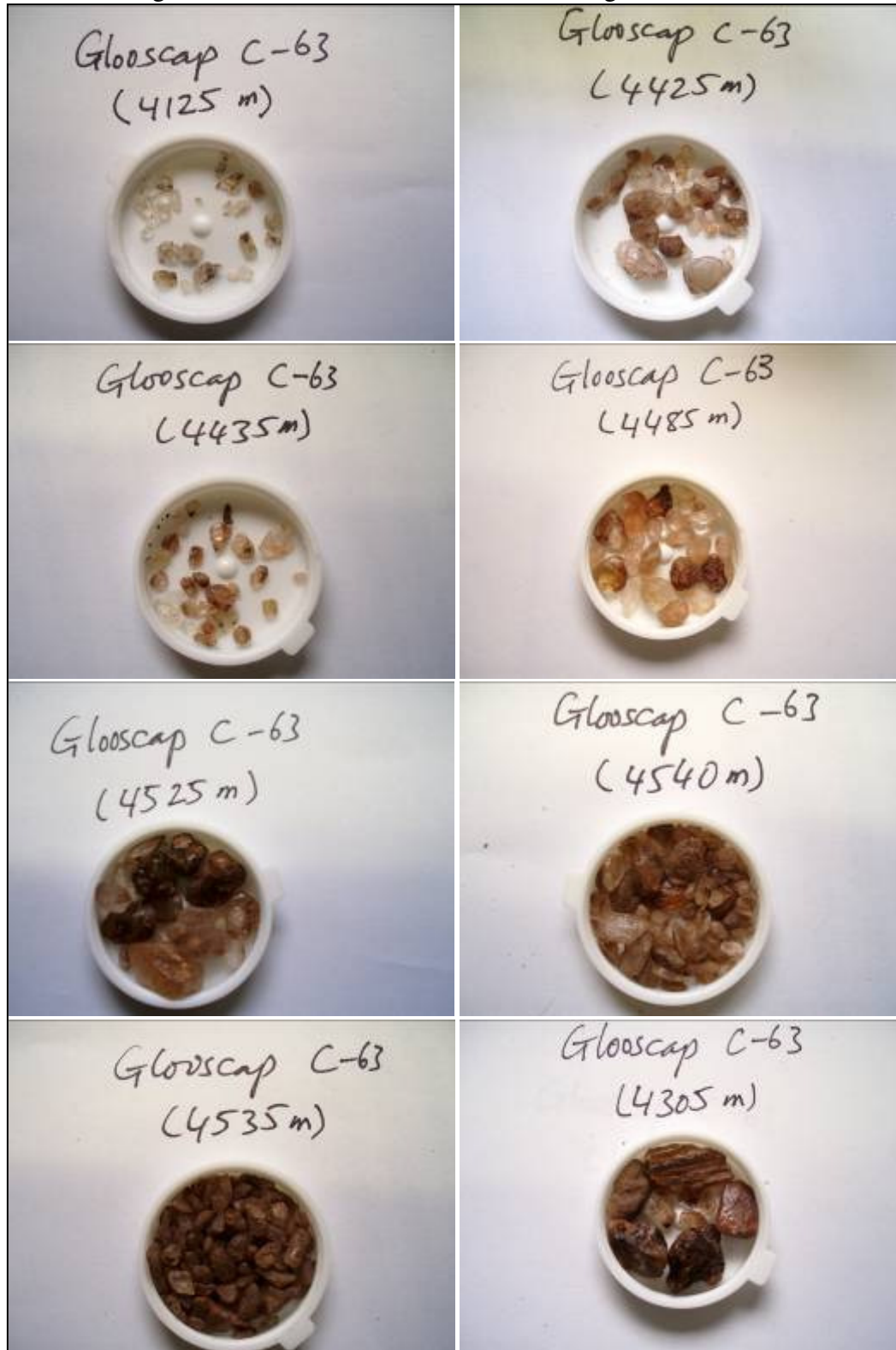
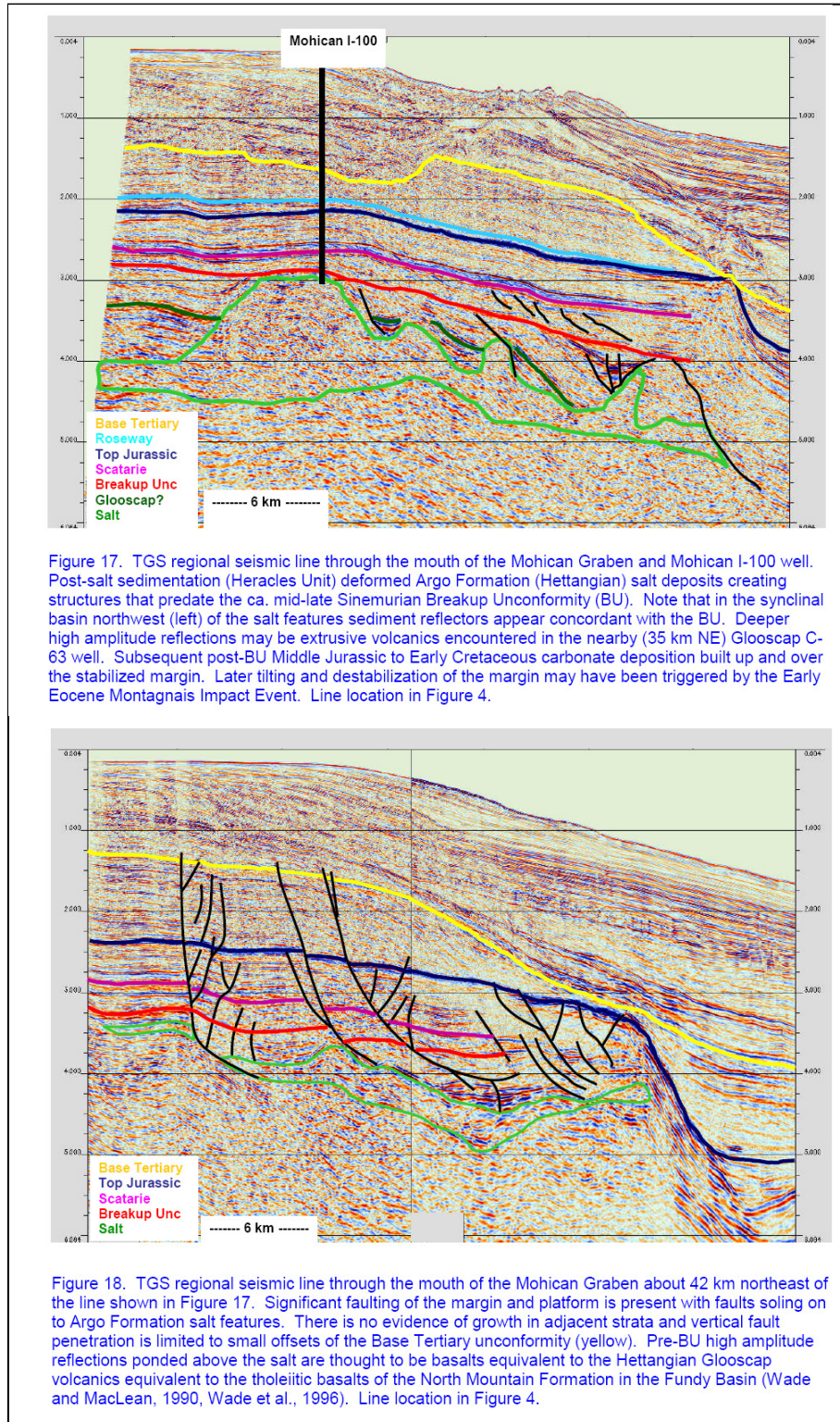


Table 4: Formations penetrated by the Glooscap-C63 well (data from the well report; the log is kindly provided by Patrick Letouzey of BeicipFranlab)

	Formation	Sample Top (m)	Log Top (m)	Prognosis Top (m)
	Banquereau	-	-	523
	Upper Cretaceous	690	-	-
	Wyandot	970	957	1048
	Dawson Canyon	1080	1078.5	1073
	Logan Canyon	1793	1794	1873
	Naskapi	1861	1865	1973
	Mississauga	1970	1965.5	2153
	O Marker	2265	2265	-
	Artimon Member	2502	2501	-
	Baccaro Member	2609	2612	2623
	Misaine Member	3254	3276.5	3393
	Scatarie Member	3331	3344	3453
	Mohican	3466	3475.5	3593
	Iroquois	3761	3770.5	3923
	Volcanics	3892	3895.5	-
	Argo	4041	4045	4143

Fig. 3. Argo salt configuration in the area around Glooscap-C63 well (from Kidston et al 2002).



Sampling and Sample Treatment

Systematic samples have been taken from Glooscap-C63 well on 10m intervals along its thickness of 497m (Table 3); the previously unwashed samples were washed on sieves to get rid of the mud and the survived salt chips were hand picked and air dried. The washed samples were kept in plastic container. Few chips have survived the drilling and washing process. The size of salt chips were ranging from <1 mm up to 5 mm (averaging 2-3 mm). The suitable transparent chips were cleaved using sharp X-acto knife into thin flakes along their cleavage planes and put on glass slides for microscopic studies without further treatment. Few of the collected samples were either not enough or dark brown and hard for cleaving which were not suitable for study.

Petrographic microscopic studies

Microscopic studies were conducted on the suitable cleaved salt chips from Glooscap-C63 well (Table 3). All samples were studied under both transmitted light polarizing microscope to identify the fluid inclusions and classify them according to their types. This was followed by studying them under fluorescence light microscope to positively identify the petroleum fluid inclusions (PFI) which shows fluorescence effect unlike the non-petroleum aqueous fluid inclusions. UV light filter as well as filters at both ends of the visible spectrum was used. The results were documented as photomicrograph images in all cases (Figures 4 to 15). These studies were followed by microthermometric studies using Linkam heating/cooling stage to get information regarding the temperature of the formation of fluid inclusions and their composition. The results of these studies showed more than one type of fluid inclusions as well as other crystal inclusions in the Argo salt.

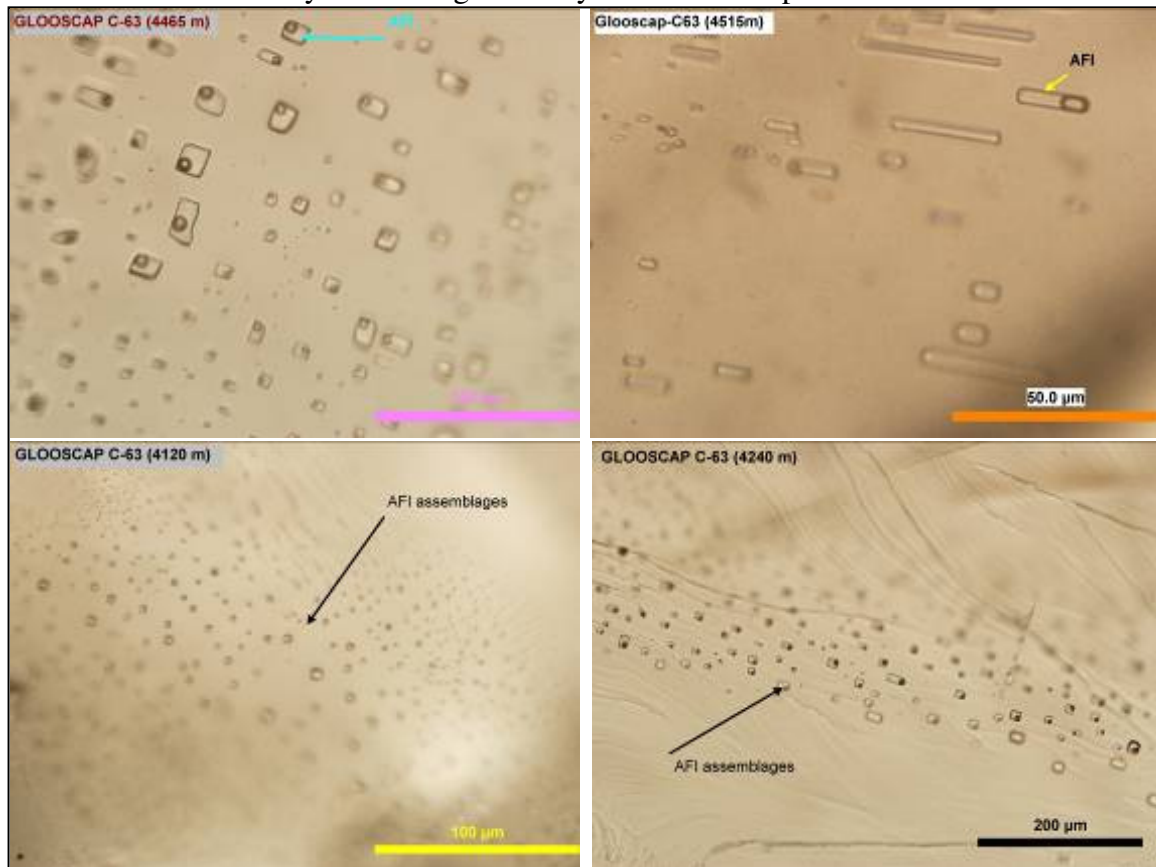
1. Aqueous Fluid Inclusions

a. Normal one- and two-phased aqueous fluid inclusions

They are very common and form as assemblages in large numbers and have relatively regular shapes ranging between parallelepipeds, cubes or cylinders (rectangular, square or elongate cylindrical in cross section view) and various sizes ranging from submicroscopic to 20 μm in average with systematic orientation and

positions relative to each other. They contain aqueous liquid (salty water) with or without vapor bubble. They are clear, colorless, transparent and apparently of primary origin formed during deposition and formation of halite crystals (Fig. 4). However, in spite of their possible primary origin, their microthermometric behavior indicated wide stretching in them as they homogenize at very high temperatures. The bubble size in most of these inclusions also suggests stretching as they look large relative to the volume of their host. Stretching and deformation has probably taken place under burial condition and also been encountered during both cooling and heating processes as part of microthermometric studies. They mostly belong to H_2O - NaCl system and in rare case to H_2O - NaCl - KCl although their eutectic point temperatures are low for such systems.

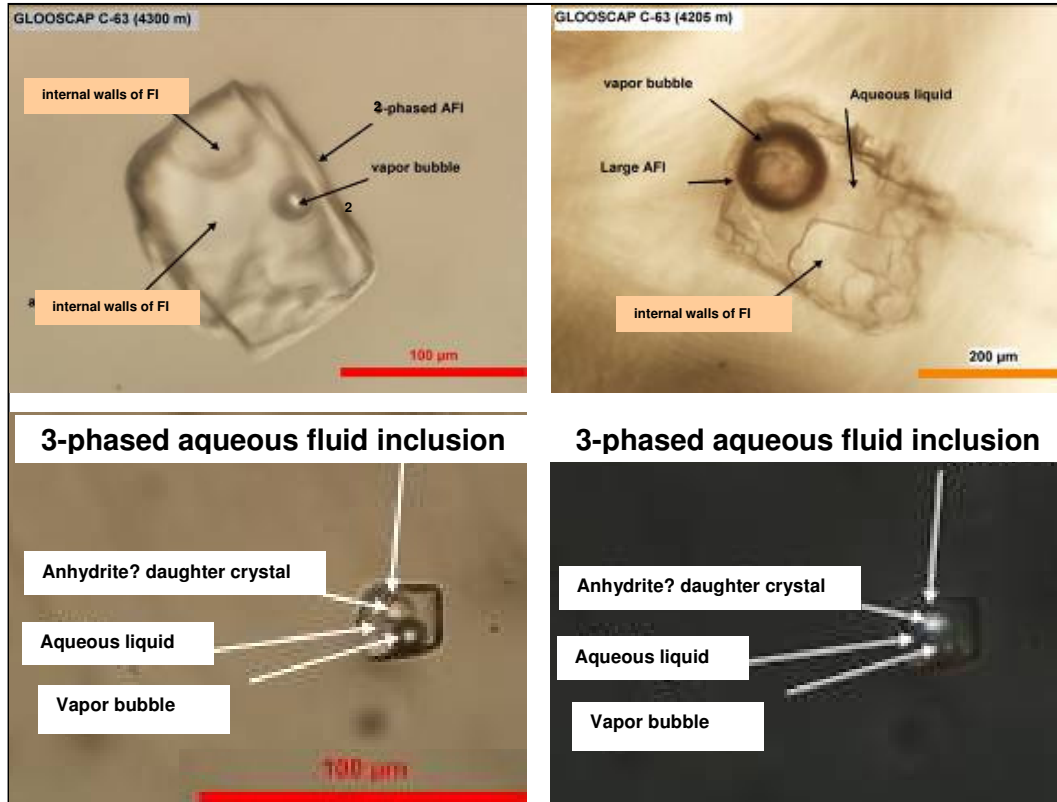
Fig. 4: Normal one- and two phased aqueous fluid inclusions assemblages in the Argo salt of Glooscap-C63 well. In most cases the vapor bubbles are large relative to the size of fluid inclusions. They are rectangular or cylindrical in shape.



b. Large two-and three-phased accidental aqueous fluid inclusions

These are large (tens to hundreds micrometers) and sporadic in their distribution and relatively not as common in their occurrence as type-a described above. They usually have parallelepiped shapes with irregular internal surfaces with clear and transparent appearance. The irregular internal walls of these large fluid inclusions can easily be mistaken by halite crystals which can form as daughter crystals in inclusions; however microthermometric studies showed that they are not daughter crystals but only block-like irregularities forming the walls as they do not melt even at very high temperatures ($>450^{\circ}\text{C}$) but deform. They mostly contain two phases and rarely three phases; a large vapor bubble, a perfect shaped solid (crystal), possibly of anhydrite which is indicated from its anisotropic character, and a liquid phase surrounding the other phases. They are probably of primary origin formed during recrystallization of salt crystals. Similar large fluid inclusions were reported by Goldstein and Reynolds (1994) who considered them primary in origin formed during recrystallization of halite crystals but they record the conditions at which recrystallization happened. They have been affected by stretching indicated by microthermometric studies (Fig. 5). Deformation of these fluid inclusions during cooling-heating process can easily be observed due to their large size as will be explained later in microthermometry section.

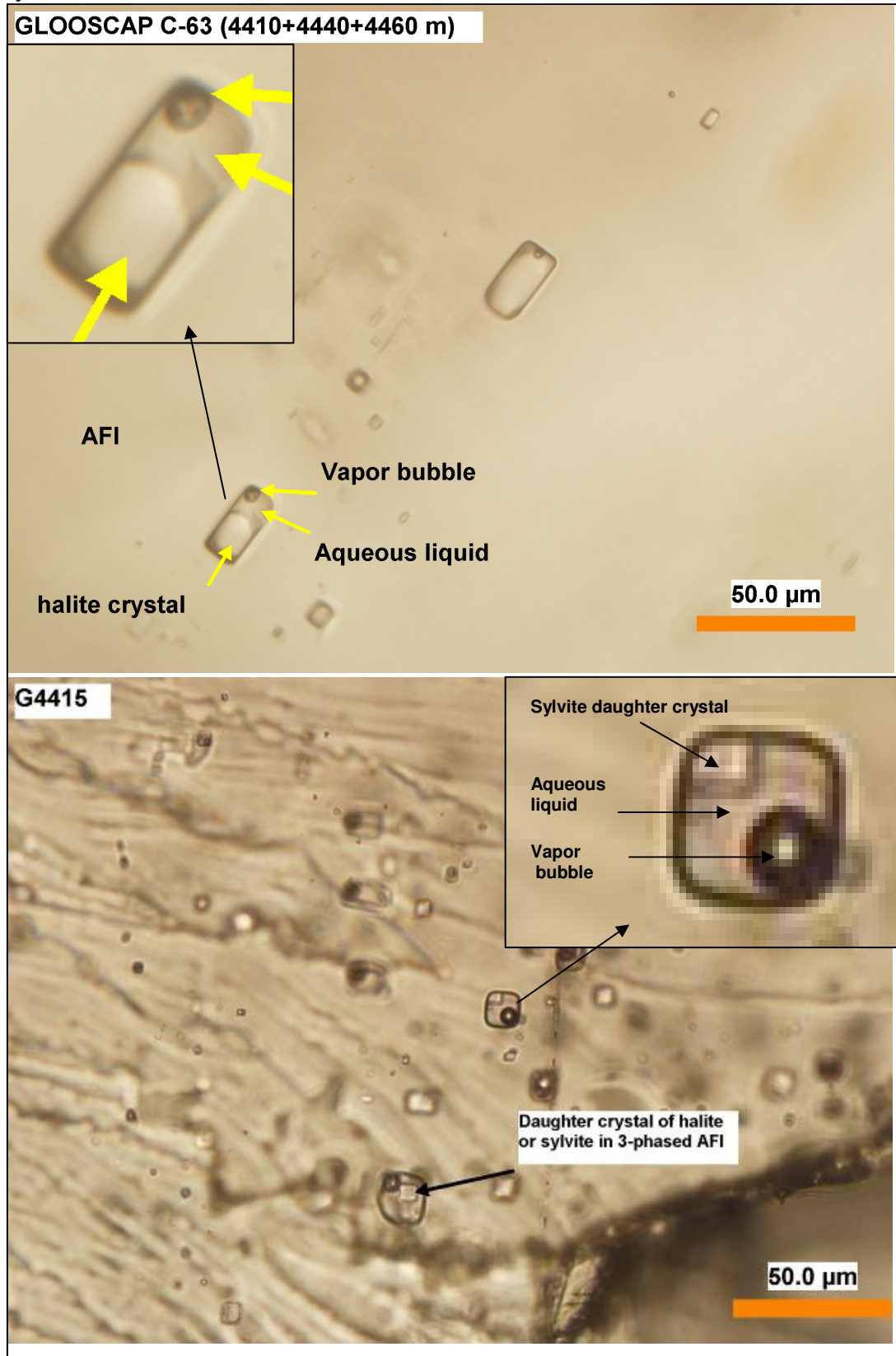
Fig. 5: Large two- and three-phased large aqueous fluid inclusions. The crystal inside the fluid inclusion of lower images is probably anhydrite indicated by its interference colors in crossed-polarized light (lower right)



c. Normal three-phased aqueous fluid inclusions

This type of fluid inclusions are not common and rarely observed where the inclusions contain a well developed euhedral (square or rectangle-shaped in cross-section view) crystal (rarely two) of sylvite or halite usually located at one of the corners and in fewer cases in the middle of the inclusion (Fig. 6). The identity of the daughter crystal as sylvite or halite daughter crystal is understandable from their behavior during microthermometric measurements. The shape, size and distribution of these inclusions suggest their primary origin; however the homogenization temperatures are too high for the formation of such inclusions at surface conditions which suggests their deformation by stretching at burial conditions. The bubble size is also relatively larger than usual for such inclusions which also indicate that they have been stretched and changed volume.

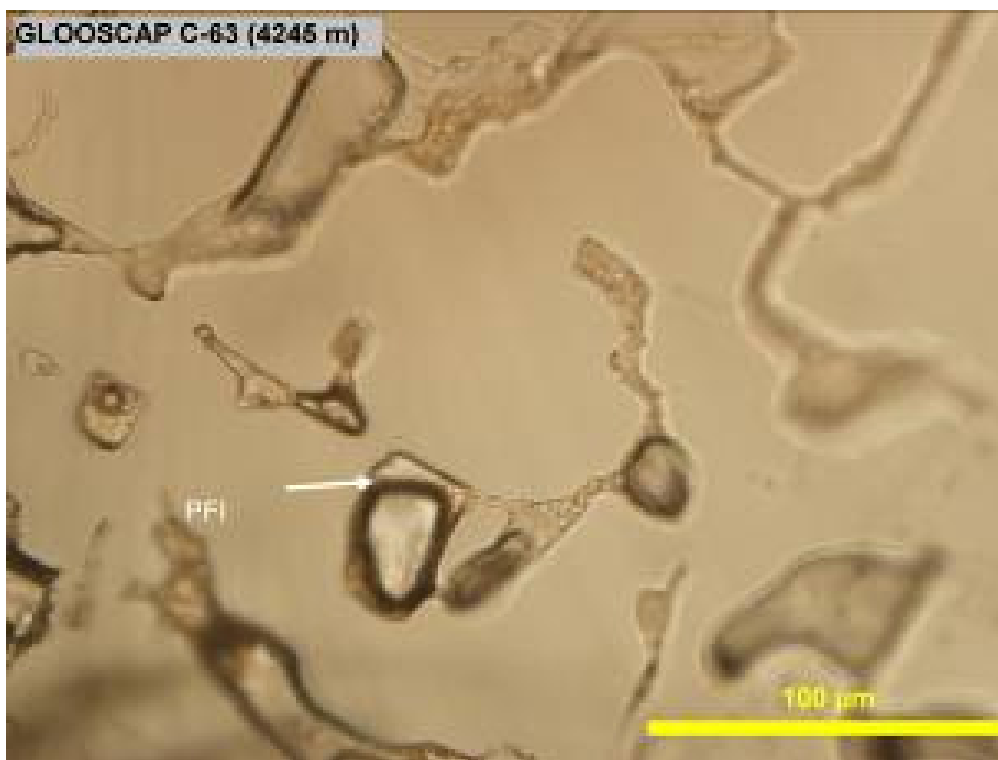
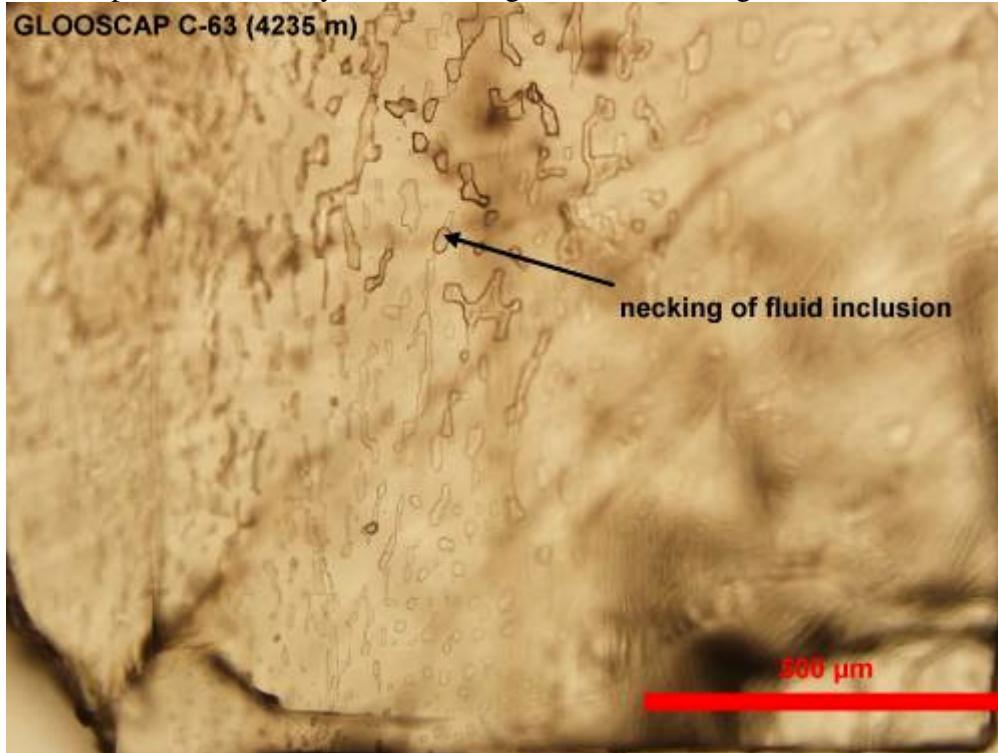
Fig. 6: Normal three-phased aqueous fluid inclusion assemblages in H_2O -NaCl-KCl system.



d. Necked aqueous fluid inclusions

Necking is a post-entrapment process in which large, irregular inclusions tend to attain morphological equilibrium by splitting into many smaller, more equant inclusions (Samson et al., 2003). Such fluid inclusions exist in the studied salts as they look different in their shape and distribution. They can form naturally or during sample treatment and study. Necking has been observed in both aqueous and petroleum inclusions (Fig. 7).

Fig. 7: Necked aqueous (top) and petroleum (bottom) fluid inclusions in the Argo salt of Glooscap-C63 well. They show necking at the lower image



2. Secondary Petroleum Fluid Inclusions

Petroleum fluid inclusions are common in the Argo salt of Glooscap-C63 well. They usually occur directly along or close to the healed fractures, cleavage planes or crystal boundaries and for this reason their shapes follow the orientation of these linear features as indication of their secondary origin (Fig. 8 and 9). The inclusions have either regular rectangular, square or needle shapes (parallelepiped, cubic and spindle in three dimensions) or irregular of any imaginable shapes such as cylindrical, tubular, network, etc. (Fig. 10). They exist either as one-phased fluid inclusions (liquid petroleum or gas petroleum) or as multi-phased aqueous-petroleum fluid inclusions (Fig. 11a and b). They exist as water dominant with methane fluid inclusion group of Goldstein and Reynolds (1994) in the $\text{H}_2\text{O}-\text{NaCl}-\text{CH}_4$ system. They will be called petroleum-bearing aqueous fluid inclusions in this report. The multi-phased inclusions are either vapor dominated or liquid dominated forming two, three or four phases (aqueous liquid + petroleum liquid usually with solid impurities \pm gas or vapor bubbles) (Fig. 11b). The vapor-dominated inclusions usually belong to the group occurring directly along the planes of weaknesses where the vapor bubbles are usually elongate surrounded by very narrow liquid counterparts. The vapor bubble is usually small and rounded surrounded within liquid in the liquid-dominated inclusions which are distributed along or on both sides of the planes of weaknesses. The petroleum content is evident from the fluorescence of the liquid part within these secondary inclusions in UV light and also at the near-ends of visible spectrum (green and red). Most of the dark colored (usually yellowish brown or dark brown) fluid inclusions are petroleum-bearing as well as many colorless ones. The other feature of petroleum-bearing inclusions is the cloudy looking liquid part which contains very tiny solid impurities of unknown identity which could be degraded petroleum or some sort of petroleum-generating bacteria or algae (Fig. 11 to 12). The nature of petroleum in these inclusions is apparently of low amount and dispersed or partially dissolved nature because they have not formed distinct isolated oil spots within the liquid part as it is usually the case in the petroleum-bearing fluid inclusions of Weymouth-A45 well (Fig. 12). Some of such inclusions fluorescence heterogeneously and by excessive heating the fluorescence become more homogeneous suggesting that the petroleum phase is of low amount and exist as scattered molecules within the more

dominant water phase. Microthermometrically the petroleum-bearing inclusions behave like aqueous inclusions but still they show distinct fluorescence.

The average length of petroleum fluid inclusions are in the range of 10-50 μm and few μm in other dimensions and occasionally have longer dimensions reaching 0.2-0.3 mm (Figures 8 to 12). These inclusions are less common than other types but have been detected in most of the studied samples (Fig. 13). The dominant aqueous liquids in the petroleum-bearing inclusions belong to H_2O -NaCl system and in rare cases to H_2O -NaCl-KCl as indicated from microthermometric studies. However, similar to the other types, these inclusions were also stretched (deformed) indicated from the very high homogenization temperatures. Both the primary looking and secondary fluid inclusions can be seen side by side and the differences between them can easily be observed from their shapes, distribution and occurrence within the halite crystals (Fig. 8).

In rare cases some salt chips contain impurities of microscopic scale showing weak fluorescence which could be remnants of dead bacteria or algae grown on salt crystals during their deposition (Fig.14).

Fig. 8: Secondary petroleum fluid inclusions grown along a fracture cross-cutting cleavage planes in the Argo Salt at the Glooscap-C63 well. The lower image shows both primary aqueous fluid inclusions (AFI) and secondary petroleum fluid inclusions (PFI).

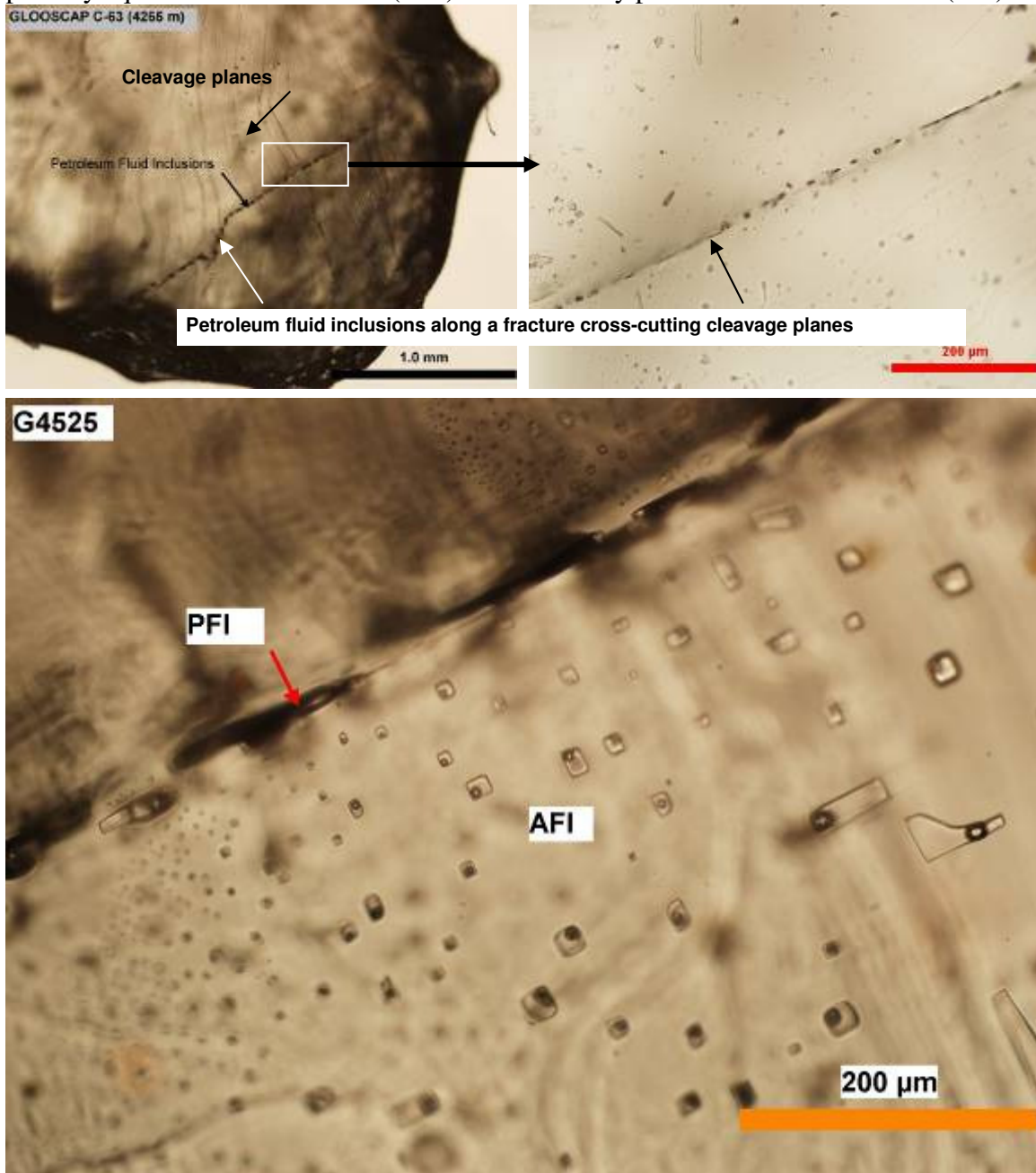


Fig. 9: Secondary petroleum-aqueous fluid inclusions grown along perpendicular cleavage planes. They show fluorescence in UV, green and red lights.

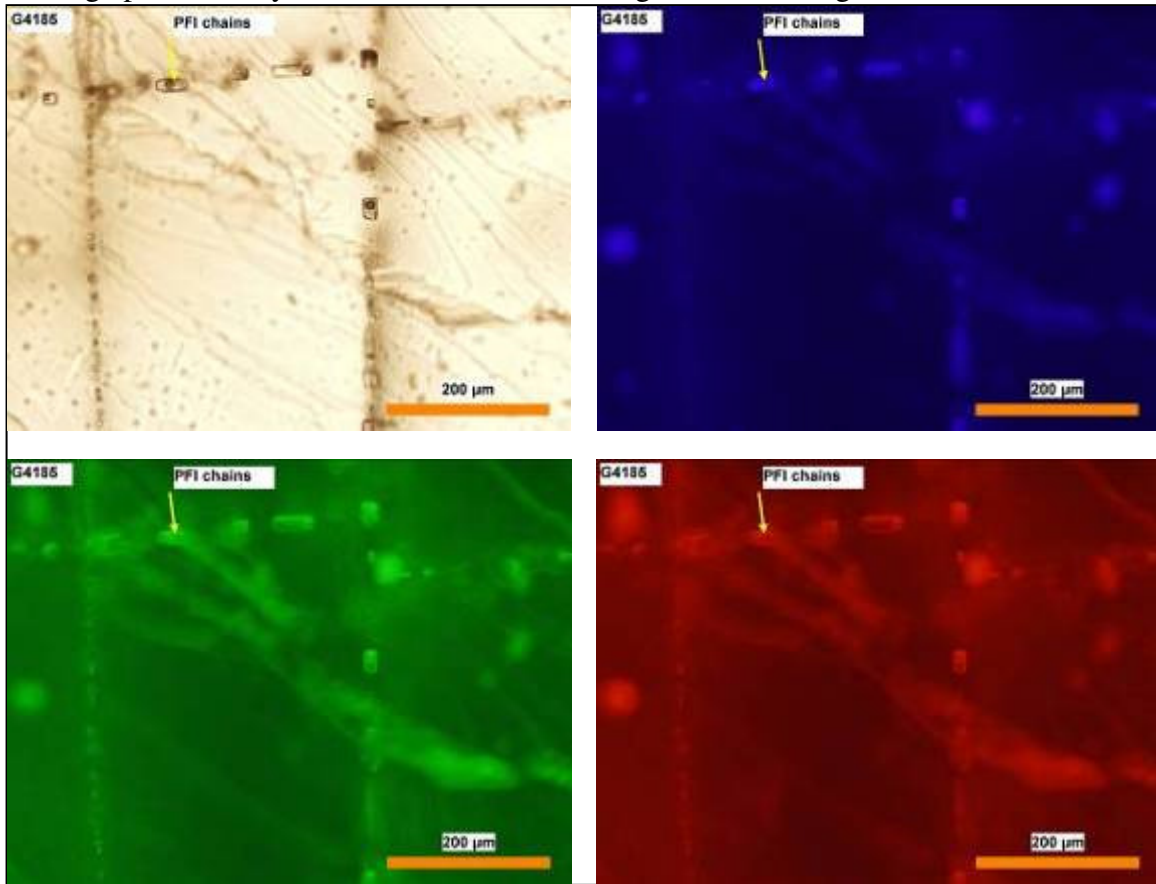


Fig. 10: Various shapes of petroleum-bearing fluid inclusions in Argo Salt at the Glooscap-C63 well.



Fig 11a: One-, two- and three-phased petroleum fluid inclusions

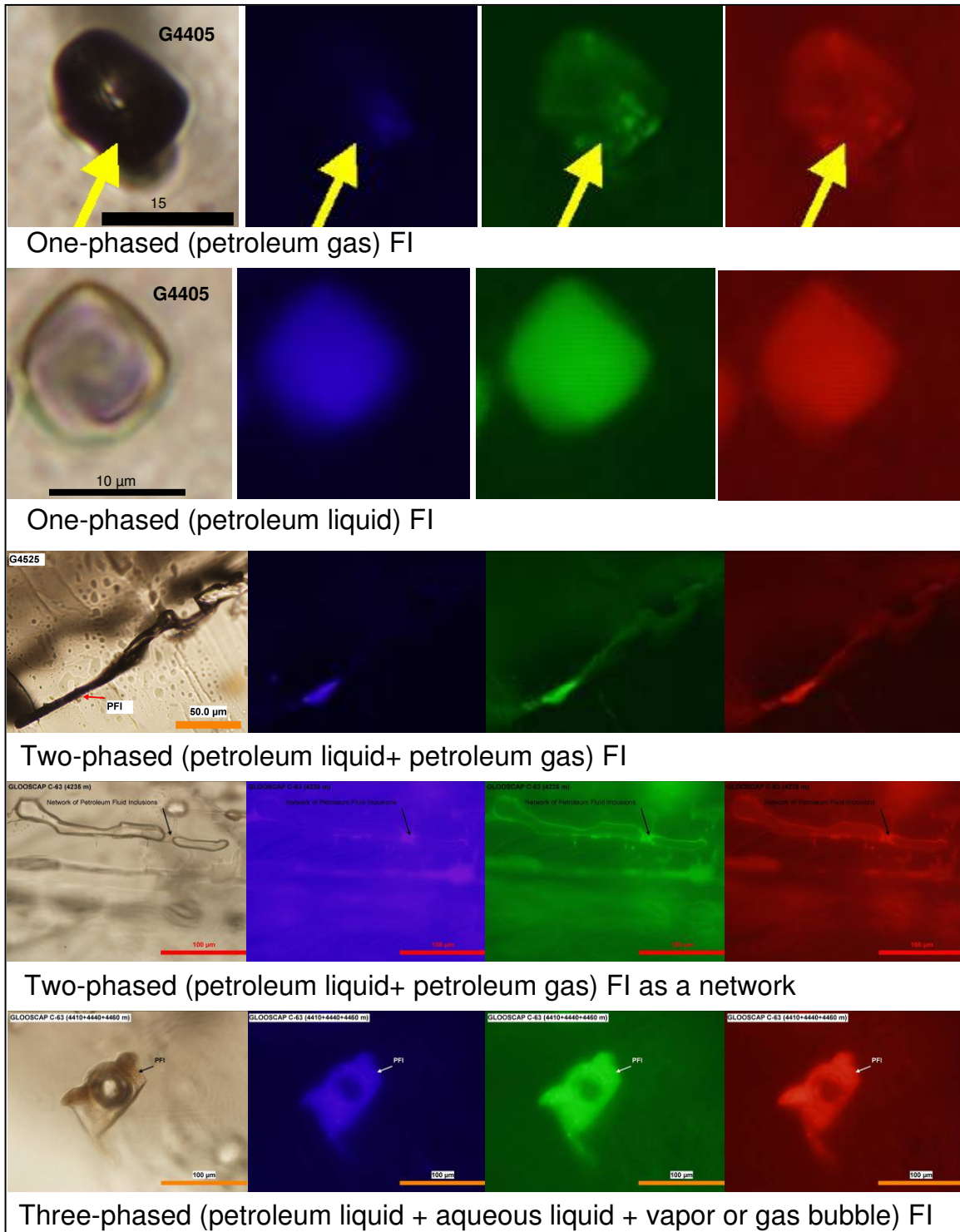
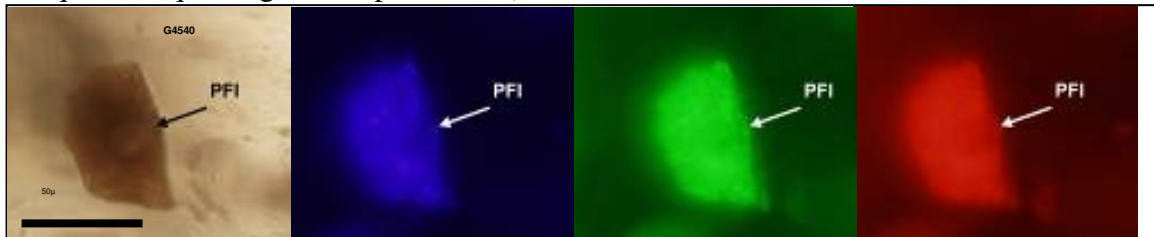
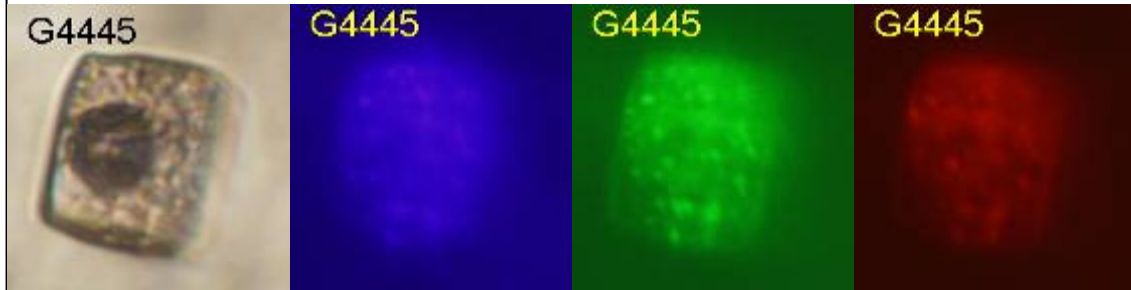


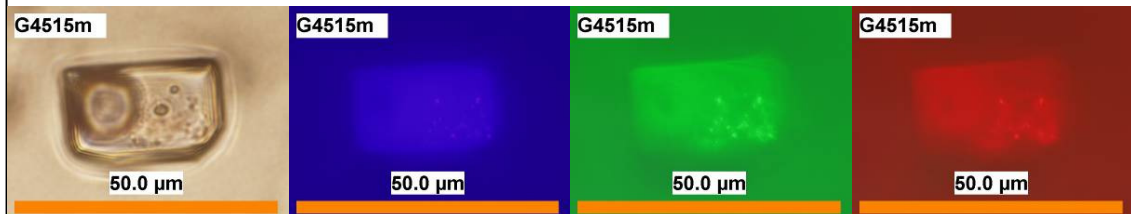
Fig 11b: Four-phased petroleum fluid inclusions (petroleum liquid with solid impurities + aqueous liquid + gas or vapor bubble).



Four-phased (petroleum liquid + aqueous liquid + impurities + vapor or gas bubble) FI



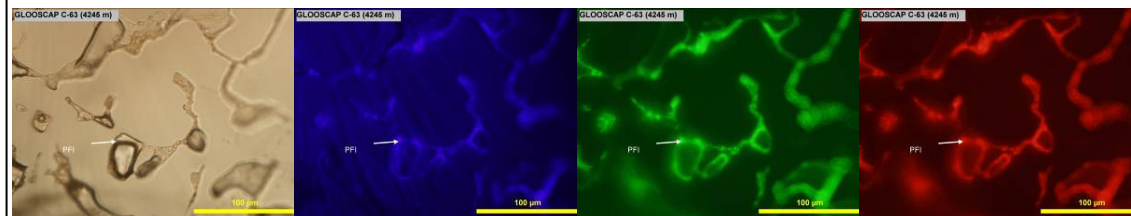
Four-phased (petroleum liquid + aqueous liquid + impurities + vapor or gas bubble) FI



Four-phased (petroleum liquid + aqueous liquid + impurities + vapor or gas bubble) FI



Four-phased (petroleum liquid + aqueous liquid + impurities + vapor or gas bubble) FI



Four-phased (petroleum liquid + aqueous liquid + impurities + vapor or gas bubble) FI as a network

Fig. 12: Aqueous-Petroleum Fluid Inclusions in Argo Salt in Glooscap-C63 (top two rows) and Weymouth-A45 (lower three rows) wells. Petroleum part is mostly impure in both but show distinct isolated liquid ring with more intense fluorescence in Weymouth and more dispersed and less fluorescent in Glooscap-C63 well samples.

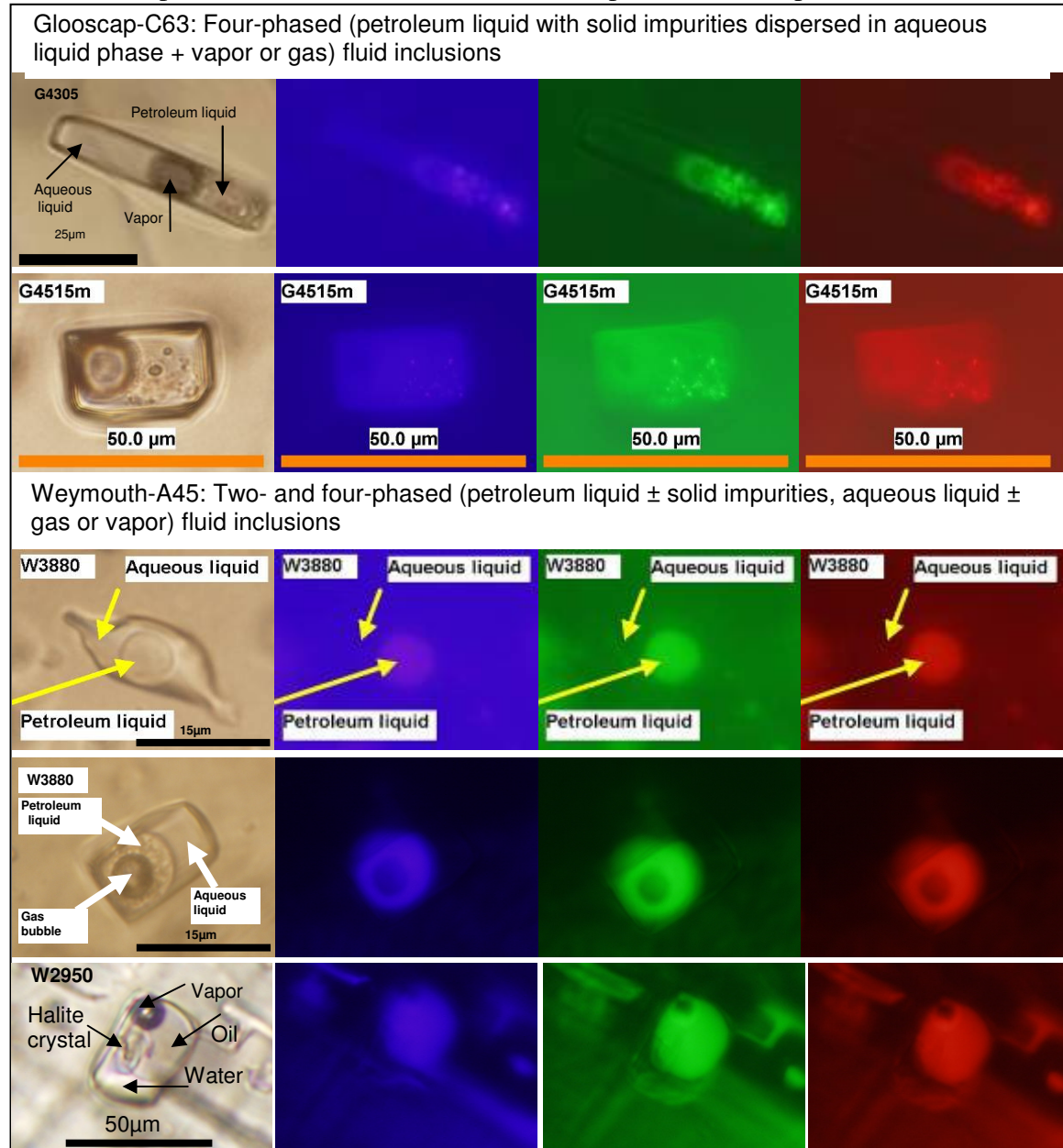


Fig. 13a: Representative images of the studied samples showing various petroleum-bearing fluid inclusions in plane polarized light (left), as well as UV light (blue) and visible spectrum green and red lights in the studied Glooscap-C63 salt samples.

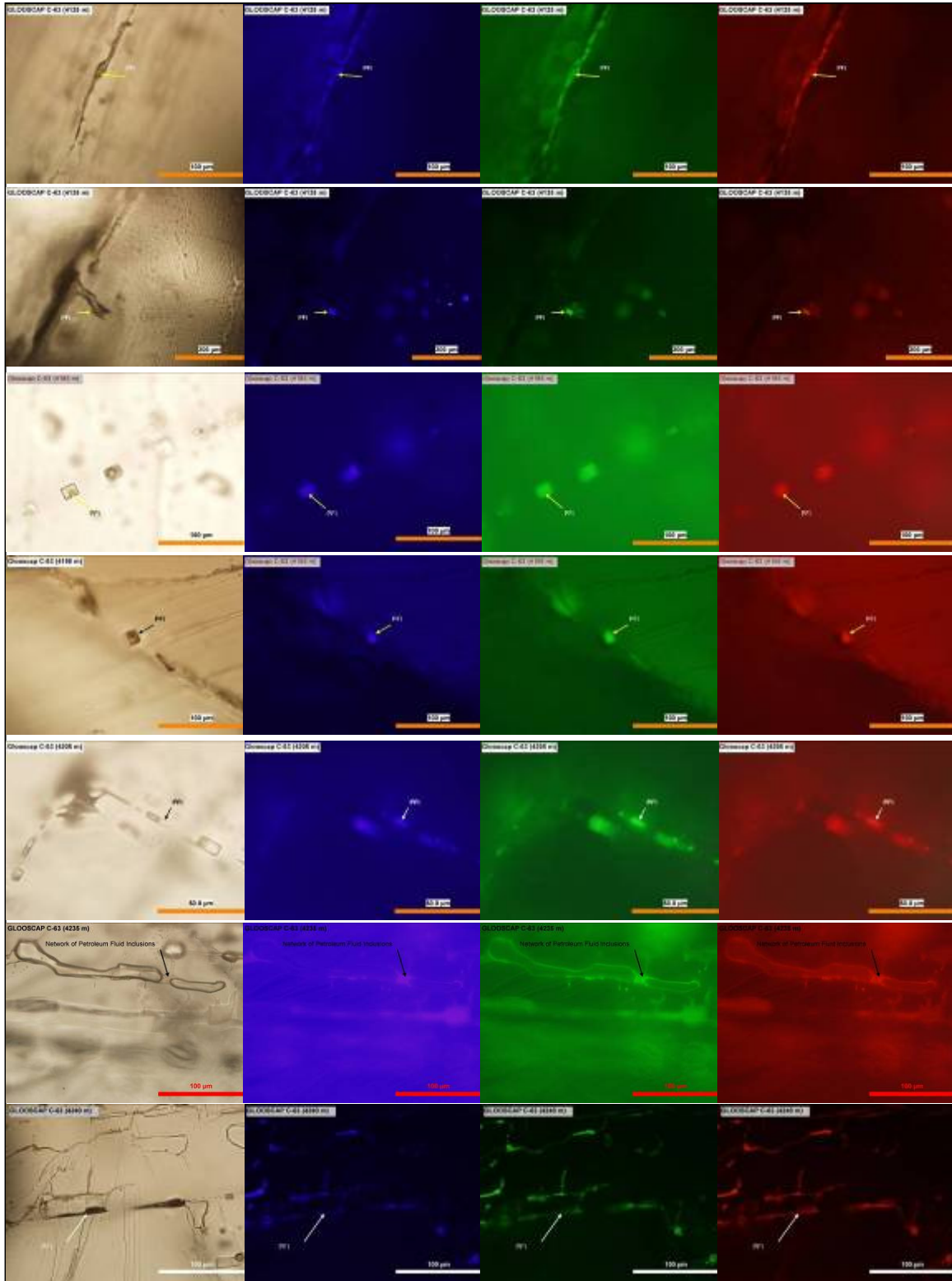


Fig. 13b: Representative images of the studied samples showing various petroleum-bearing fluid inclusions in plane polarized light (left), as well as UV light (blue) and visible spectrum green and red lights in the studied Glooscap-C63 salt samples.

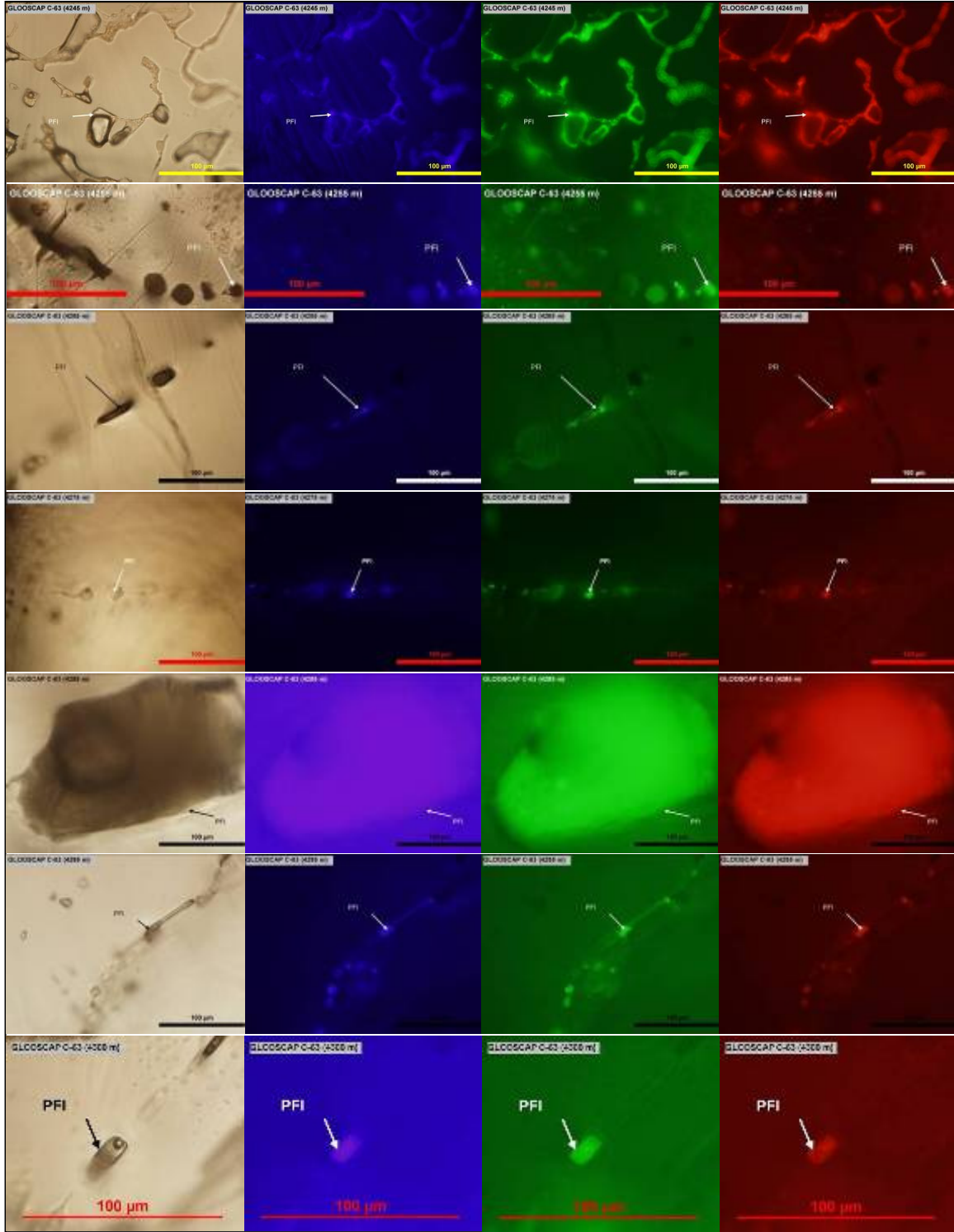


Fig. 13c: Representative images of the studied samples showing various petroleum-bearing fluid inclusions in plane polarized light (left), as well as UV light (blue) and visible spectrum green and red lights in the studied Glooscap-C63 salt samples.

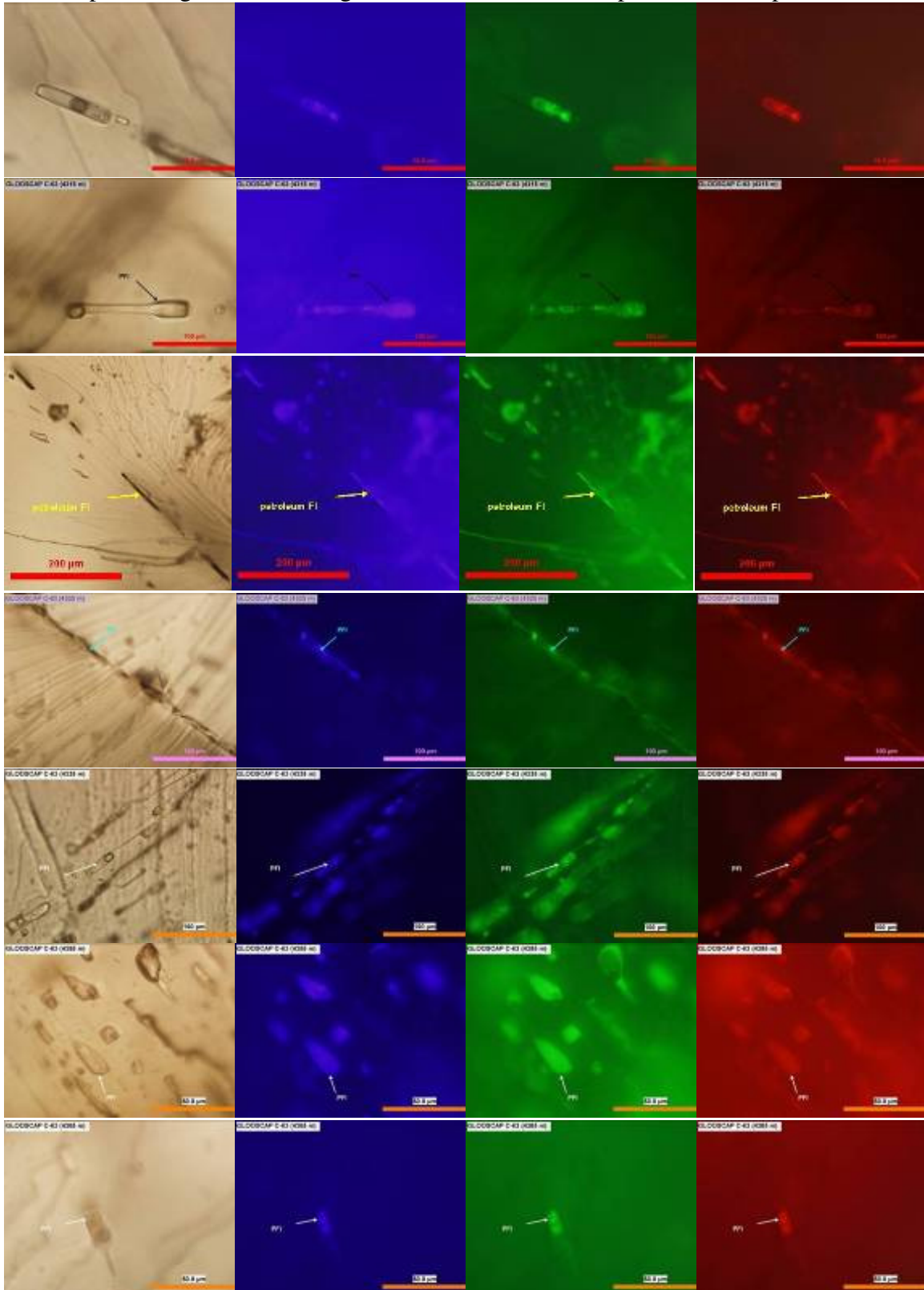


Fig. 13d: Representative images of the studied samples showing various petroleum-bearing fluid inclusions in plane polarized light (left), as well as UV light (blue) and visible spectrum green and red lights in the studied Glooscap-C63 salt samples.

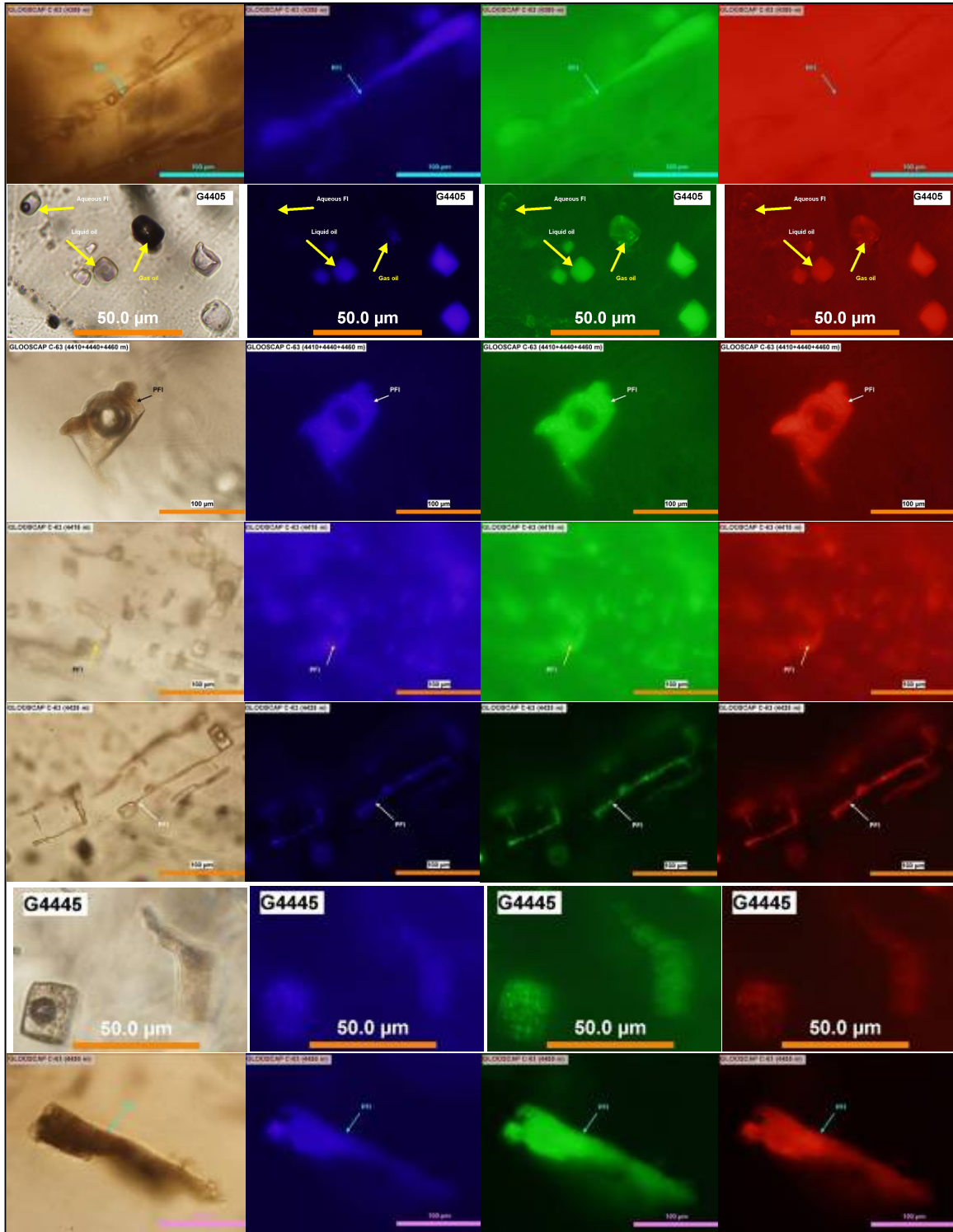


Fig. 13e: Representative images of the studied samples showing various petroleum-bearing fluid inclusions in plane polarized light (left), as well as UV light (blue) and visible spectrum green and red lights in the studied Glooscap-C63 salt samples.

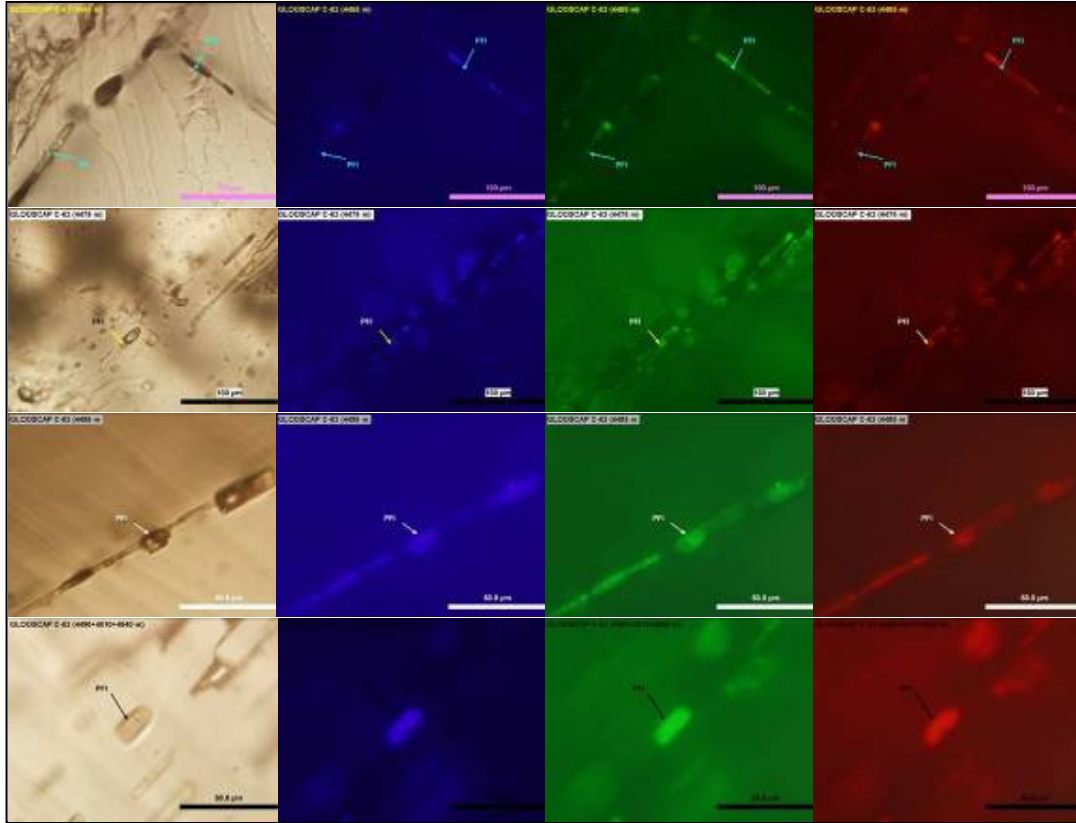


Fig. 13f: Representative images of the studied samples showing various petroleum-bearing fluid inclusions in plane polarized light (left), as well as UV light (blue) and visible spectrum green and red lights in the studied Glooscap-C63 salt samples.

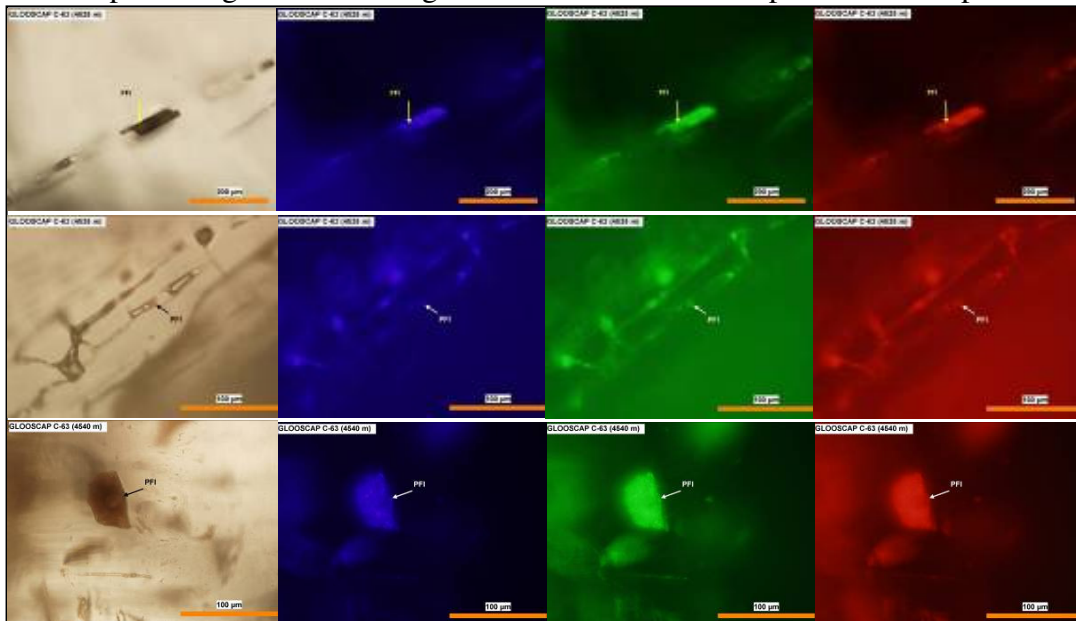
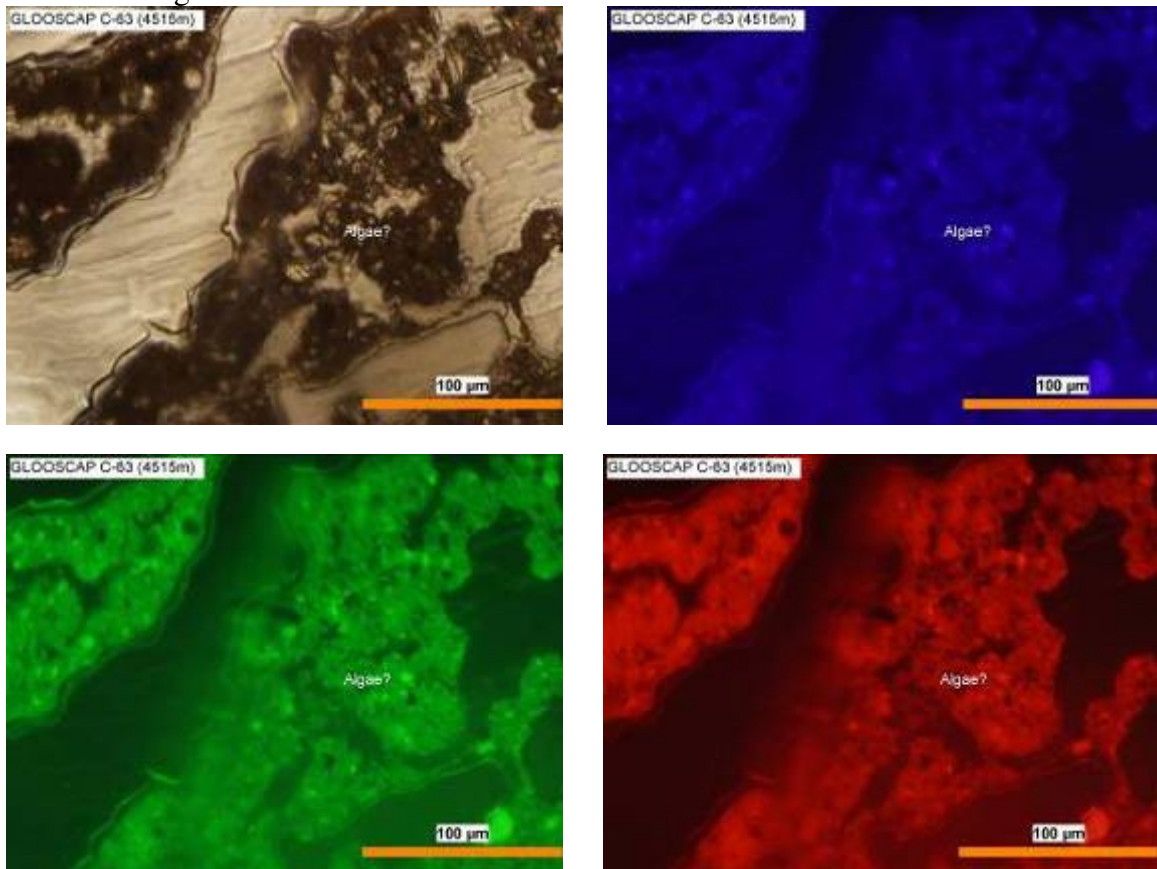


Fig. 14: Impurities on the salt chips showing weak fluorescence which could be dead bacteria or algae.



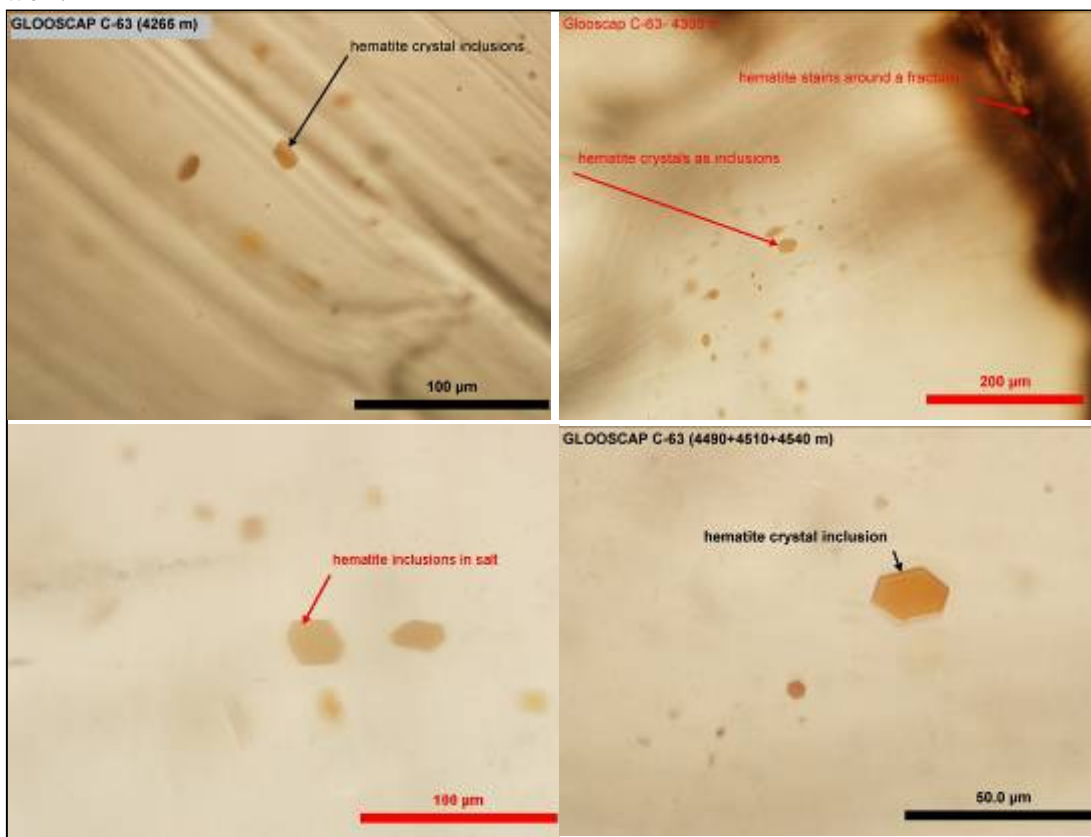
3. Other Inclusions

In addition to the abundant primary and secondary fluid inclusions in the studied salt at Glooscap-C63 well, there are solid (crystal) inclusions such as hematite, anhydrite and rarely quartz as well as a liquid which is found on the surface of salt.

a. Hematite crystal inclusions

Perfectly shaped euhedral hematite inclusions are common in the studied salt. They are usually less than 20 μm in size. In addition to these crystals, iron stain also exists as very thin films within the salt along fractures and has resulted in brown coloration (Fig. 15). The presence of iron oxides is an indication of the oxidizing conditions during deposition of Argo salt in Late Triassic time.

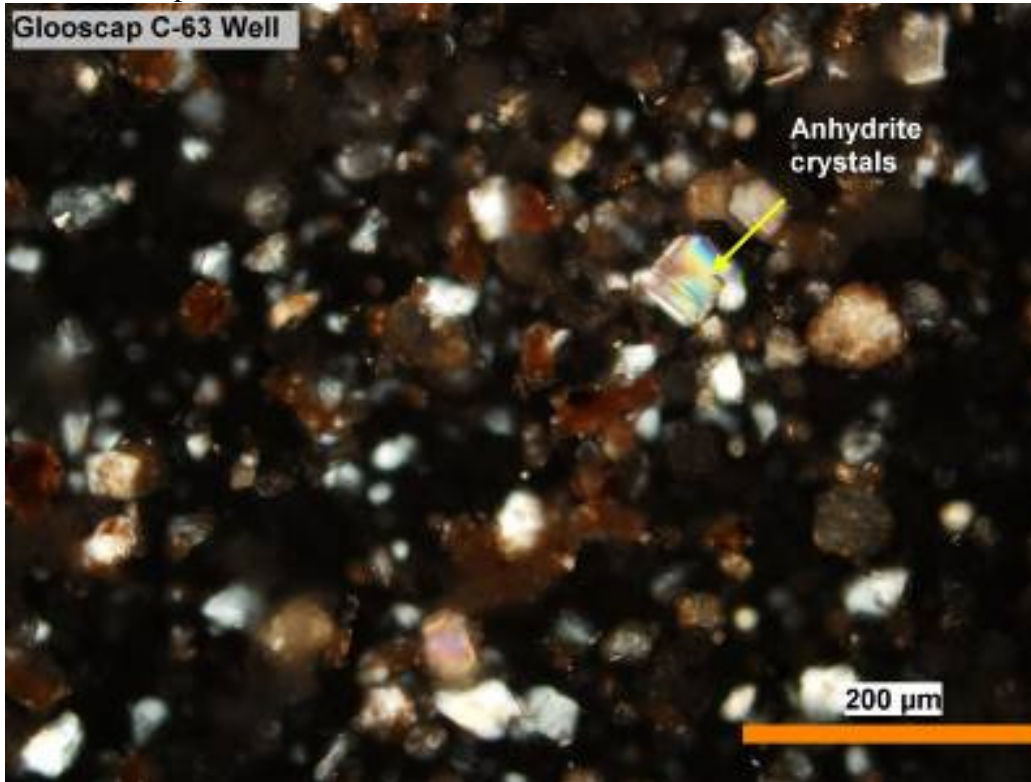
Fig. 15: Perfect euhedral hematite inclusions and iron stain in halite of Glooscap-C63 well.



b. Anhydrite crystal inclusions

Tiny anhydrite crystals exist as part of impurities in halite crystals. They become more evident when a chip of halite dissolves in water leaving behind anhydrite and iron oxides as insoluble residue (Fig. 16).

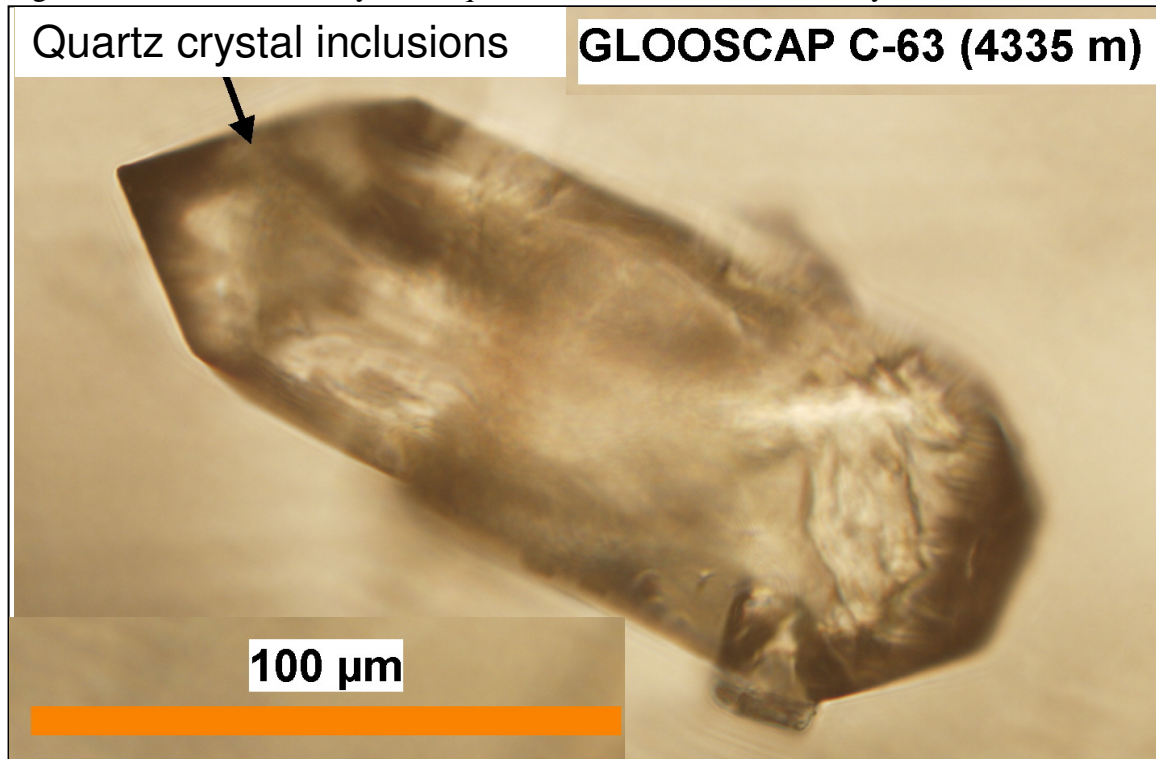
Fig. 16: Tiny anhydrite (light colored) and iron oxides (brown) inclusions left over from dissolved chips as insoluble residue.



c. Quartz crystal inclusions

Quartz crystal inclusions can rarely be seen within halite of Glooscap-C63 well. These crystals are very well developed euhedral crystals (Fig. 17). They are obviously of detrital origin brought to the site of salt depositional environment from nearby land areas. The perfect shape of the crystal with no broken tips and edges suggests that the source rocks were very close to the site of deposition which did not require much transportation.

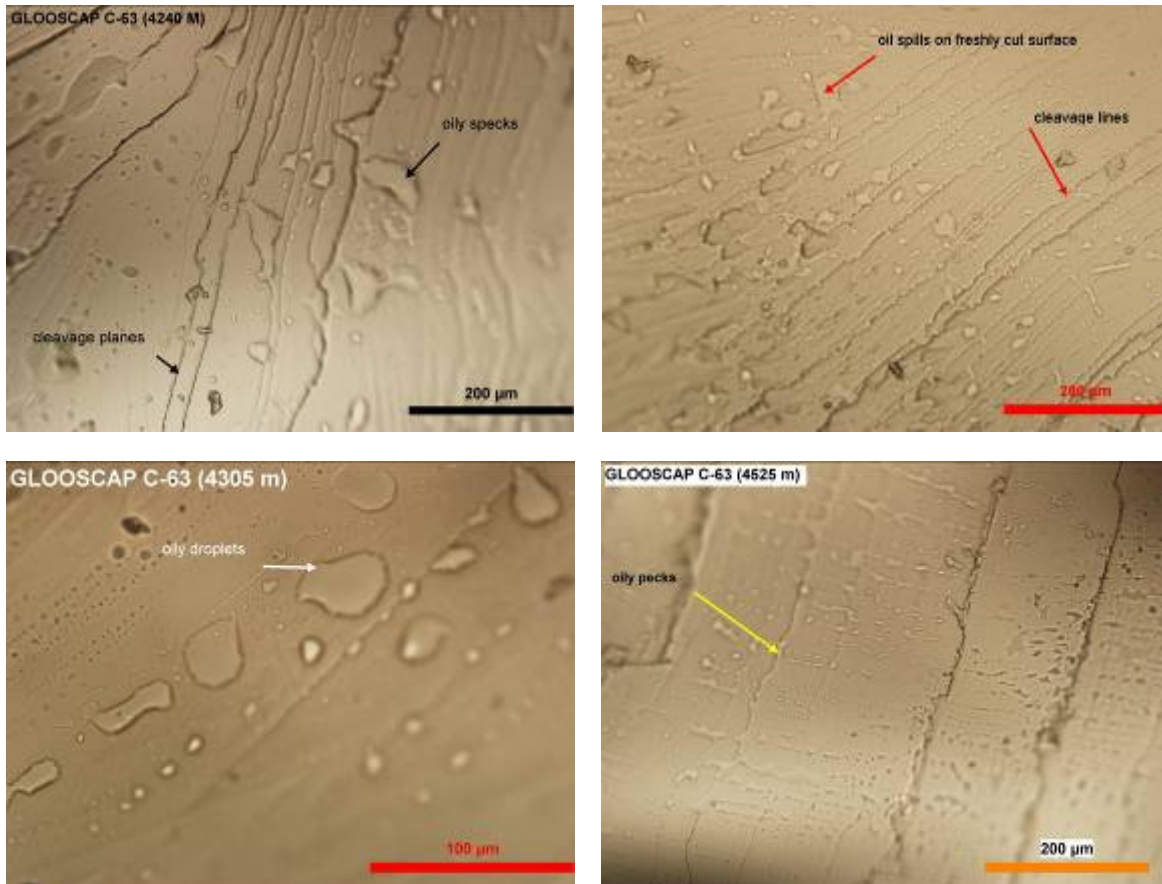
Fig. 17: Perfect euhedral crystal of quartz as inclusion in salt of Weymouth-A45 well.



d. Lubricant-like liquid:

The salt chips also contain a lubricant-like liquid as specks which are especially obvious in the newly cleaved pieces. They spill over the cleavage planes and other parts and look like oily material but do not show fluorescence. The source of these fluids could be the fluid inclusions which leaked during preparation (Fig. 18).

Fig. 18: Lubricant-like liquid on the surface of the salt grains and along cleavage planes.



WEYMOUTH-A45 WELL

Well Summary:

The Weymouth A-45 M (main) is an exploration well drilled at a water depth of 1689.7m to a total depth of 4348m on an inland plateau within the Scotian Slope (Fig.1). The Weymouth A-45 ST is a sidetrack portion of the Weymouth A-45 M which was undertaken at 4453m and continued to a total depth of 6520m. A mud system of water based Guar Gum + bentonite was used in drilling from the ocean bottom to 2702m, and synthetic oil base mud (PARADRIL IA) was used from 2702m to the total depth. Sampling was performed at 5m interval to the depth of 6128m and 2m interval to final TD. The basic information on the well is given in Tables 2 and 5. It is located in the southern half of EL 2380 (Weymouth), ~295 km southeast of Halifax and ~84 km south of deep Panuk Field. The well was drilled to evaluate the deep water equivalent of the lower (Berriasian) and Middle (Hauterivian) Members of the Early Cretaceous Missisauga Formation turbidite sandstone reservoirs which is believed to be enclosed in a broad anticlinal structure with four way dip closure overlying a remnant core of the Argo Salt member. The primary targets were the Middle Missisauga and Lower Missisauga formation sands at 5711m and 6502m depths respectively. The Argo Formation's salt forms a canopy and according to the EnCana's end of well report (Datalog Canada Ltd, 2004), the subsalt seismic markers are: Naskapi and the Upper, Middle and Lower Missisauga equivalent formations. However the lithostratigraphic units encountered in this borehole according to basin database (<http://basin.gdr.nrcan.gc.ca/wells>) are: Banquereau Formation, Argo Salt, Logan Canyon equivalent, Naskapi equivalent, and then the Upper, Middle and Lower Missisauga Formation equivalents (Table 5).

Table 5: Lithostratigraphy of Weymouth A-45 well (Datalog Canada Ltd, 2004; <http://basin.gdr.nrcan.gc.ca/wells>)

Year	Author	Top (m)	Bottom (m)	Formation	Age	Lithology (from well report)
2004	Macinnis, D. and Macdougall, B.	2761	2840	Banquereau	Tertiary	Claystone
		2840	4348	Argo Salt	Late Triassic - Early Jurassic	Halite with dolostone interval (3590-3620m)
		4348	4607.5	Logan Canyon Equiv ?	Cretaceous	Mudstone/claystone/shale
		4607.5	5108	Naskapi Equiv	Early	Shale
		5108	5709	Missisauga Fm (Upper) Equiv	Cretaceous	Shale (dominant) /siltstone (minor)
		5709	6156	Missisauga Fm (Middle) Equiv		Shale/siltstone
		6156	6520	Missisauga Fm (Lower) Equiv		Shale

Argo salt in Weymouth-A45 well

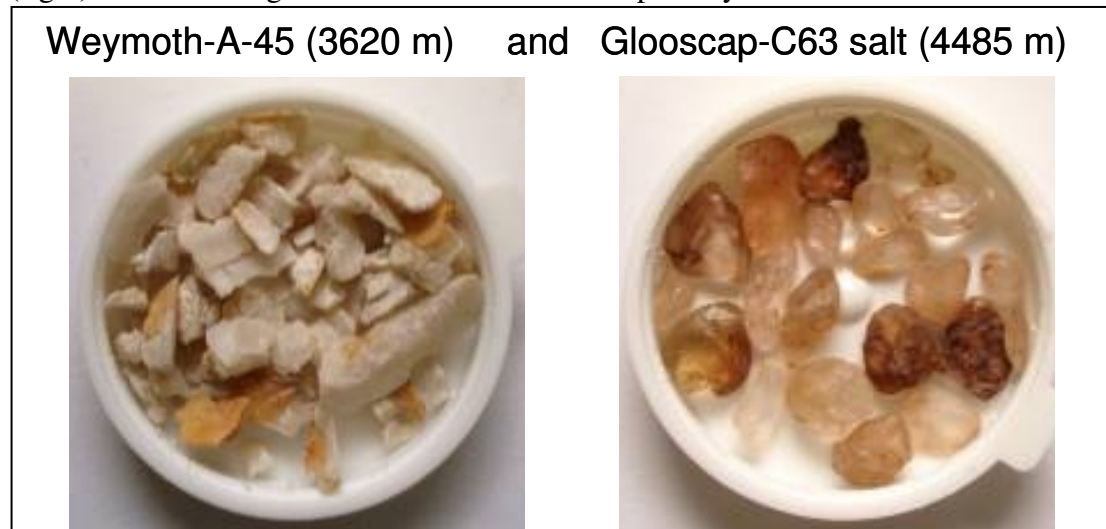
Based on the well history report (Datalog Canada Ltd, 2004), the Argo Formation (Late Triassic - Early Jurassic) in Weymouth A-45 well exists as an allochthonous salt canopy at the top of a diapir overlying younger Cretaceous formations and underlying the Tertiary Banquereau Formation (Table 5). The salt has been intersected between 2840-4348m depth with a total thickness of 1508m (Table 2). Other than dolostone which is reported in the well history report at 3590 to 3620m depth interval, the salt exists as a massive body of halite without any interbeds by other lithologic units. Two samples taken from 3590m and 3620m depths proved to be halite and not dolostone. The Argo salt in Weymouth-A45 well has many differences than that of Glooscap-C63 well (Fig. 19). The most obvious macroscopic difference is the color. It is buff colored with occasional brown tint due to iron staining, non-transparent and waxy in appearance; it is also slightly harder than that of Glooscap-C63 salt which is mostly clear and transparent (Fig. 2).

Sampling and Sample Treatment

Sampling was made from the washed and dried cutting samples available at the Canada-Nova Scotia Offshore Petroleum Board store. Thirty nine samples were collected at approximately every 35m intervals for this study (Table 3). The Argo salt in Weymouth A-45 well has many differences than that studied in Glooscap-C63 well (Fig. 19). The nature and properties of salt of Weymouth-A45 well mentioned above including color, transparency and hardness (Fig. 19) resulted in additional ways of treating and preparing the samples for microscopic study since the normal cleaving procedure of salt chips followed in dealing with Glooscap-C63 well's salt did not work for Weymouth salt. Twenty of the forty collected samples were fixed by epoxy on glass slides and cut from the surface to make them flat and smooth and then polished using mineral oil as lubricant; then the polished surface was fixed on another glass slide and the previous glass slide was removed. The new surface was again cut for flattening and smoothing, grinded and polished resulting in double-polished surface which is the ideal case for studying fluid inclusions under the microscope. However, as a result of using lubricants for polishing process, the polished surfaces gained dark stained dirt especially along

planes of weaknesses in salt chips. For this reason and for making sure that the polishing process has not affected the fluid inclusions study, the other nineteen samples were prepared for study using the same previous procedure but this time without polishing which was replaced by dry-grinding to make both surfaces of the salt chips flat and smooth. Both the polished 20 and unpolished 19 samples were studied for their fluid inclusions content using transmitted and fluorescent light microscopic settings. After these microscopic studies, the samples were separated from the glass slide by immersing them in acetone overnight for microthermometric studies. In spite of all these preparation procedures, ideal salt chips for microthermometric studies could not be found in many samples which required additional preparations. This time few new salt chips were hand grinded on fine-grained sand paper to smooth both surfaces and for final finishing the flattened chips were polished on the bare skin of the hand which proved to be even more efficient than the above mentioned methods.

Fig. 19: Representative salt samples from Weymouth-A45 (left) and Glooscap-C63 (right) wells showing the obvious color and transparency differences between the two.



Petrographic Microscopic Studies

Microscopic studies were conducted on Thirty nine cutting samples (Table 3). Transmitted light polarizing microscope was used to identify the fluid inclusions and classify them according to their types as well as to study the other material within the salt. This was followed by studying the fluid inclusions under fluorescence light microscope to positively identify the petroleum fluid inclusions (PFI) which shows fluorescence effect unlike the non-petroleum fluid inclusions. UV light as well as the light at the near ends of the visible spectrum (green and red) was used. The results were documented as photomicrograph images in all cases. This was followed by microthermometric studies using heating-freezing stage to get information regarding the temperature of the formation of fluid inclusions and their composition. It has been mentioned earlier in this report that the salt in Weymouth-A45 well has many macroscopically evident differences than the salt in Glooscap-C63 well. The Weymouth-A45 salt is buff colored, non-transparent, waxy and harder. Microscopic studies showed that these differences are attributable to the relatively high content of impurities dominated by anhydrite crystals as large inclusions in halite and also possibly to their rich petroleum content. The halite crystals constituting the Argo salt in the studied samples of Weymouth-A45 well is usually fine grained ranging from 0.01 to >1.5 mm (Figures 20 and 21); however this is not conclusive evidence of the overall crystal sizes since the studied material are few millimeter cuttings (chips) which will not show the real size of crystals if they are larger than the cuttings themselves. The microscopic studies also showed more than one type of fluid inclusions as well as other crystal inclusions in the Argo salt. Some inclusions are similar to those found in Glooscap-C63 well salt and some others are different. More than one type of primary looking (PFIs) and secondary (SFIs) fluid inclusions were found in Weymouth-A45 well salt. The petroleum-bearing fluid inclusions (PFIs) are of secondary origin and shows some differences compared to those found in Glooscap-C63 well salt. Just like the salt at Glooscap-C63 well, the PFIs in the salt of Weymouth-A45 well occurs between cleavage planes within growth zones and parallel to the halite crystal boundaries growth zones (Fig. 21); meanwhile the SFIs including the PFIs were trapped along and on the nearby zones of cleavage planes, healed

fractures mostly cross-cutting cleavage and along crystal contacts (Fig. 21). It is evident that the SFIs have elongate shapes oriented parallel to the planes of weaknesses which acted as pathways and traps for the source fluids which created these fluid inclusions under burial conditions. The details of these fluid inclusions found in each of the studied samples are given below and were documented as images in Figures 22 to 24.

Fig. 20: Fine grained (10 to >300 μ m) halite crystals constituting the Argo salt in the Weymouth-A45 well. Larger grains are shown in Fig. 19.

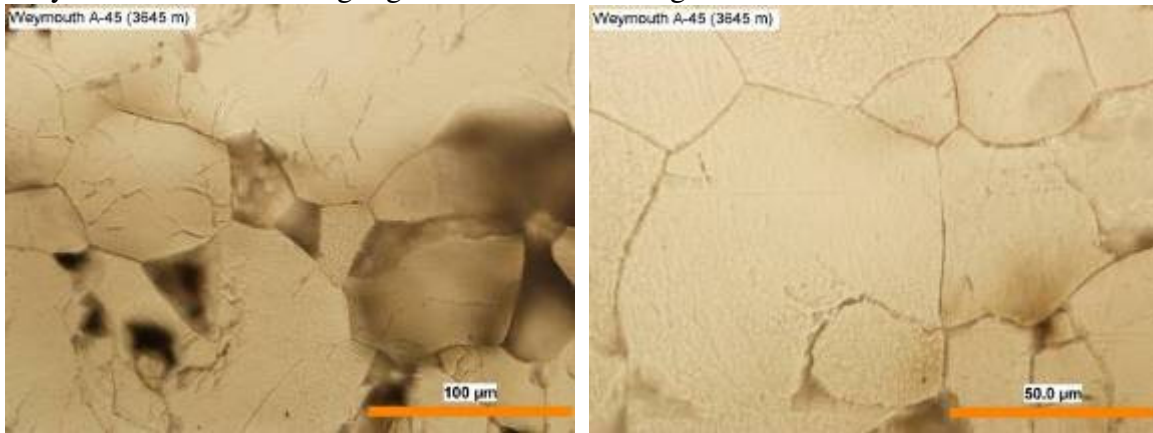
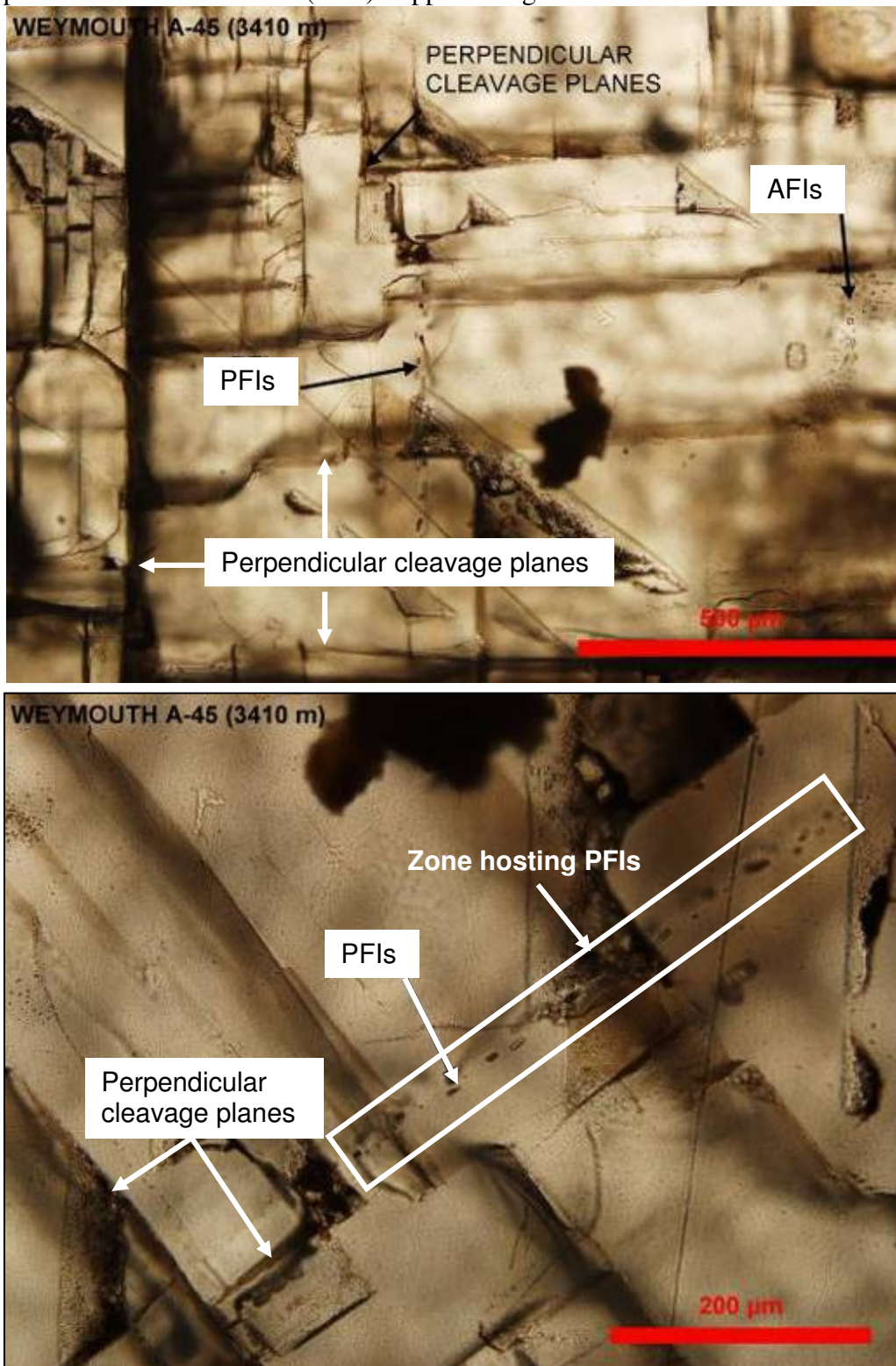


Fig. 21: Halite crystals of the Weymouth-A45 well showing perpendicular cleavage planes and assemblages of primary aqueous fluid inclusions (AFIs) between cleavages planes parallel to growth zones as well as a linearly oriented assemblages of secondary petroleum fluid inclusions (PFIs) trapped along a healed fracture zone.



1. Aqueous Fluid Inclusions (AFI)

They are less common than those in Glooscap-C63 well salt. They exist as assemblages and have relatively regular shapes. They have various sizes ranging from submicroscopic to $>10\text{ }\mu\text{m}$ with systematic orientation and positions relative to each other. These inclusions contain aqueous liquid with or without vapor bubble. They are clear, colorless, and transparent and possibly are of primary origin formed during deposition and formation halite crystals but later reequilibrated under deep burial conditions (Fig. 22 and 23). According to their shapes, they can be grouped into two types:

- a.** Fluid inclusions with parallelepiped and cube shapes (square and rectangular in cross-section views (Fig. 22). They are liquid-dominated mostly one- or occasionally two-phased inclusions. They have some similarity to the primary fluid inclusions of the Glooscap-C63 well salt in shape but are generally less common, smaller in size (mostly $<10\mu\text{m}$), mostly one-phased (liquid dominated) and have smaller vapor bubbles when found in two-phase, liquid-dominated inclusions. These AFIs belong to $\text{H}_2\text{O-MgCl}_2\text{-NaCl}$ or $\text{H}_2\text{O-CaCl}_2\text{-NaCl}$ system.
- b.** Fluid inclusions with ellipsoid (oval), lens-like, pin-like and even polygons (ellipse to oval shape with or without needle-like tail and hexagons in cross-section views) (Fig. 23). This type is normally of one-phase nature, rarely contain bubbles and have strange microthermometric behavior during heating and cooling as they do not show any changes as if they are empty vacuoles. Their size range from submicroscopic up to around $100\text{ }\mu\text{m}$. It is not certain whether these inclusions are of primary origin or of secondary origin. They have not been found in the salt of Glooscap-C63 well.

Fig. 22: One-phased rectangular-shaped aqueous fluid inclusions assemblages (AFI) of possibly primary origin along side with secondary AFI-PFI and PFI which crosscut the PFI .and show fluorescence in the salt of Weymouth-A45 well.

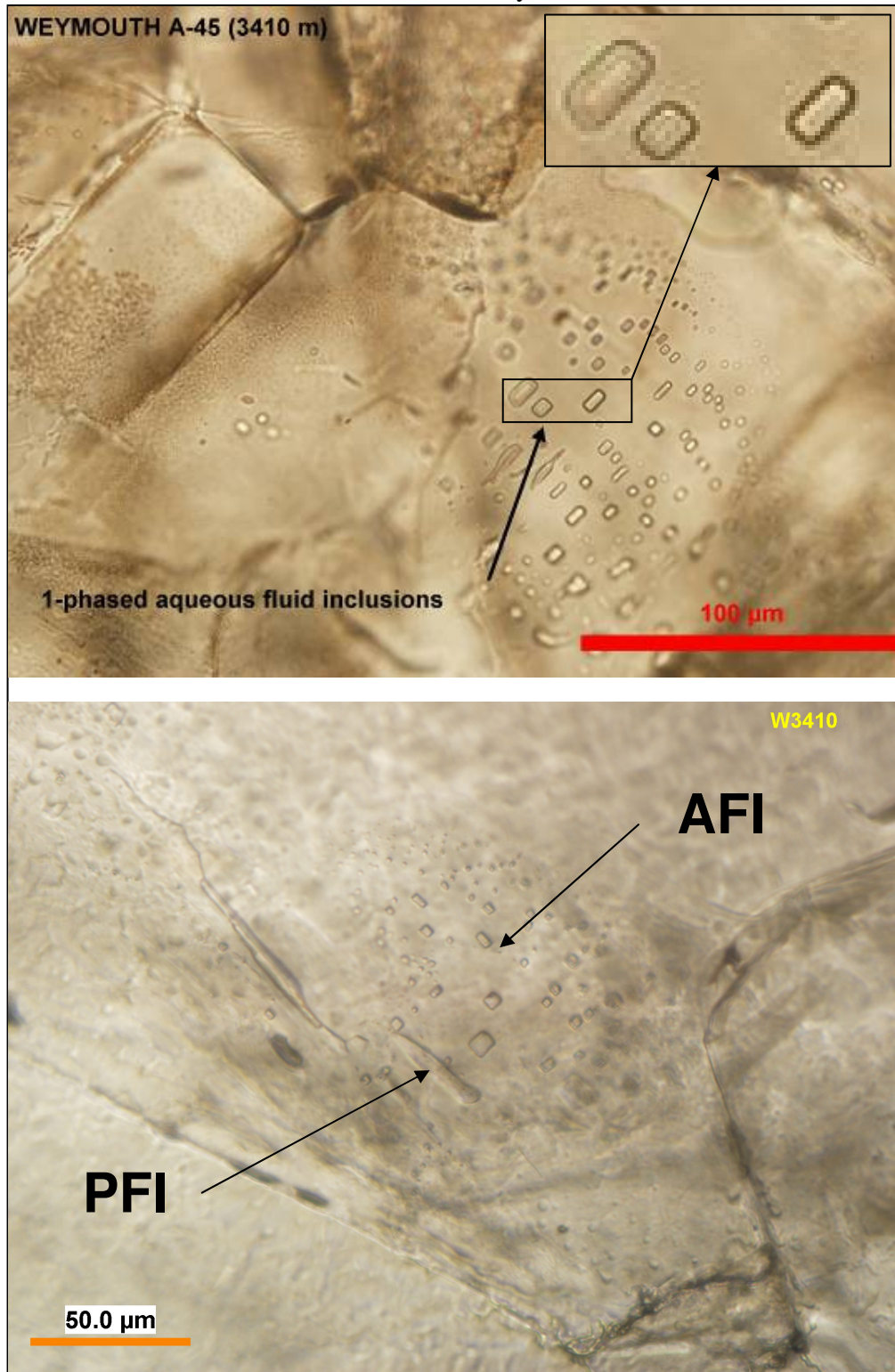


Fig. 23a: One-phased pin-like (a and b), elliptical (c, d and f), hexagonal (g) and lens-shaped (a, d, e, h, I, j) aqueous fluid inclusions in the salt of Weymouth-A45 well.

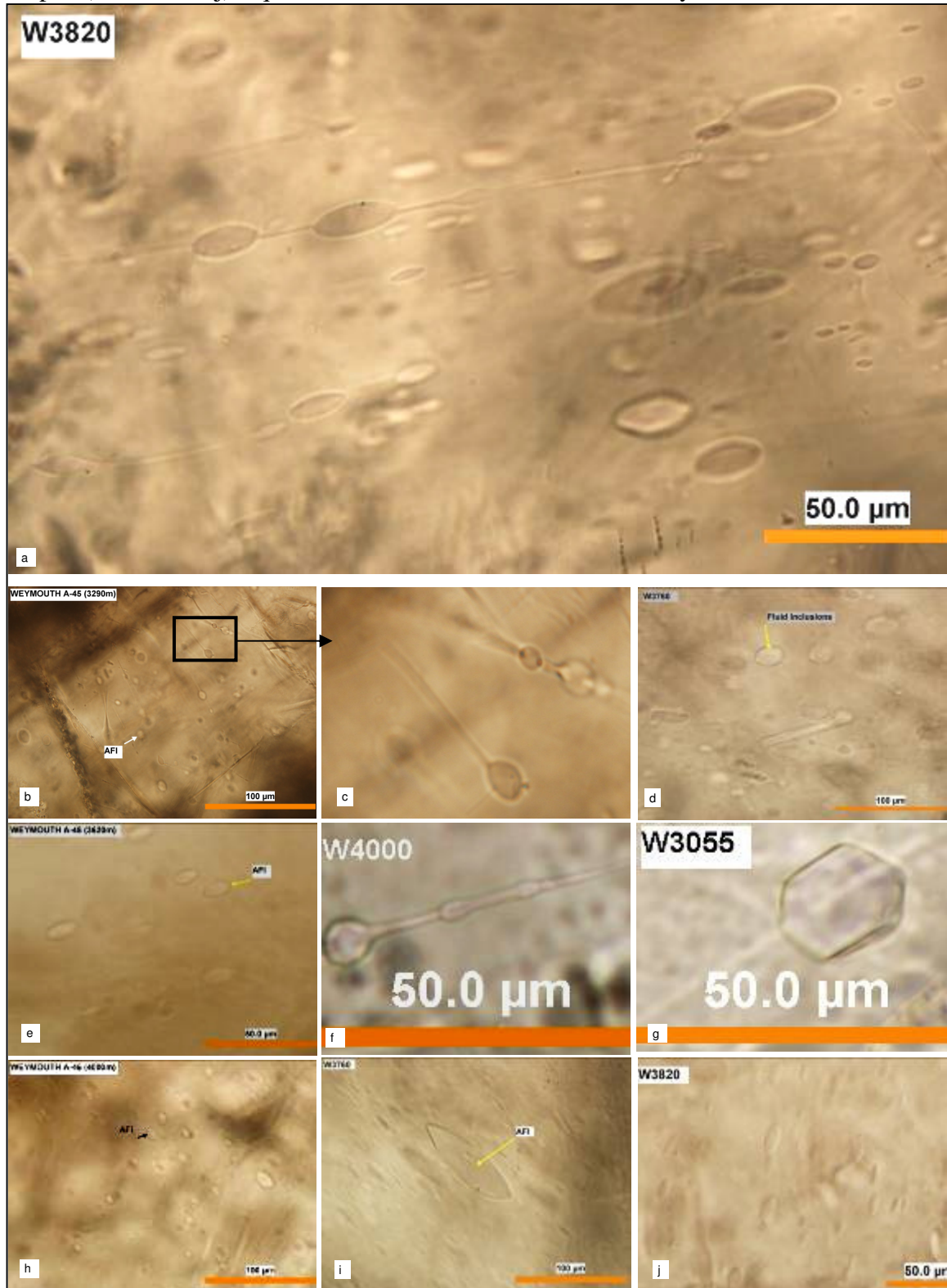
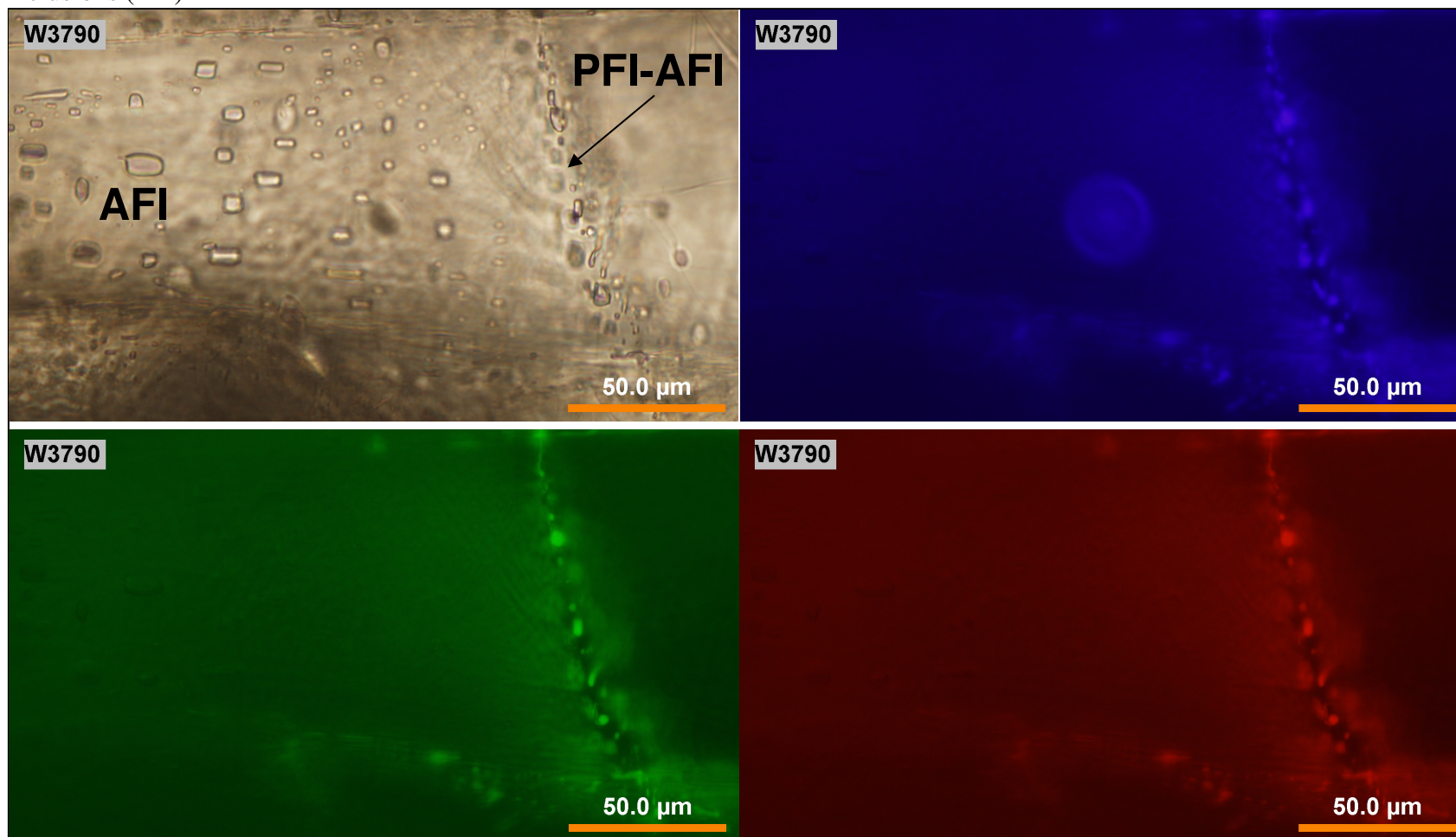


Fig. 23b: One-phased rectangular aqueous fluid inclusions (AFI) in the salt of Weymouth-A45 well. Side by side with petroleum fluid inclusions (PFI)



2. Secondary Petroleum and Petroleum-Aqueous Fluid Inclusions

These secondary fluid inclusions are more common than the primary looking aqueous ones. They are usually but not always follow linear features in the halite crystals and concentrated along micro-fractures (Fig. 21). They have various shapes (rectangular, tubular, spindle-like, cylindrical, needle-shaped, network and many other irregular shapes) (Fig. 24). They are either clear in color or with faint yellowish brown to dark brown tint liquid and dark colored gas bubbles. Some of these inclusions contains only petroleum in liquid or gas phase and in most cases both petroleum and aqueous phases coexist together in the same inclusions but distinctly separated as immiscible phases (Fig. 24 and 25). They exist as one-, two-, three- and four-phased inclusions (Fig. 25a, b and c). The hydrocarbon identity of these fluid inclusions is reflected in the bright fluorescent behavior of its liquid part under UV light as well as under green and red lights of the visible spectrum. The size of PFIs is variable but mostly range between 10-20 μ m in average and occasionally have longer dimensions reaching 0.2-0.3 mm (Fig 26). These inclusions are common and have been found in almost all studied samples as inclusions of secondary origin developed under burial conditions along cleavage and fracture planes and spread into the structure of halite crystals (Fig. 27). The secondary origin of these inclusions is evident from their mode of occurrence as they usually form within or close to linear features such as healed fractures (Fig. 28). They are much more numerous and varietals than those found in the salt of Glooscap-C63 well.

The multi-phased PFI are more common than the one-phased ones and more distinct. They are characterized by their petroleum liquid part occurring as distinct immiscible phase within the aqueous part (Fig. 25) and usually containing very fine grained solid impurities. The number of petroleum spots within the API-PFIs varies between one to five (Figures 24, 25 and 29). The origin and identity of the dust like solid particles within the petroleum part is unknown and could be degraded petroleum products or petroleum-generating bacteria or algae. The AFI-PFIs of the Glooscap-C63 salt also contain these tiny solid particles but the main difference is that the petroleum liquid part does not form a distinct immiscible phase with boundaries within the aqueous phase as it is the case in the Weymouth-A45 salt (Fig. 12). In many cases the

petroleum part of these AFI-PFIs is more dominant than their aqueous counter-parts (Fig. 25b- e and f); in these cases where the fluid inclusions are relatively large in size the solid impurities within these petroleum parts are much more prominent and obvious than those found in inclusions of smaller size (Fig. 24). In some cases the petroleum spots within these inclusions look clear with no obvious impurities (Figures 25a-f, 24b-a, and 24c-f). These petroleum phases are characterized by their strong and bright fluorescence standing out of the surrounding non-fluorescent aqueous phases (Figures 25, 28 and 29). The one-phased PFIs are usually clear and do not contain tiny solid impurities as it is usually but not always the case with the multi-phased PFIs; and also they show bright fluorescence in UV and visible light spectrums (Fig. 25a and 30). The PFI some times exist as assemblages while in many other cases they occur together with the multi-phased AFI-PFI (Fig. 30). Representative images for the petroleum fluid inclusions found in Weymouth-A45 well salt samples are presented in Figure 27 and more examples are given in Figures 28 to 34 to show some of their detailed features.

Fig.24: Petroleum fluid inclusions of various shapes and characters in the Argo salt of Weymouth-A45 well.

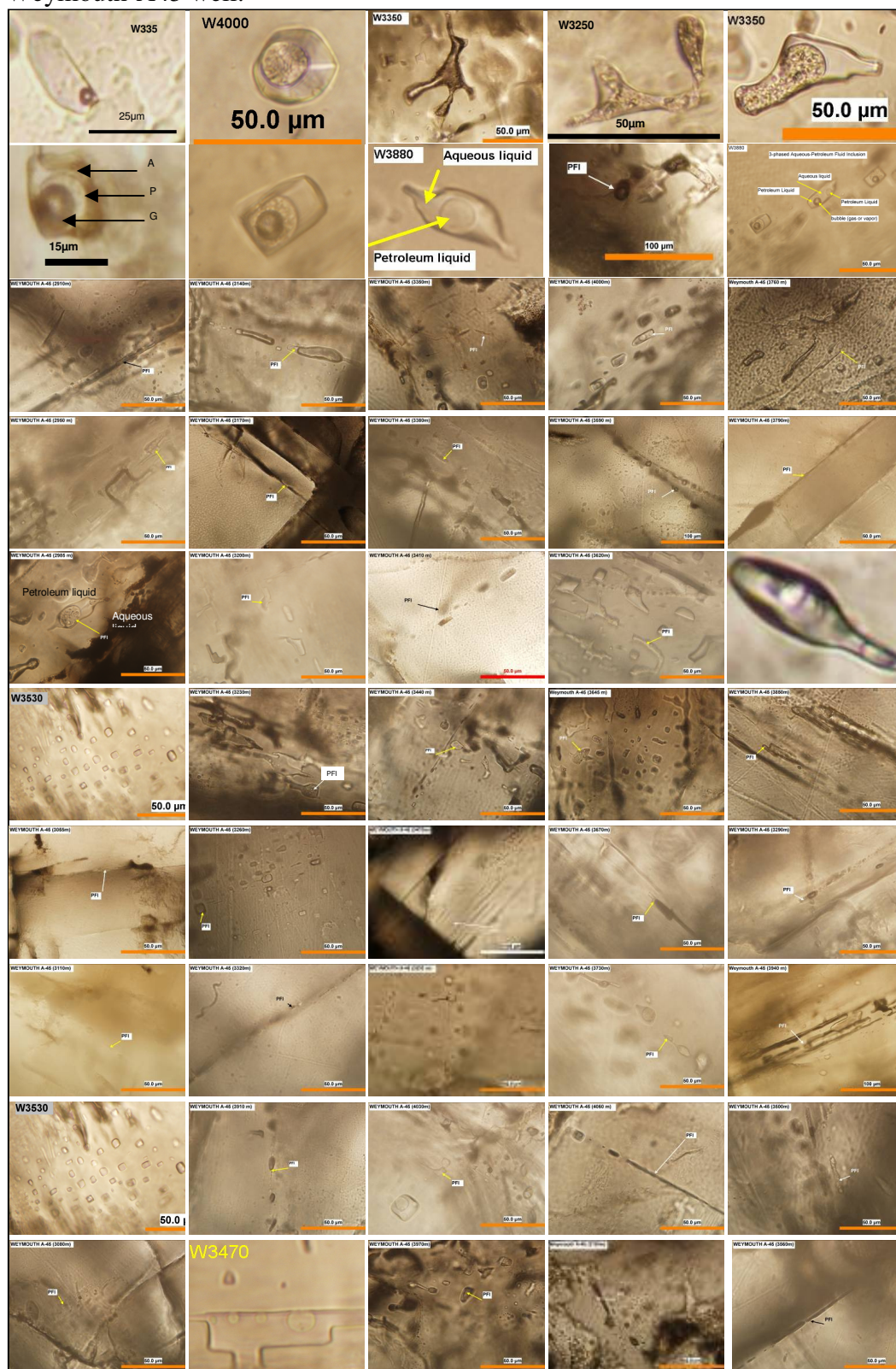


Fig. 25a. Petroleum fluid inclusions showing one- and two-phased types.

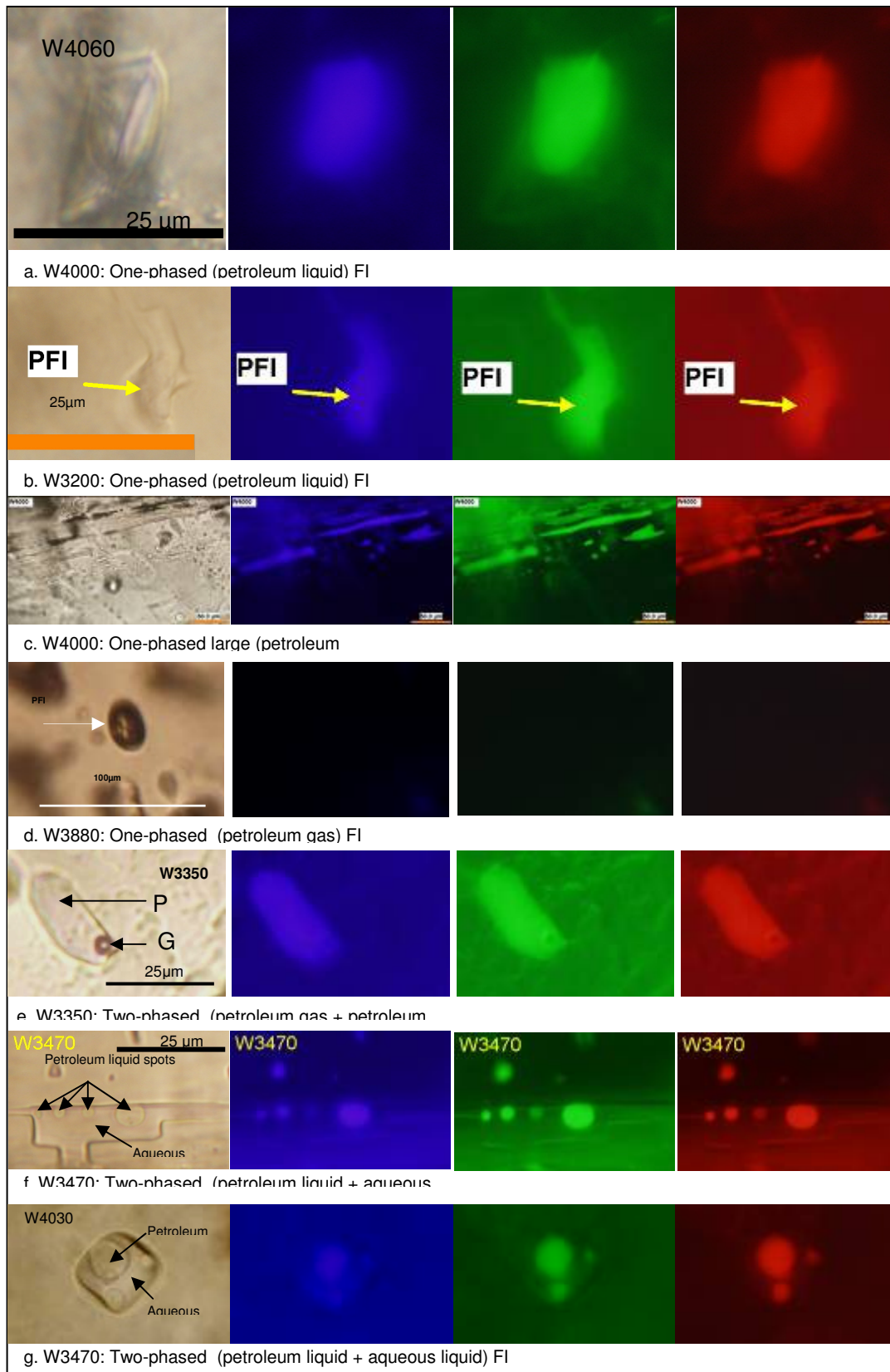


Fig. 25b. Petroleum fluid inclusions of two- and three-phases types (A = aqueous; P = petroleum)

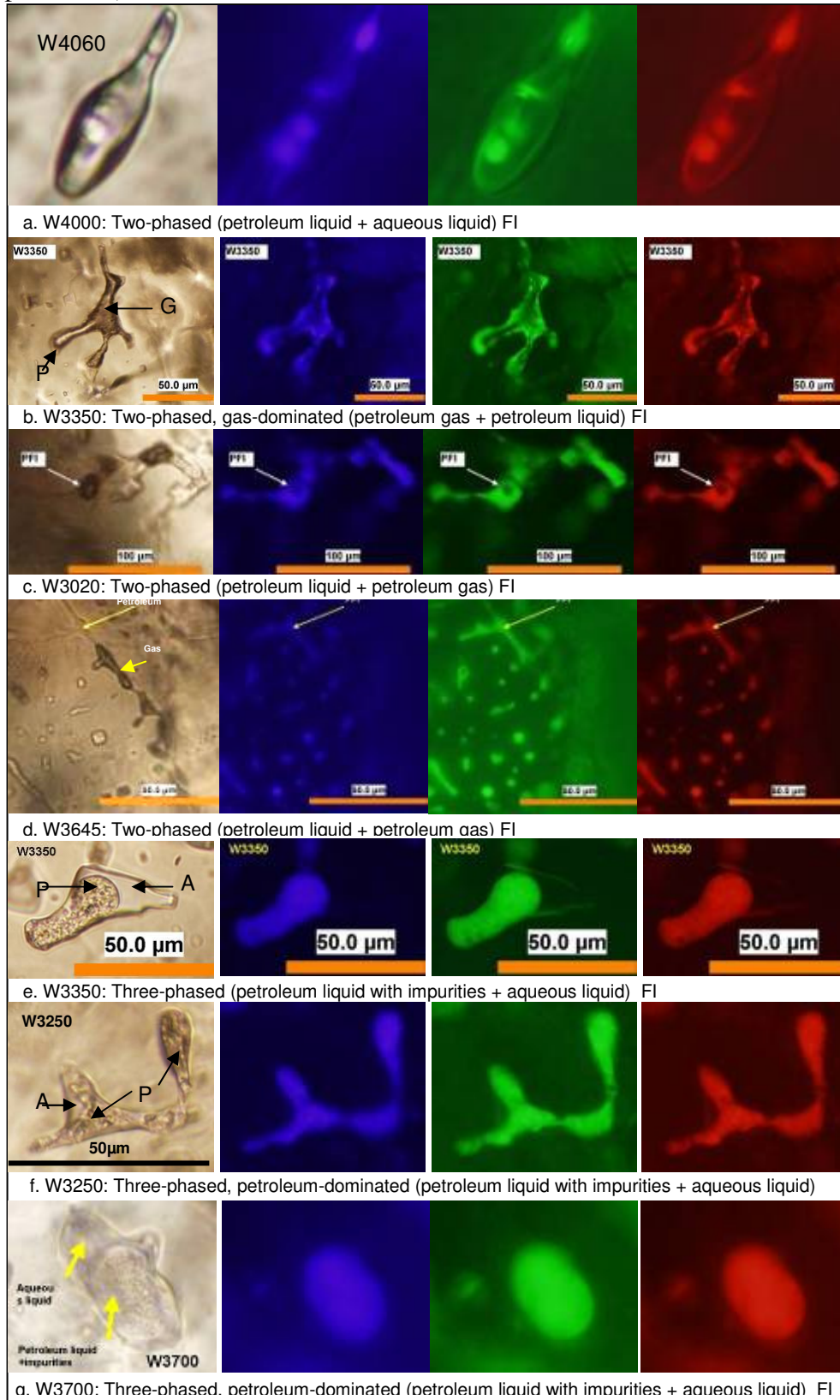


Fig 25c. Petroleum fluid inclusions showing three- and four-phased types

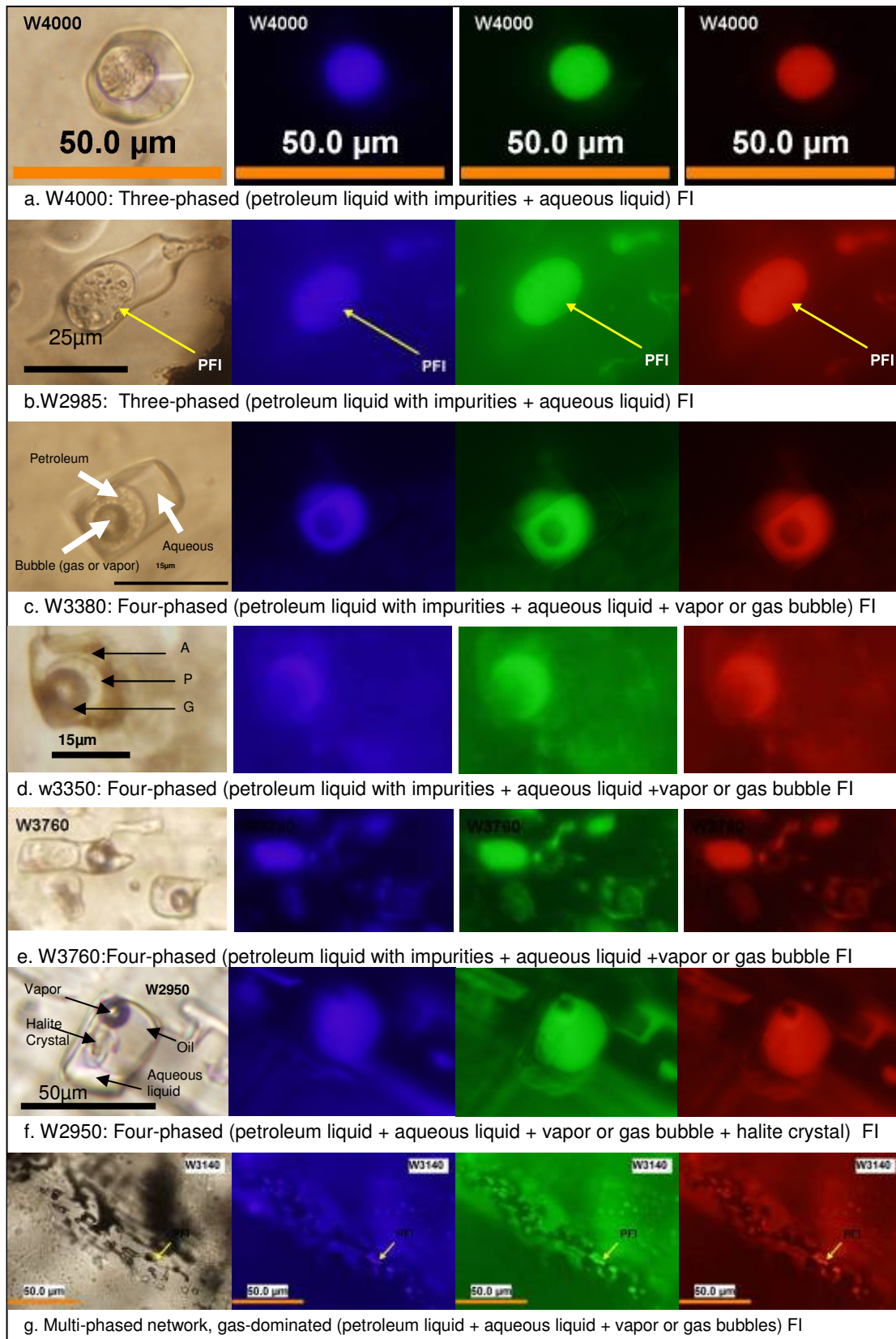


Fig. 26: A very long pin-shaped, three-phased aqueous-petroleum-vapor or gas fluid inclusion (A = aqueous; P = petroleum; G = gas or vapor).

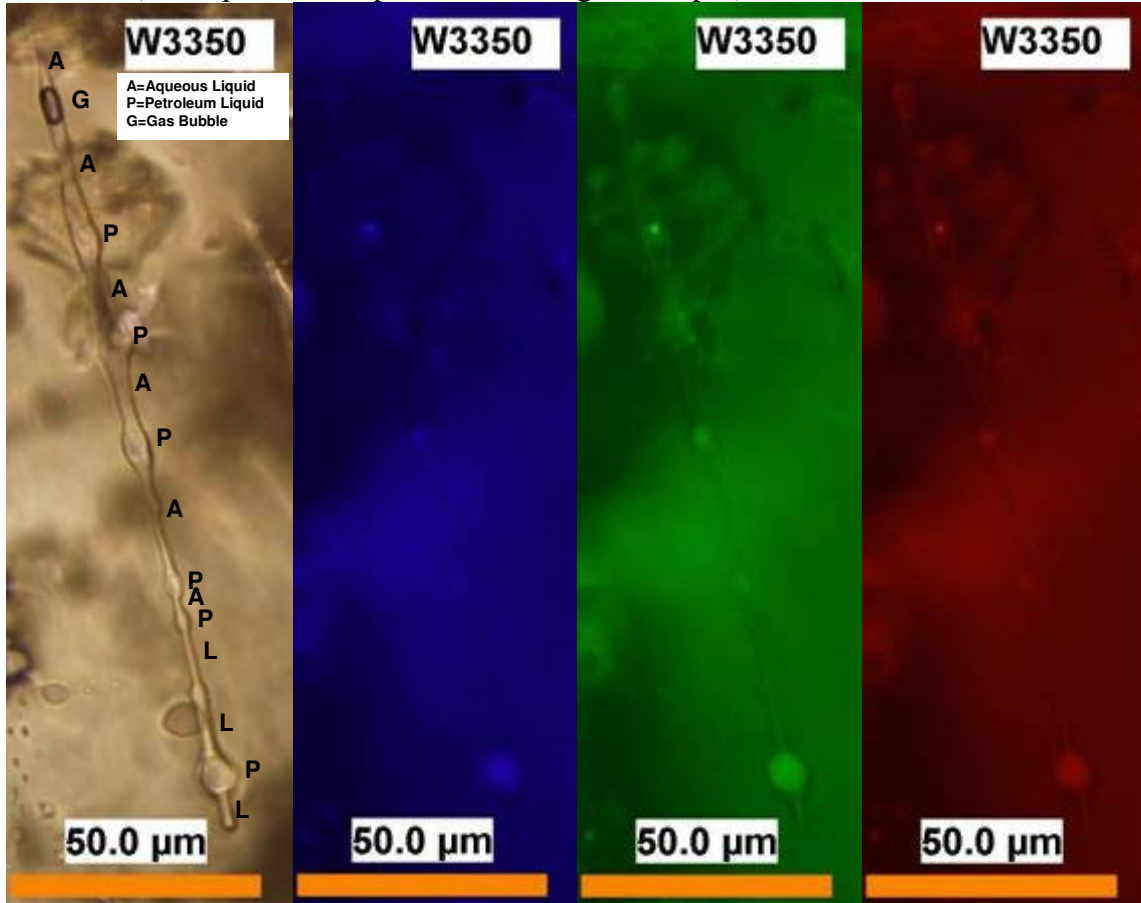


Fig. 27a: Representative images of petroleum fluid inclusions in the studied samples. The colored images show fluorescence of liquid petroleum in UV, green and red light.

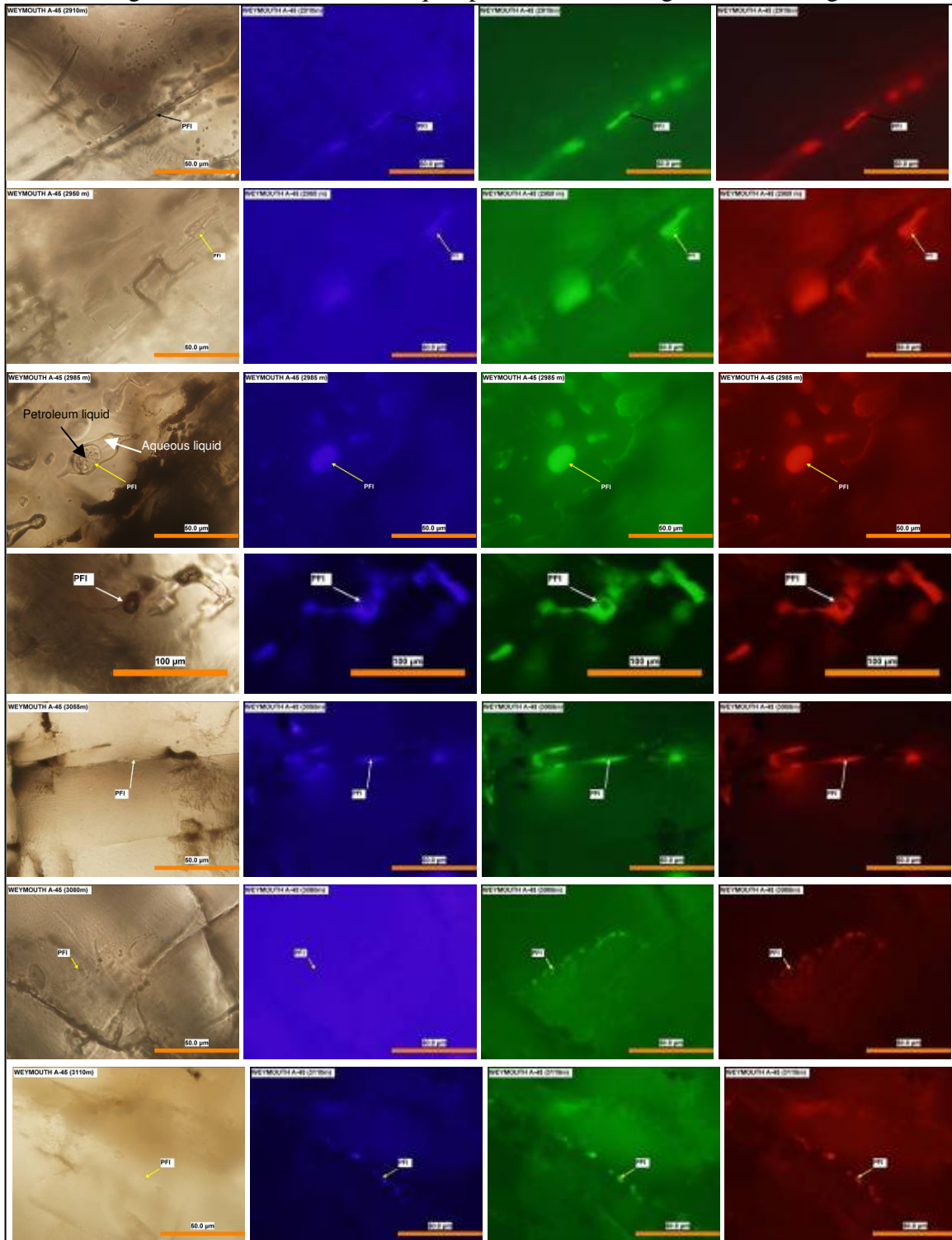


Fig. 27b: Representative images of petroleum fluid inclusions in the studied samples. The colored images show fluorescence of liquid petroleum in UV, green and red light.

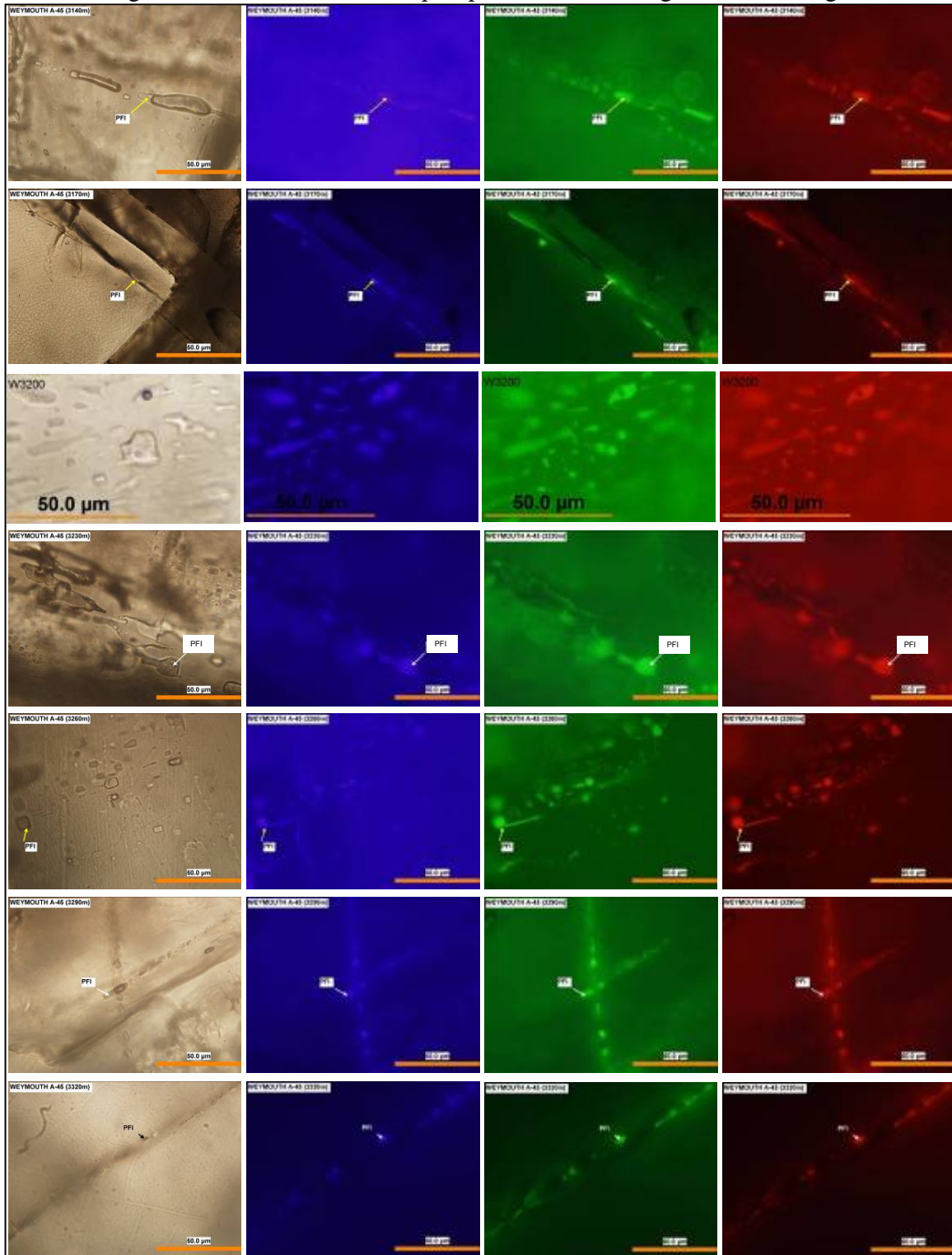


Fig. 27c: Representative images of petroleum fluid inclusions in the studied samples. The colored images show fluorescence of liquid petroleum in UV, green and red light.

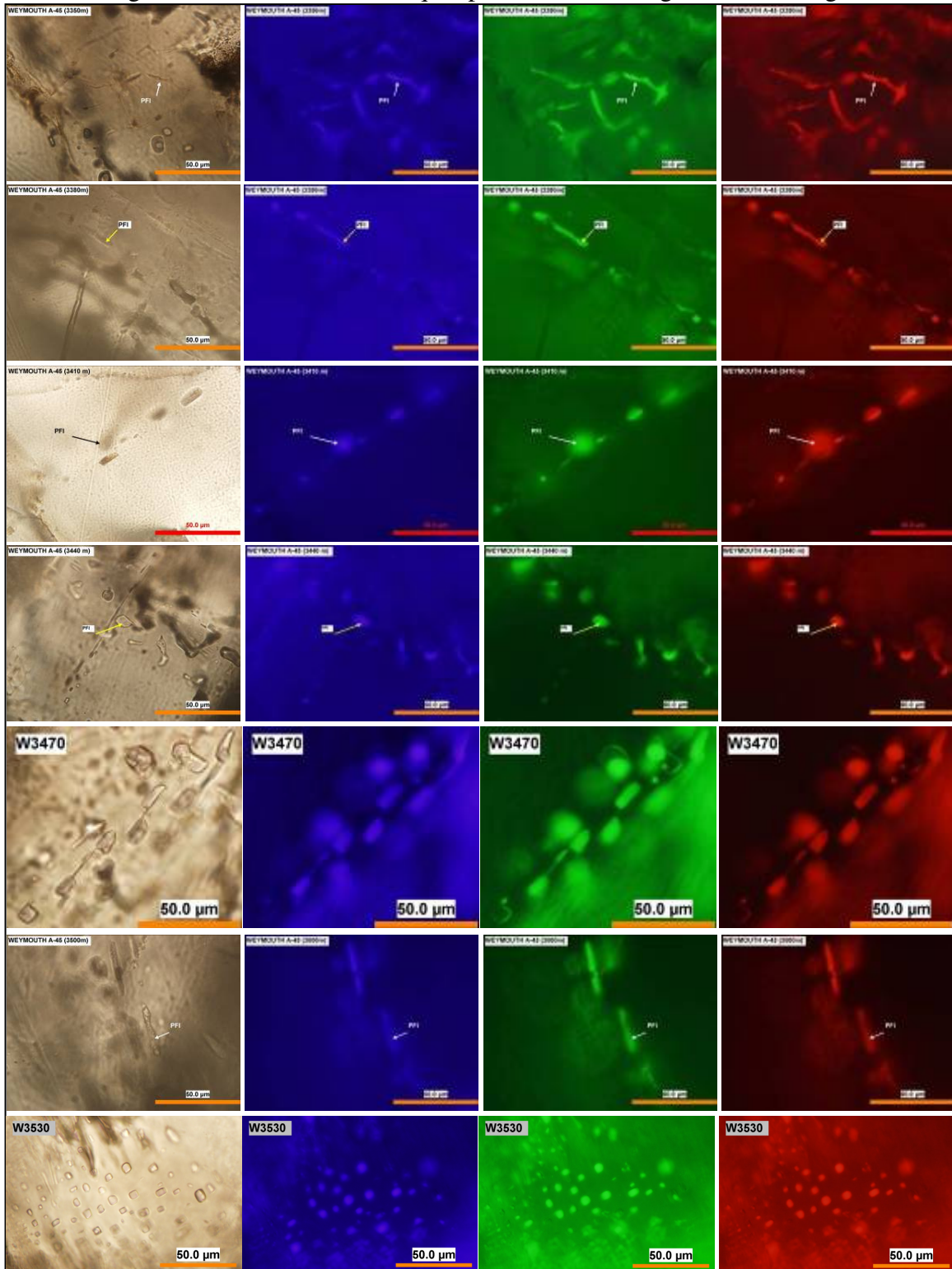


Fig. 27d: Representative images of petroleum fluid inclusions in the studied samples. The colored images show fluorescence of liquid petroleum in UV, green and red light.

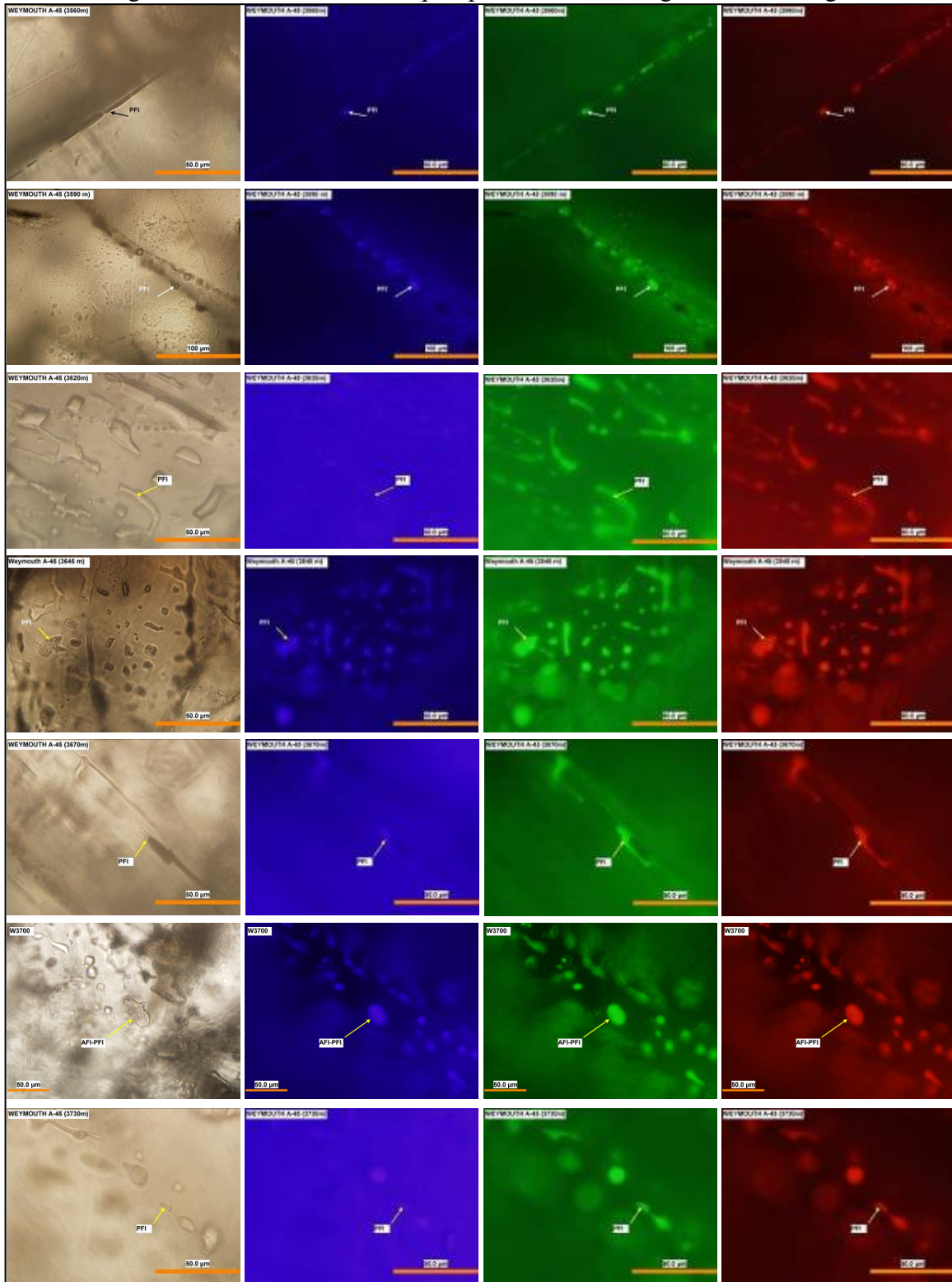


Fig. 27e: Representative images of petroleum fluid inclusions in the studied samples. The colored images show fluorescence of liquid petroleum in UV, green and red light.

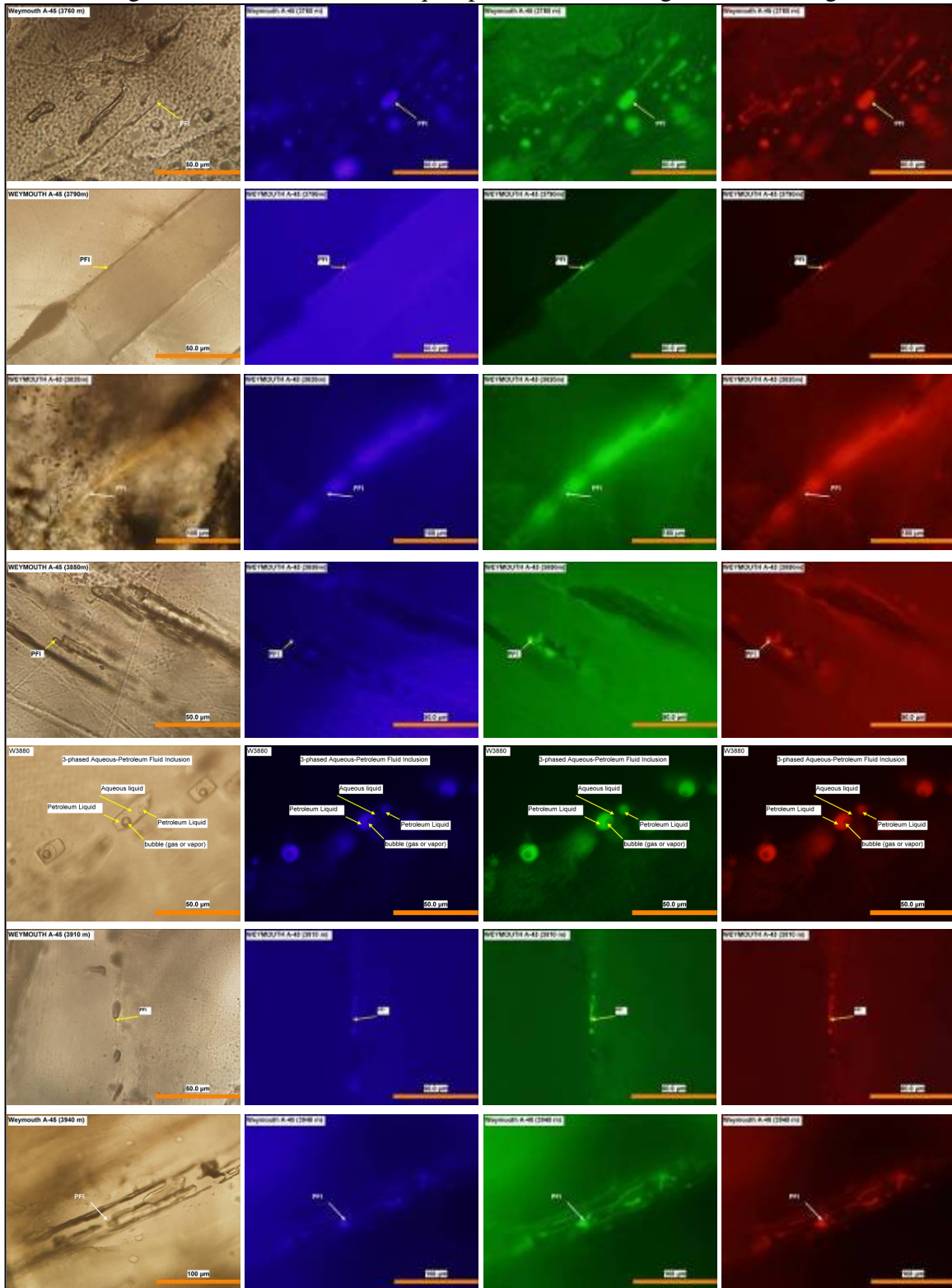


Fig. 27f: Representative images of petroleum fluid inclusions in the studied samples. The colored images show fluorescence of liquid petroleum in UV, green and red light.

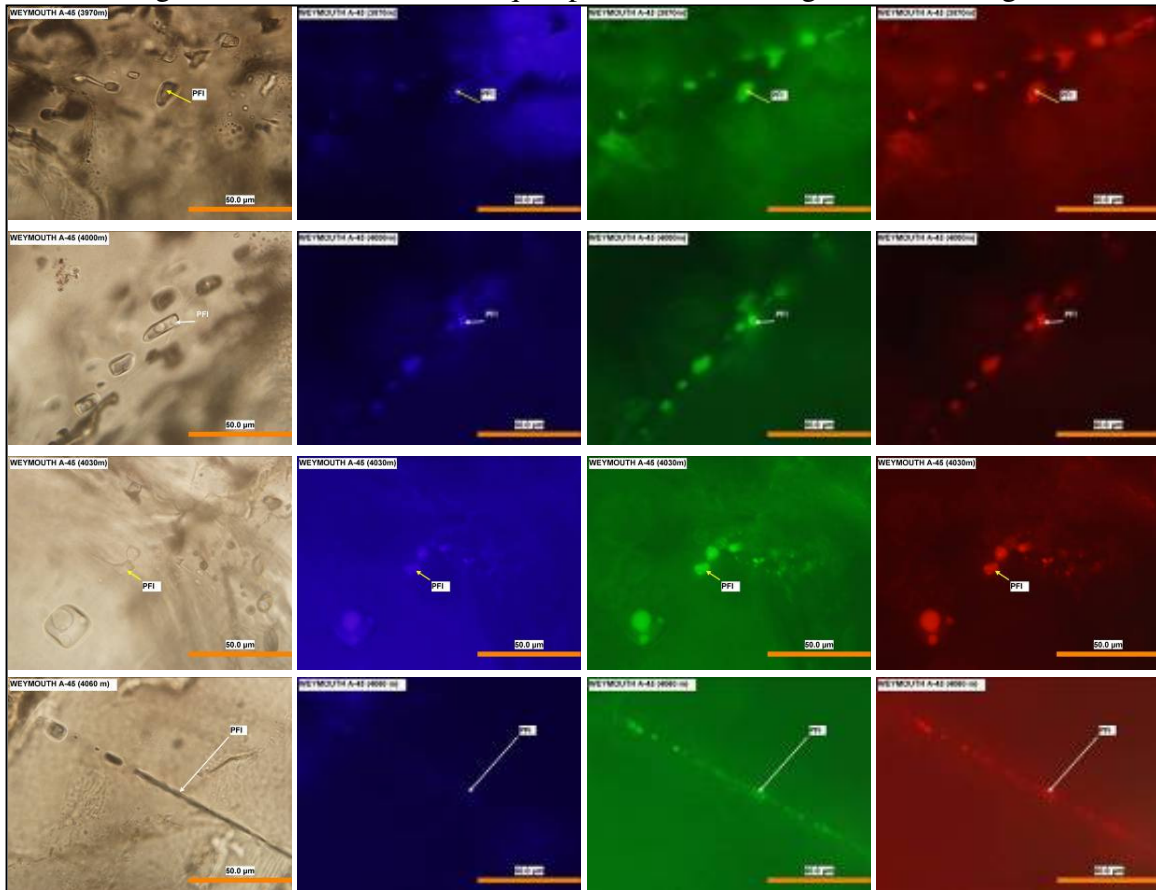


Fig. 28a: One-phased and two-phased petroleum fluid inclusions showing linear pattern of distribution in the salt of Weymouth-A45 well.

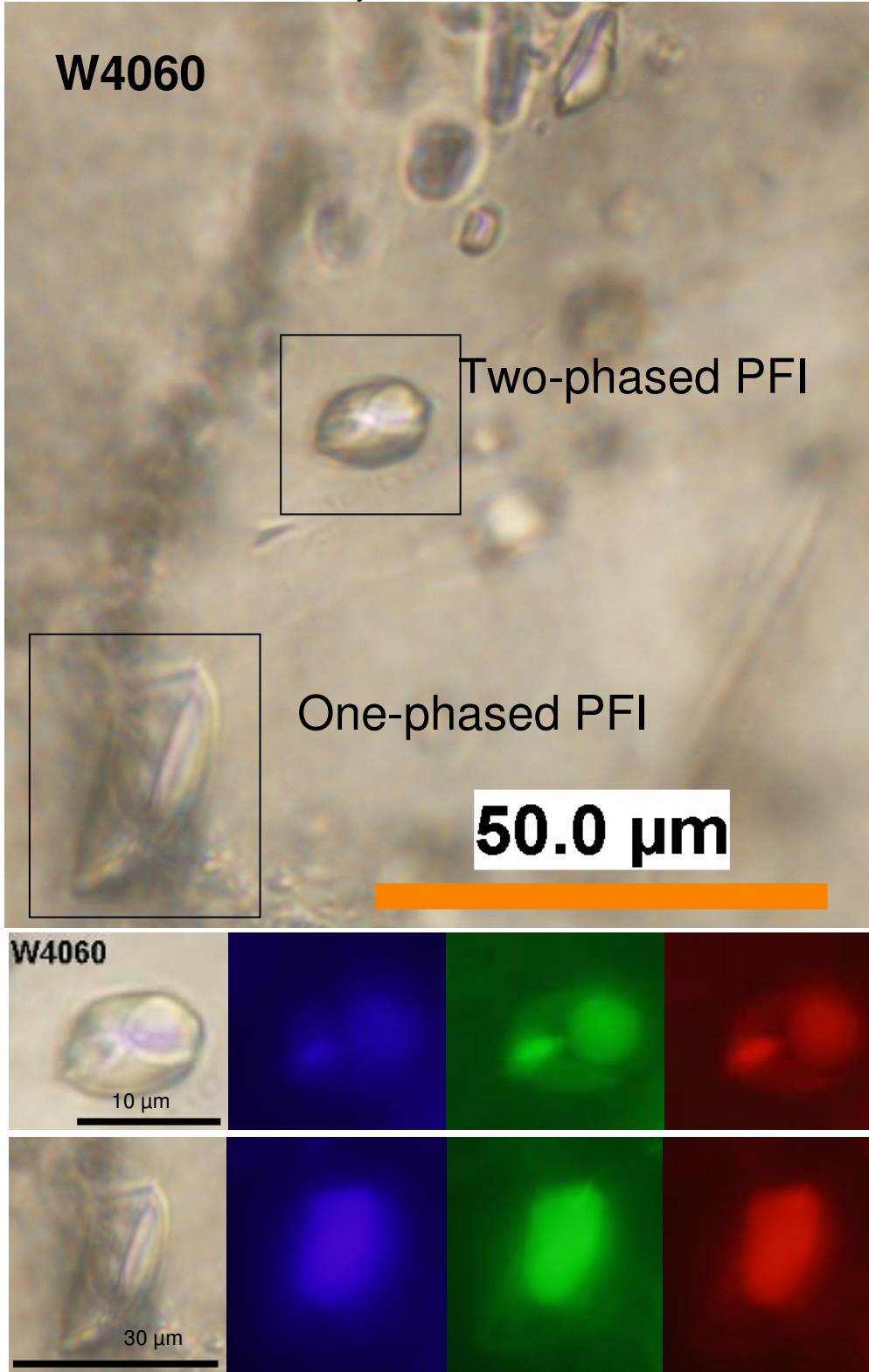


Fig. 28b: Two-phased petroleum-aqueous fluid inclusions showing linear pattern of distribution in the salt of Weymouth –A45 well.

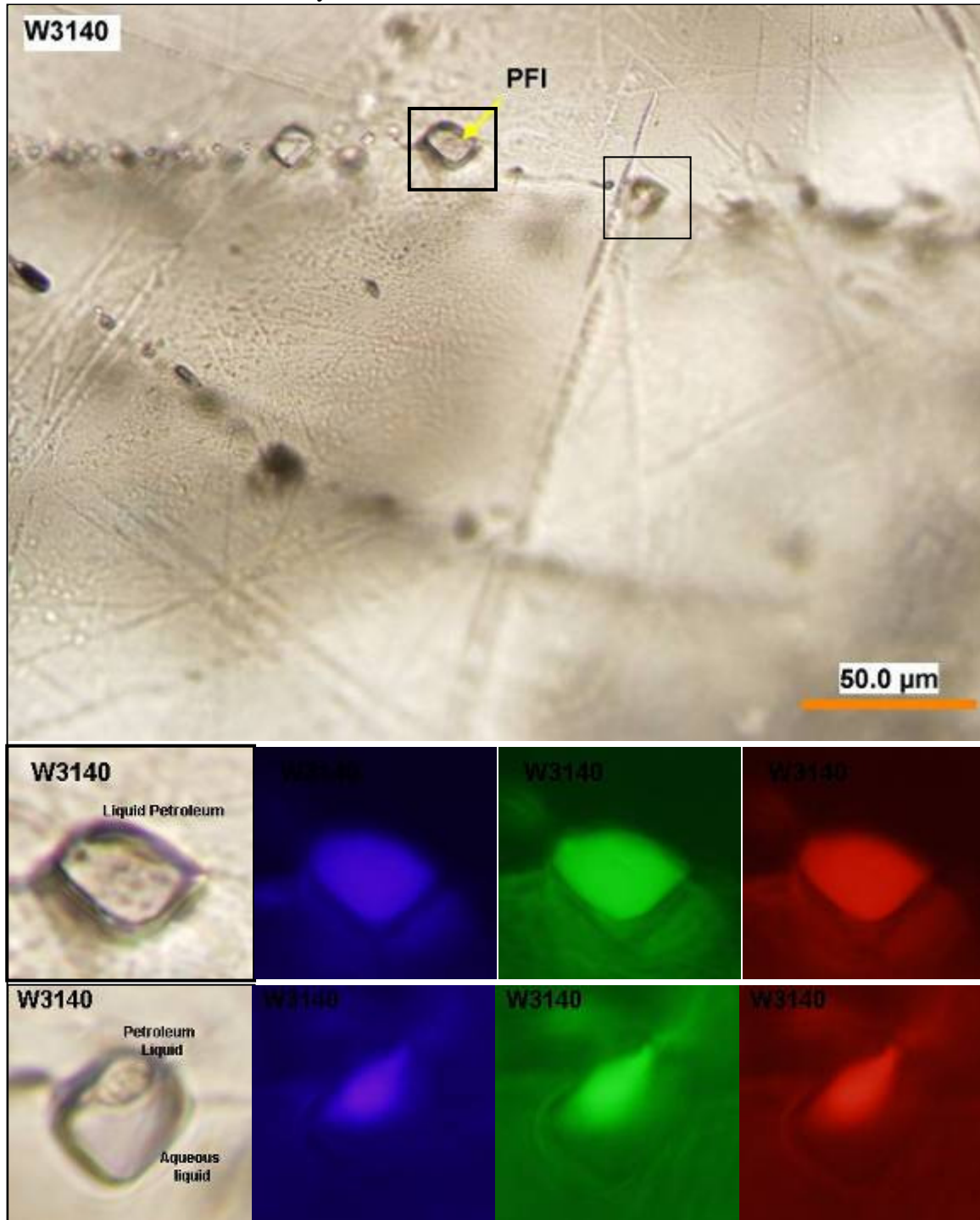


Fig.29: Irregular-shaped aqueous-petroleum fluid inclusion showing 5 (top) and 3 (bottom) separate spots (rings) of liquid petroleum within the aqueous liquid.

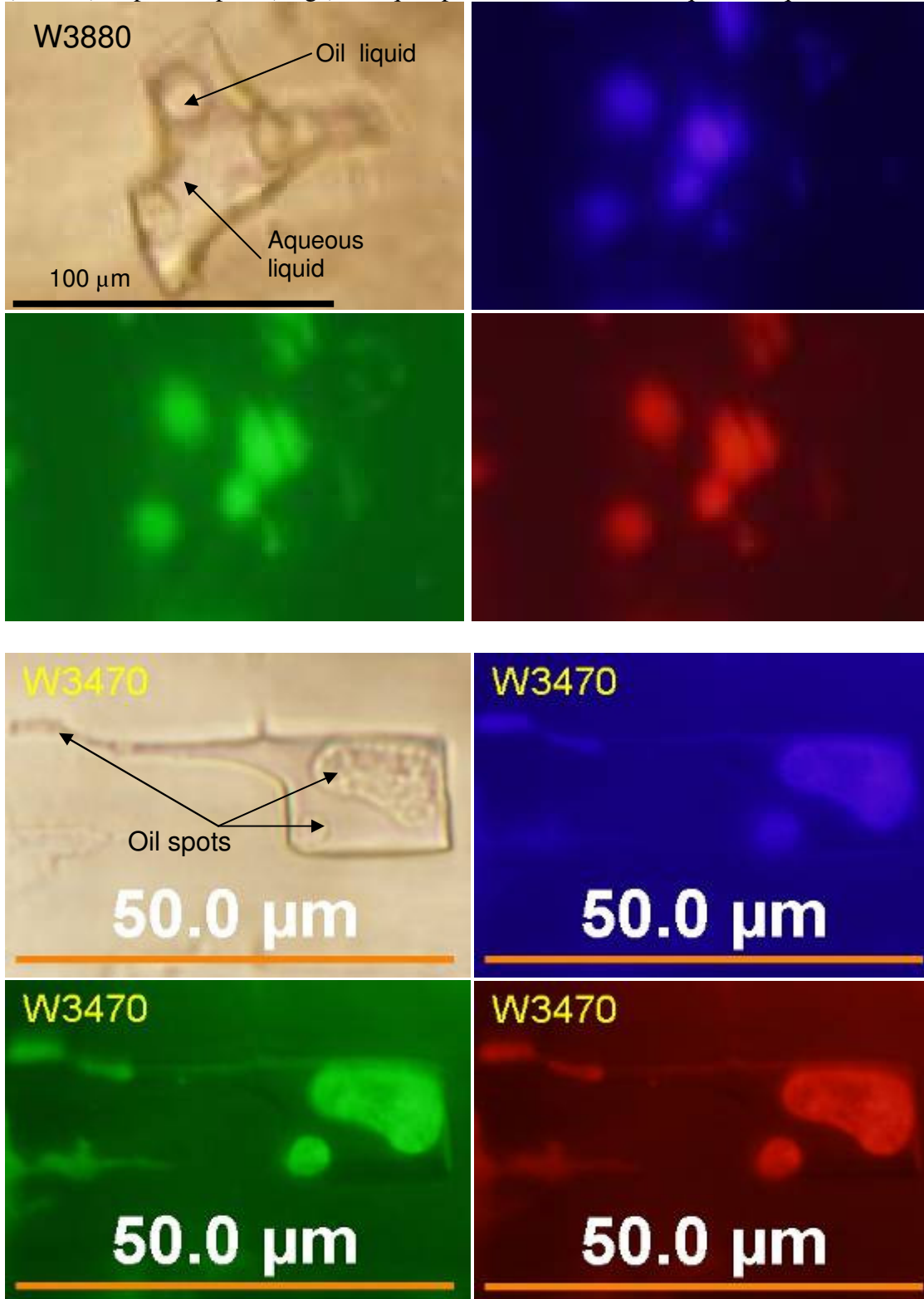


Fig. 30: Mode of occurrence of PFI and AFI-PFI. They either exist alone as assemblages or together in the same sample.

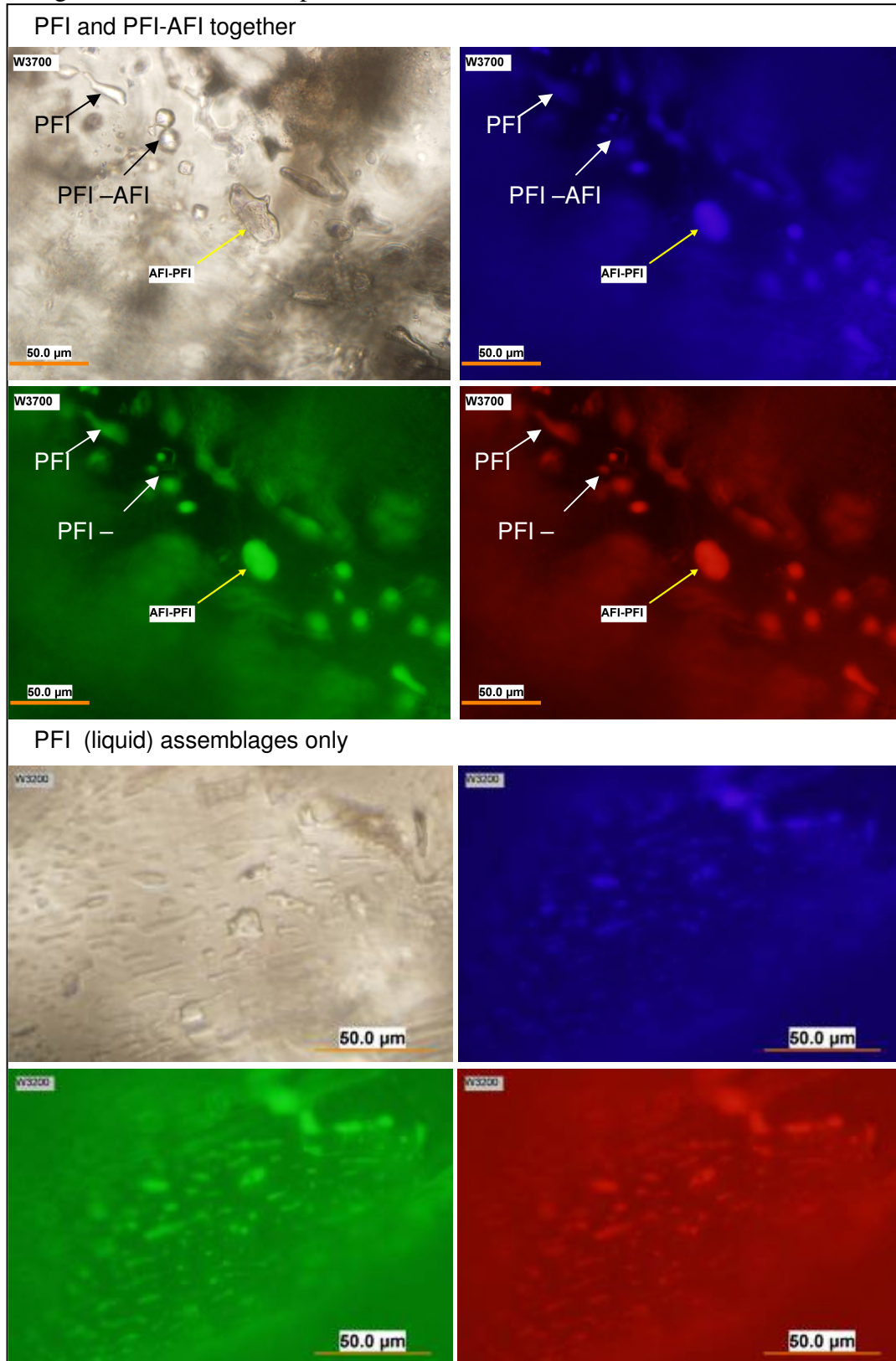


Fig. 31: Petroleum-bearing fluid inclusions showing linear elongate nature (top) and orientation of many small inclusions along dissected fractures (bottom).

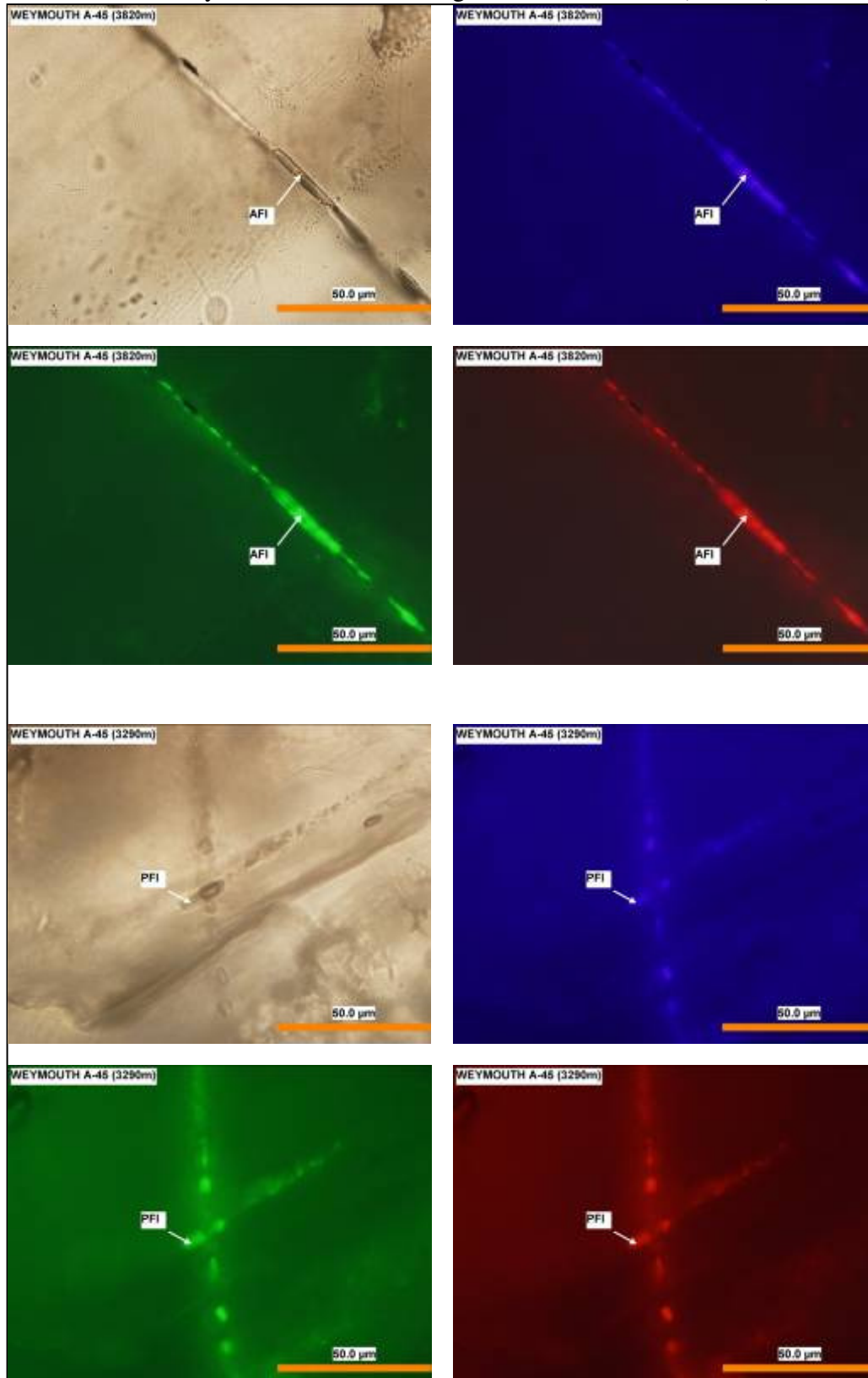


Fig. 32: Gas-dominated petroleum-bearing fluid inclusions showing elongate net-like pattern and fluorescence of the minor liquid part only as thin rims around gas bubbles.

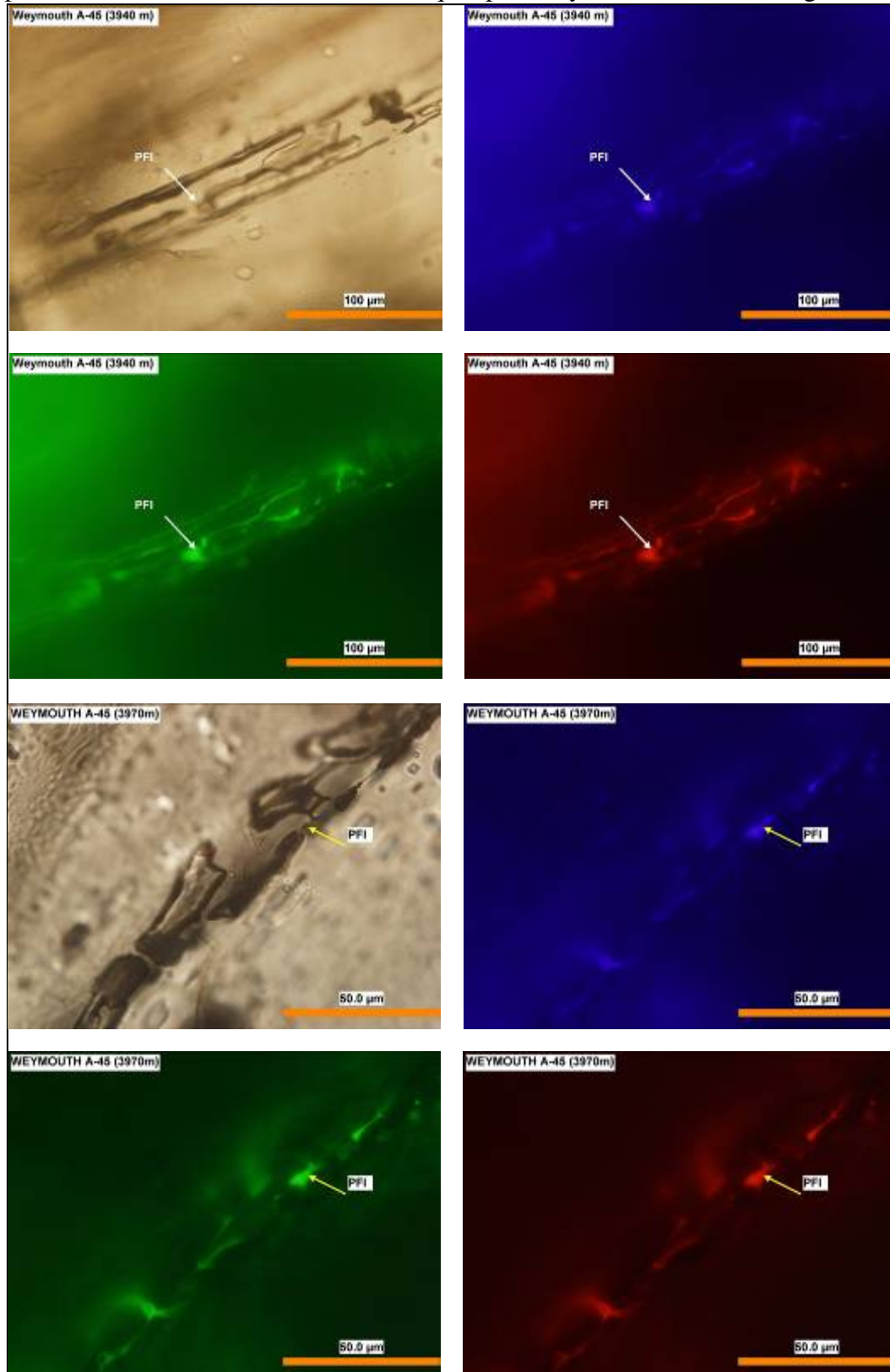


Fig. 33: One and multi-phased petroleum-bearing fluid inclusion assemblages with no obvious relation to fractures; however they are probably situated parallel to such planes of weaknesses which can not be seen in such images for this reason.

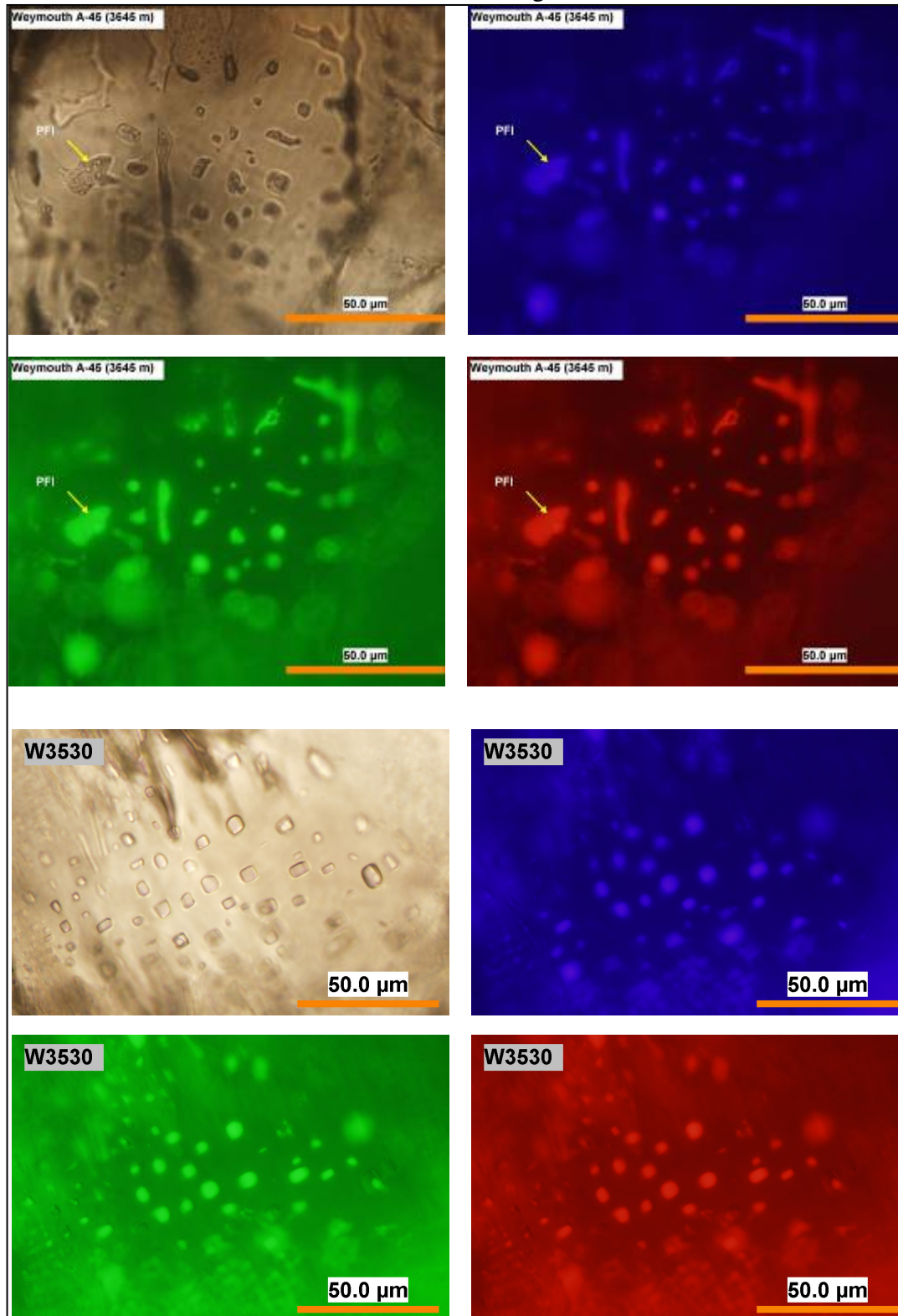
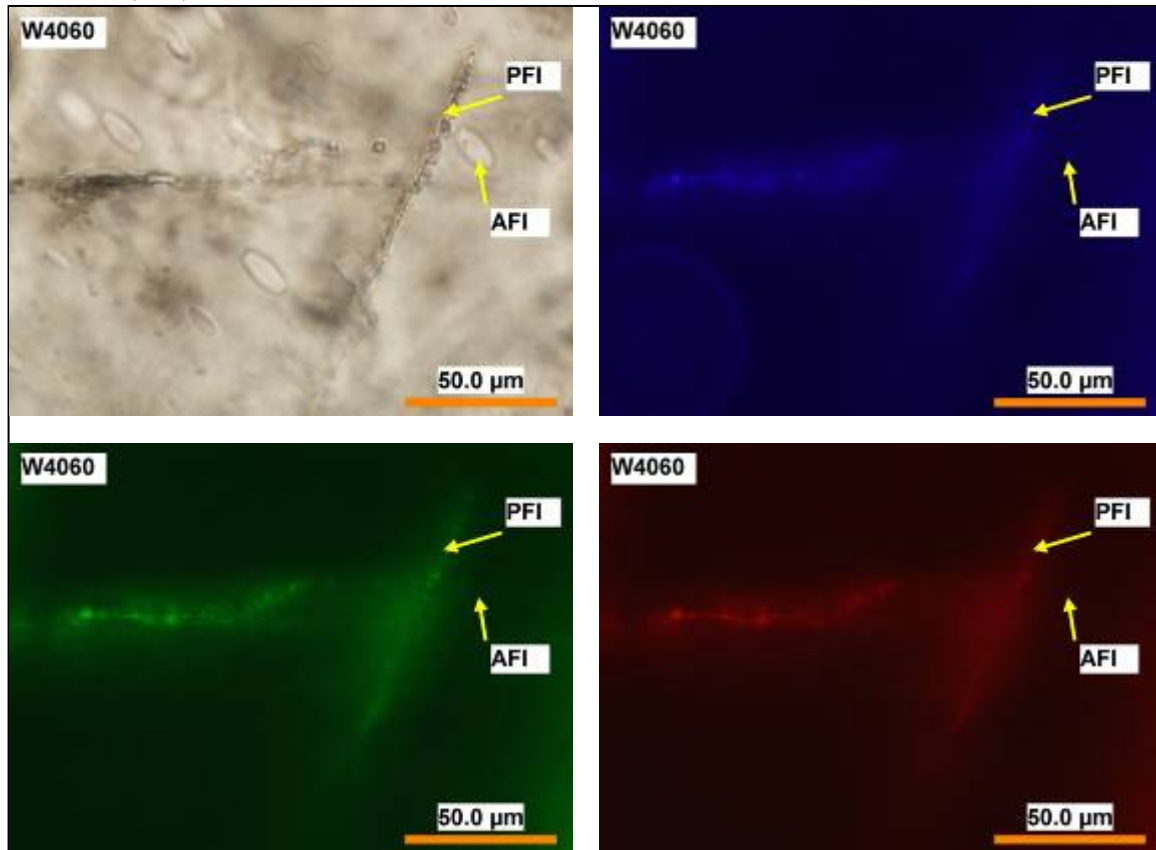


Fig. 34: Oval shaped aqueous fluid inclusions (could be of primary or secondary origin) (AFI) side-by-side with secondary petroleum fluid inclusions oriented along dissecting fractures (PFI).



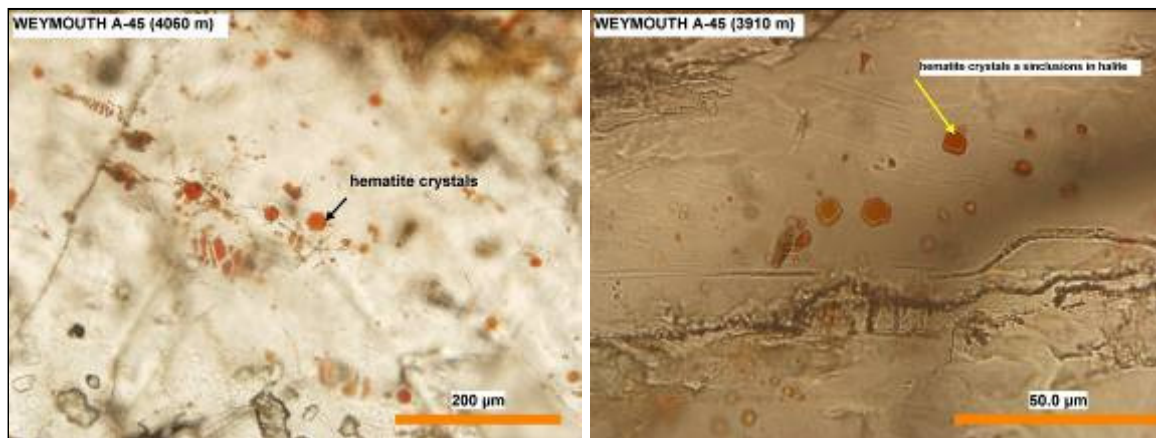
3. Other inclusions

In addition to the aqueous and petroleum fluid inclusions, the salt samples of Weymouth-A45 well also contain a number of other inclusions similar to those found in the salt samples of Glooscap-C63 well. These inclusions are hematite crystals and iron stains, evaporate crystals (anhydrite), rarely quartz crystals and some lubricant-like liquids.

a. Hematite crystal inclusions

Perfect six-sided euhedral small crystals of hematite are common in Weymouth-A45 salt (Fig. 35). Similar hematite crystals are also common within the salt of Glooscap-C63 well. (Fig. 15).

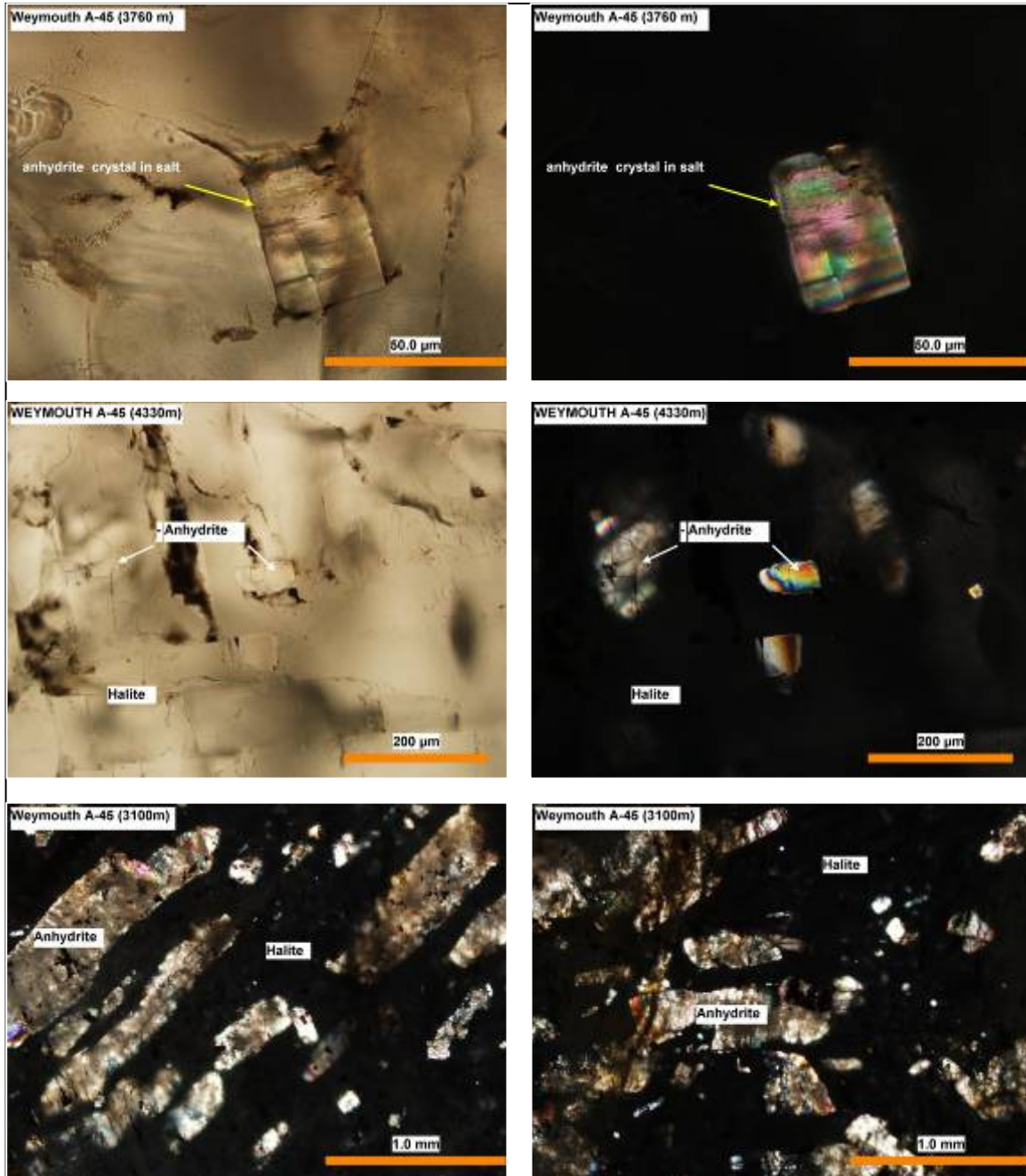
Fig. 35: Euhedral hematite crystals as inclusions in the Weymouth-A45 salt



b. Anhydrite crystal inclusions

Anhydrite crystals are very common within the halite crystals of Weymouth-A45 salt (Fig. 36). These crystals are relatively large in size (up to 0.5 mm in length) and constitute an important portion of the salt volume. The high content of anhydrite within this salt is the main reason of non-transparent, cloudy (buff colored) and waxy appearance of the salt which makes it different than the salt of Glooscap-C63 well (Figures 2, 19 and 36). It has also made the salt slightly harder and not easily cleavable for study in the same way as Glooscap-C63 well's salt behaved. For these reasons, the salt chips have to be smoothed, flattened, grinded and/or polished to make it possible for microscopic studies. In many cases the anhydrite crystals show parallel alignment within the salt (Fig. 36) as an indication of their earlier crystallization during deposition and then sinking through the salty water which was subsequently depositing halite crystals. The salt of Glooscap-C63 also contains anhydrite but of much smaller size and quantity than that of Weymouth-A45 samples; it can be detected as an insoluble residue when a salt chip is dissolved (Fig. 16).

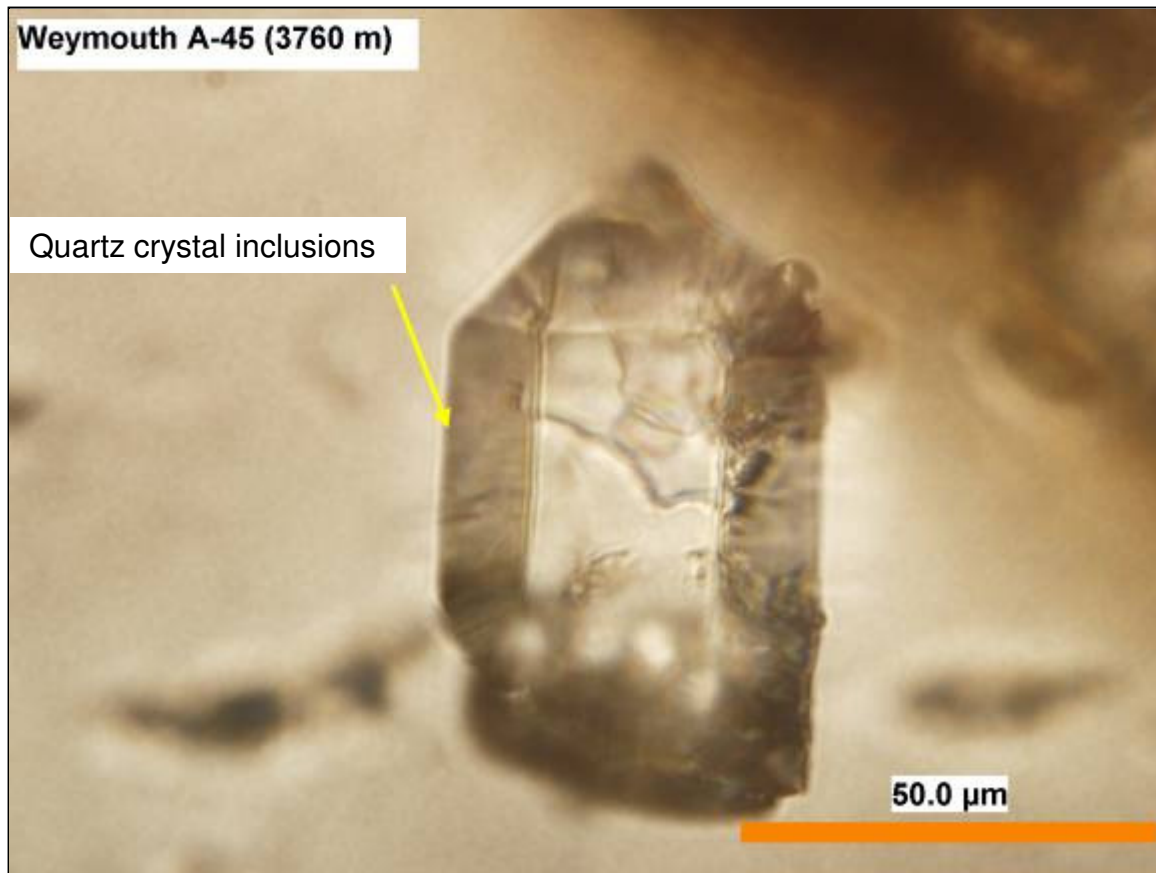
Fig. 36: Anhydrite crystal inclusions in Weymouth A-45 salt. The dark images are taken under crossed polars showing the isotropic nature of halite and anisotropic behavior of anhydrite.



c. Quartz crystal inclusions

Quartz crystal inclusions can also rarely be found within halite of Weymouth-A45 well. These crystals are very well developed euhedral crystals (Fig. 37) of obviously detrital origin brought to the site of salt depositional environment from nearby land areas. The perfect shape of the crystal with no broken tips and edges suggests that the source rocks were very close to the site of deposition which did not require much transportation. Similar quartz crystals were also observed in the salt samples of Glooscap-C63 well (Fig. 17).

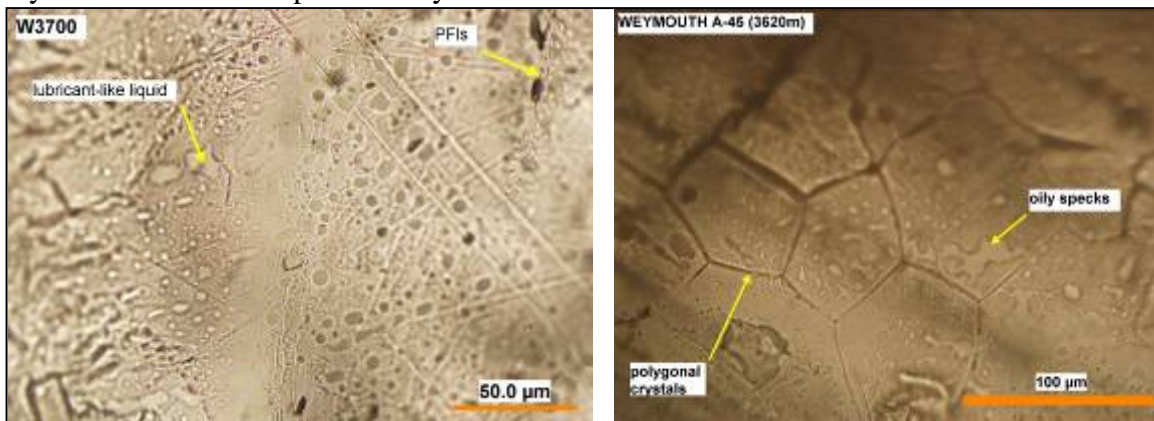
Fig. 37: Perfect euhedral crystal of quartz as inclusion in salt of Weymouth-A-45 well.



d. Lubricant-like liquid

Lubricant-like liquids are common within the salt along cleavage surfaces (Fig. 38). The identity of these fluids is not certain as they normally do not show fluorescence but have lubricant-like, oily appearance. They are probably liquids spilled over from fluid inclusions along cleavage planes and spread on the surface of salt chips. These fluids are also common in the Glooscap-C63 salt samples.

Fig. 38: Lubricant-like liquid along cleavage planes and on the surface of the halite crystals in the salt samples of Weymouth-A45 well.



MICROTHERMOMETRY

Microthermometric fluid inclusion study can be used to give useful data on trapping conditions only if they satisfy “Roedder’s Rules” (Roedder, 1984; Bodnar, 2003). These roles are (1) the fluid inclusion must trap a single homogeneous phase, (2) the inclusions must remain a constant volume (isochoric) system after trapping (excluding reversible elastic volume changes), and (3) nothing has been added or removed from the inclusion following trapping event (Bodnar, 2003). Reequilibration which can occur naturally during burial or uplift of the host rock or during sample preparation and/or laboratory studies such as microthermometry must also be taken into consideration during interpretation of fluid inclusions study results for constructing thermobaric history of the host rocks (Bodnar, 2003). Reequilibration means that the fluid inclusion has changed volume (stretched), or some material have been added or removed from the inclusions following trapping process. Evaporites are generally considered to be the weakest rocks in the sedimentary basins (Davison, 2009). The hardness of halite is 2.5 on Mohs Scale which is equivalent to that of fingernail. Tugarinov and Naumov (1970) (in Bodnar, 2003) are the first to note a direct relationship between the mineral hardness and the ease with which the included fluid inclusions reequilibrate; they recognized a linear relation between the hardness of many minerals and the pressure required to decrepitate fluid inclusions in them. For this reason halite which can easily reequilibrate (naturally or during study) is considered by many fluid inclusionists a problematic mineral during microthermometric studies and the results must be dealt cautiously.

Taking all the above mentioned facts into consideration, twenty one samples from Glooscap-C63 and eighteen samples from Weymouth-A45 wells were studied microthermometrically (Table 6). The results for Glooscap-C63 well proved that the aqueous liquids whether they are petroleum-bearing or not, belong to $\text{H}_2\text{O}-\text{NaCl}$ ($\pm\text{CH}_4$) system and in rare cases also to $\text{H}_2\text{O}-\text{NaCl}-\text{KCl}$ ($\pm\text{CH}_4$) system; while those of Weymouth-A45 well proved to belong to $\text{H}_2\text{O}-\text{MgCl}_2-\text{NaCl}$ ($\pm\text{CH}_4$) and/or $\text{H}_2\text{O}-\text{CaCl}_2-\text{NaCl}$ ($\pm\text{CH}_4$). These studies further confirmed earlier results of fluorescence microscopic studies in proving the existence of both aqueous and petroleum fluid inclusions in both studied wells.

1. Microthermometry of the fluid inclusions in the salt of Glooscap-C63 well

Microthermometric studies performed on twenty two samples covering all intervals along the intersected salt proved the existence of a variety of fluid inclusions. These inclusions are aqueous (AFI), aqueous-petroleum (AFI-PFI) and petroleum (PFI) (Figures 11 and 12, and Table 7). The aqueous and aqueous-petroleum fluid inclusions are generally belonging to $\text{H}_2\text{O}-\text{NaCl}$ ($\pm\text{CH}_4$) and rarely to $\text{H}_2\text{O}-\text{NaCl}-\text{KCl}$ ($\pm\text{CH}_4$) systems. The identity of petroleum fluid inclusions which are usually expected to be methane-rich could not be determined but are possibly of complex nature.

In spite of the fact that the petrographic studies showed the primary-looking nature of the aqueous fluid inclusions, the microthermometric results indicated wide spread reequilibration and or stretching (deformation) under burial conditions and/or as a result of treatment during study (cooling-heating). They usually contain large vapor bubbles which are not proportional to the size of the inclusions (Fig. 4 to 6) as a sign of reequilibration. The other sign of reequilibration is microthermometric results (Table 7 and Fig. 39) which showed very high homogenization temperatures and lower temperatures of metastable eutectic and eutectic points. The homogenization temperatures (T_h) of the AFIs which range between 110°C to 380°C with a median of 283°C and average of 282°C (Fig. 39e) can not be justified for inclusions formed from evaporating oceanic waters neither for those which were formed under burial conditions. For this reason the only explanation for such very high homogenization temperatures is reequilibration and/or deformation by stretching during burial conditions and sample treatment and microthermometric study. Apparently both reasons have contributed in the deformation of these fluid inclusions because these samples were only cleaved and then studied so there is no preparation treatments (grinding or polishing) which might slightly affect the inclusions; furthermore the size of vapor bubble looked too large even before microthermometric studies (freezing-heating). The deformation of both the vapor bubbles and of the host inclusions and accompanied phase changes during freezing and heating is indicated in figures 40a to d. The phase changes taking place indicate that these aqueous fluid inclusions belong to $\text{H}_2\text{O}-\text{NaCl}$ system as described by Roedder (1984), Bodnar (2003) and Davis et al. (1990). Upon cooling of these inclusions, they freeze at a range of -64°C to -119°C with a median of -81°C and average of -82°C (Table 7 and Fig. 39a).

Freezing is indicated by sudden color change usually to light or dark brown and less commonly to creamy white and rarely to gray (Fig. 40a to c). The color change is accompanied by the formation of granular texture composed of granular or cryptocrystalline mixture of ice and halite; or some times remain clear and glassy in texture. Upon heating following freezing process, the fluid inclusions wall become dark and thickens at a range of temperature of -51°C to -34°C with a median value of -38°C and average of -40°C as a result of initial ice melting “metastable eutectic temperature” as ice reacts with the walls of halite inclusion to produce hydrohalite crystals (Table 7 and Figures 39b and 40a to c). Irregular black patches appear and rims thicken as melting increases from the walls inward producing double-rimmed appearance; as melted area on the edges increase and become clear, the black patches move toward the center to produce a clear dark concentrated oval- or circular-shaped spot around the bubble in the core of the inclusions as an indication of eutectic phase change (Fig. 40a to c). The “eutectic temperature” ranges between -38°C to -22°C with a median of -25°C and average of -26°C (Table 7 and Fig. 39c). The eutectic point for primary aqueous fluid inclusions in salt normally takes place at -21.2 for H_2O - NaCl systems (Davis et al, 1990). The reason for the lower metastable eutectic and eutectic temperature values of the studied aqueous fluid inclusions suggests reequilibration and deformations of these inclusions which resulted in loosing their original status or due to the impure nature of the fluids which formed as secondary inclusions under burial conditions rather than keeping their primary identity as petrographic studies suggests. The other possible reason for the low eutectic temperature is the possible presence of impurities such as calcium or other divalent cations in solution (Bodnar, 2003). The possibility of the presence of calcium in these fluid inclusions is probable because the halite crystals contain anhydrite crystals as solid inclusions suggesting that the original solutions from which the halite crystals were deposited were containing calcium and possibly other cations such as magnesium. As heating continued, final melting of takes place at the “peritectic temperature” range of -6.8°C to 0°C with a median of -1.8°C and average of -2°C (Table 7 and figures 39d and 40a to c). Further heating passing the peritectic temperature, results in homogenization which takes place at very high temperatures by disappearance of the vapor bubble at a range of 110°C to 380°C with a median of 286°C and average of

282°C (Table 7 and figures 39e and 40a to c). These homogenization temperatures further support the reequilibration and deformation of these inclusions because such temperatures are neither possible for the primary fluid inclusions formed during the crystallization of halite from ocean water nor are expected for secondary fluid inclusions forming at a depth interval of ~4 to 4.5 km which is the current depth of the salt in the Glooscap-C63 well.

The large accidental aqueous fluid inclusions (Figures 5 and 40 d) which supposed to be of primary origin behave strangely. They either behave similar to those of normal aqueous fluid inclusions described above or do not show any phase changes during cooling-heating processes (Table 7 and Fig. 40d). This is due to the reequilibration and deformation which resulted in leaking of fluid out and thus filled by air with no signs of phase changes. Fig. 40d clearly shows that there are no phase changes other than changing of the size of included bubble and continuous deformation in the internal walls and change in the size and shape of the inclusion. Some of them never homogenize as indicated in the example given in Fig.40d; as the homogenization temperature approaches near 280 and the bubble became hardly visible, it grows again and continues increasing in size until the whole inclusion collapses upon decrepitation. Very few samples show daughter crystals of halite or sylvite within the aqueous fluid inclusions (Fig. 6 and Table 7); they show similar behavior to the other aqueous fluid inclusions and homogenize at very high temperatures (sample G4415).

The petroleum-aqueous fluid inclusions behave similar to the dominant aqueous inclusions described above which supposed to be of primary origin but have been reequilibrated, suggesting that all fluid inclusions have been formed/reformed and affected by the same conditions such as recrystallization at burial conditions and redistribution of liquids. These events were apparently coincidental with the generation of hydrocarbon fluids which were mixed together and heterogeneously trapped in newly formed secondary inclusions. The petrographic results support this assumption since many PFI-AFI show mixed character indicated by partial and/or heterogeneous fluorescence within the same inclusion (Fig. 11).

The pure petroleum fluid inclusions are relatively much less common than the other types which can be found in few samples in different forms along side with the aqueous fluid

inclusions (Figures 11 and 40). Many of these inclusions are two-phased and exist as elongate needle-like or narrow tubes mostly along fractures and cleavages. Others exist as pure petroleum of either liquid or gas forms indicated by their fluorescence behavior as only liquids fluoresce. Microthermotrically these PFIs do not show any of the sudden changes indicating phase changes described by Goldstein and Reynolds (1994) and mentioned earlier in the “background on fluid inclusions” of this report. These expected phase changes in the methane inclusions which form >80% of natural gases (Selley, 1998) include freezing below -190°C accompanied by sudden movement “jerk” of the gas bubble, eutectic temperature at -182.5°C indicated by instantaneous snap back of the bubble to a smooth surface status and finally homogenization at -82.1°C by the disappearance of the bubble. It was not possible to detect any of these phase changes in the studied PFIs in spite of careful observation of the bubble. The only changes was gradual increase in the size of the bubble and its deformation during cooling up to the limit temperature of -196°C, followed by gradual decrease in the bubble size and return to its original spherical shape during heating stage until final homogenization at a range of 51°C to 107°C with a median and average of 79°C (Table 7).

Table 6: Microthermometrically studied salt samples from Glooscap-C63 and Weymouth-A45 wells

Glooscap-C63 Well Samples	Weymouth-A45 Well Samples
Sample No = Depth (m)	Sample No = Depth (m)
G4135	W2950
G4185	W3055
G4195	W3140
G4205	W3200
G4235	W3260
G4245	W3350
G4275	W3410
G4300	W3470
G4315	W3530
G4335	W3620
G4355	W3700
G4375	W3790
G4385	W3820
G4405	W3880
G4415	W3910
G4445	W3940
G4465	W4000
G4485	W4060
G4505	
G4525	
G4540	
21 samples	18 samples

Table 7: Micrometric results for the fluid inclusions in the salt of Glooscap-C63 well. AFI = Aqueous fluid inclusions; PFI = Petroleum fluid inclusions; AFI-PFI = Aqueous + petroleum phases within the same fluid inclusion; AFI* = Large accidental primary fluid inclusions; T_f = Freezing Temperature; T_{im} = Metastable Eutectic (initial melting) temperature; T_e = Eutectic melting temperature; T_m = Peritectic (final melting) temperature; T_h = Temperature of homogenization; n.o.= not observed.

Sample	Type	Origin	T_f	T_{im}	T_e	T_m	T_h	Notes
4135	AFI-PFI	primary	(-66) – (-77)	-38	-24	-1.4	279-283	
	AFI	primary	(-75)	-38	-24	-1.5	280	Freezing is indicated by sudden change of color to brown
4185	AFI	primary	(-82)	-38	-25	-1.8	252-285	
	AFI	primary	(-81)	-39	-24	-1.6	292-297	
	AFI	primary	(-119) – (-128)	-49	-38	-6.8	260-261	
4195	AFI	primary	(-90) – (-118)	-40	-27	-5.1	301-305	
4205	AFI*	primary	n.o.	n.o.	n.o.	n.o.	n.o.	AFI*: Large accidental FI
4235	AFI	primary	(-67)	-39	-30	0	240	
4245	AFI	primary	(-91) – (-96)	-37	-27	-2.9	281-290	
	AFI*	secondary	(-81)	-39	-24	0	252-259	The shape of FI changed a lot during cooling-heating process
4275	AFI	primary	(-72)	-51	-25	-2.1	280	
4300	PFI	secondary	n.o.	n.o.	n.o.	n.o.	107	
	AFI	primary	(-71) – (-86)	-42	-25	-2.9	110-164	
	AFI*	primary	(-95)	-47	-27	-1	121	AFI*: Large accidental FI
4315	AFI	primary	(-76)	-38	-28	-1	280	Normal AFI
4335	AFI*	primary	(-84)	-70	n.o.	n.o.	n.o.	AFI*: Large accidental FI
	AFI	primary	(-72)	-41	-31	-3	291	
	AFI -PFI	secondary	(-75)	-50	-28	-4	>380	
4355	AFI*	primary	n.o.	-39	-25	n.o.	n.o.	AFI*: Large accidental FI
4375	AFI	primary	(-75)	-34	-24	-0.3	320	
4385	AFI-PFI	secondary	(-91) – (-95)	-37	-27	-3.5	286-288	

4405	PFI	secondary	n.o.	n.o.	n.o.	n.o.	51	
	AFI	primary	(-70)	-40	-24	-1.6	259	27C (halite disappeared) and 259C bubble disappeared
4415	AFI-3p	primary	(-69) – (-84)	-38	-23	-1.9	256-270	3-phased NaCl-KCl-H ₂ O system. Sylvite daughter crystals melted at 70-90C (mostly at 74C).
	AFI-3p	primary	(-77) – (-87)	-38	-27	-2	280-312	
4445	AFI-PFI	secondary	(-64) – (-76)	-37	-24	-3	286	
4465	AFI	primary	(-84)	-40	-23	-1.3	302	
	AFI*	primary	(-113)	-47	-26	-4.8	338	AFI*: Large accidental FI
4485	AFI	secondary	(-84)	-38	-25	-1	334	
4505	AFI	primary	(-92) – (-106)	-36	-27	-1.8	362	
	AFI	primary	(-95)	-38	-27	-1.6	360	
4525	AFI	primary	(-83)	-38	-24	-1.9	308-313	
	AFI	primary	(-81) – (-91)	-38	-26	-1.8	136	
	AFI	primary	(-70) – (-77)	-38	-22	-0.4	314-320	
4540	AFI	primary	(-96)	-38	-27	-2.9	352-360	
	AFI-PFI	secondary	(-90)	-38	-22	0	360	
Median	AFI and PFI-AFI		-81	-38	-25	-1.8	286	
Average			-82	-40	-26	-2	282	
Minimum			-119	-51	-38	-6.8	110	
Maximum			-64	-34	-22	0	380	
Median	PFI		n.o.	n.o.	n.o.	n.o.	79	
Average			n.o.	n.o.	n.o.	n.o.	79	
Minimum			n.o.	n.o.	n.o.	n.o.	51	
Maximum			n.o.	n.o.	n.o.	n.o.	107	

Fig. 39a: Histogram of freezing point temperatures (T_f) versus depth in the fluid inclusions of Glooscap-C63 well. T_f average = -82°C ; median = -81°C ; minimum = -119°C ; maximum = -64°C

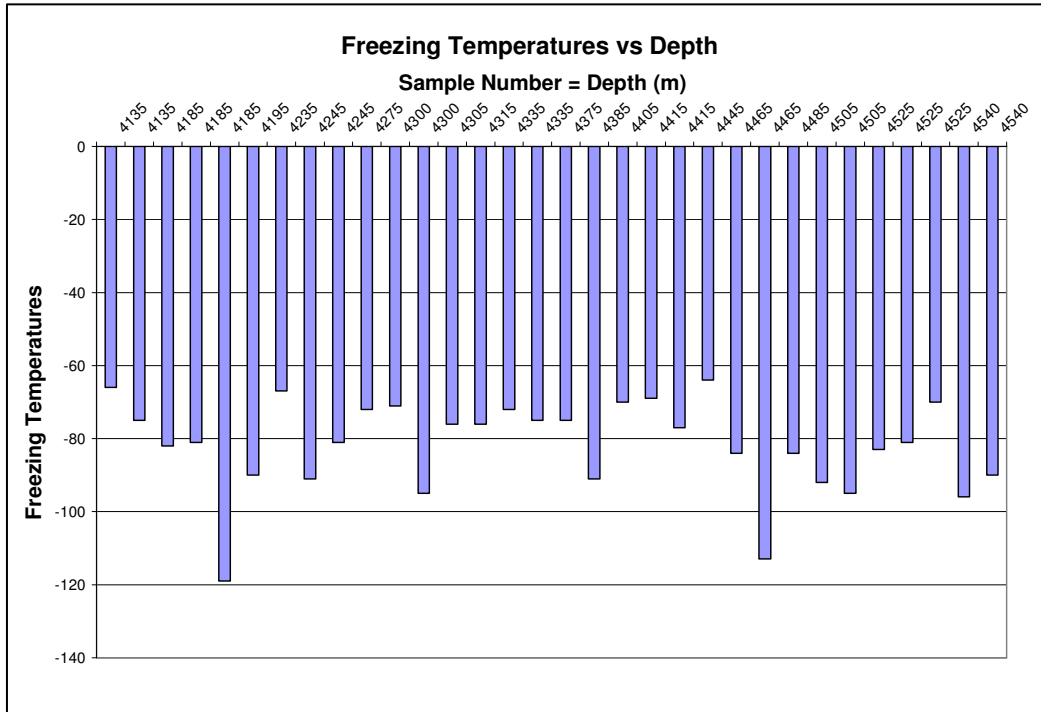
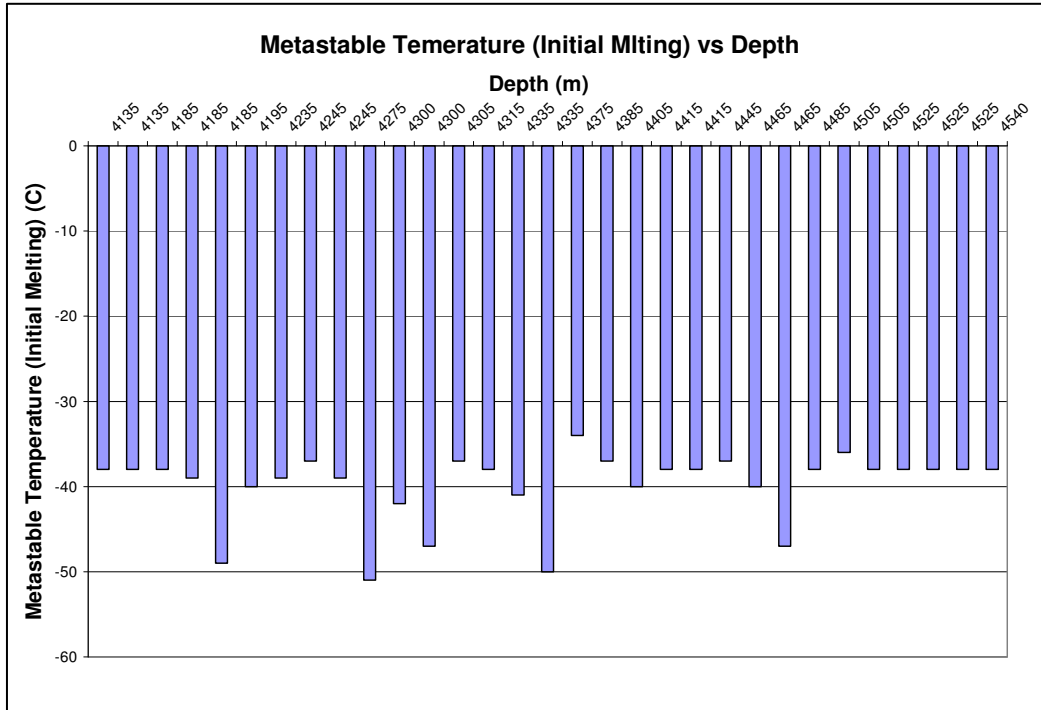


Fig. 39b: Histogram of metastable eutectic temperatures (initial melting - T_{im}) versus depth in the fluid inclusions of Glooscap-C63 well. T_{im} average = -40°C ; median = -38°C ; minimum = -51°C ; maximum = -34°C



Eutectic Temperature vs Depth

Depth (m)	Eutectic Temperature (C)
4135	-24
4135	-24
4185	-25
4185	-24
4185	-38
4185	-27
4195	-27
4195	-30
4235	-27
4245	-24
4245	-25
4275	-25
4275	-27
4300	-27
4300	-25
4305	-28
4315	-31
4335	-24
4335	-28
4375	-27
4385	-24
4405	-23
4415	-27
4415	-24
4445	-23
4465	-26
4465	-25
4485	-27
4485	-27
4505	-24
4505	-26
4525	-26
4525	-22
4525	-27
4540	-27

Peritectic Temperature (Final Melting) vs Depth

Depth (m)	Peritectic Temperature (Final Melting) (°C)
4135	-1.4
4135	-1.5
4135	-1.8
4185	-1.6
4185	-6.8
4185	-5.1
4195	-2.9
4235	-2.9
4245	-2.1
4245	-2.9
4275	-1.0
4300	-1.2
4300	-1.3
4305	-1.0
4315	-3.0
4335	-4.0
4335	-0.3
4375	-3.5
4385	-1.6
4405	-1.9
4415	-2.0
4415	-3.0
4445	-1.3
4465	-4.8
4465	-1.0
4485	-1.8
4505	-1.6
4505	-1.9
4525	-1.8
4525	-0.4
4525	-2.9
4540	-2.9

Fig. 39e: Histogram of homogenization temperatures (T_h) versus depth in the fluid inclusions of Glooscap-C63 well. T_h average = 282°C; median = 283°C; minimum = 110°C; maximum = 380°C

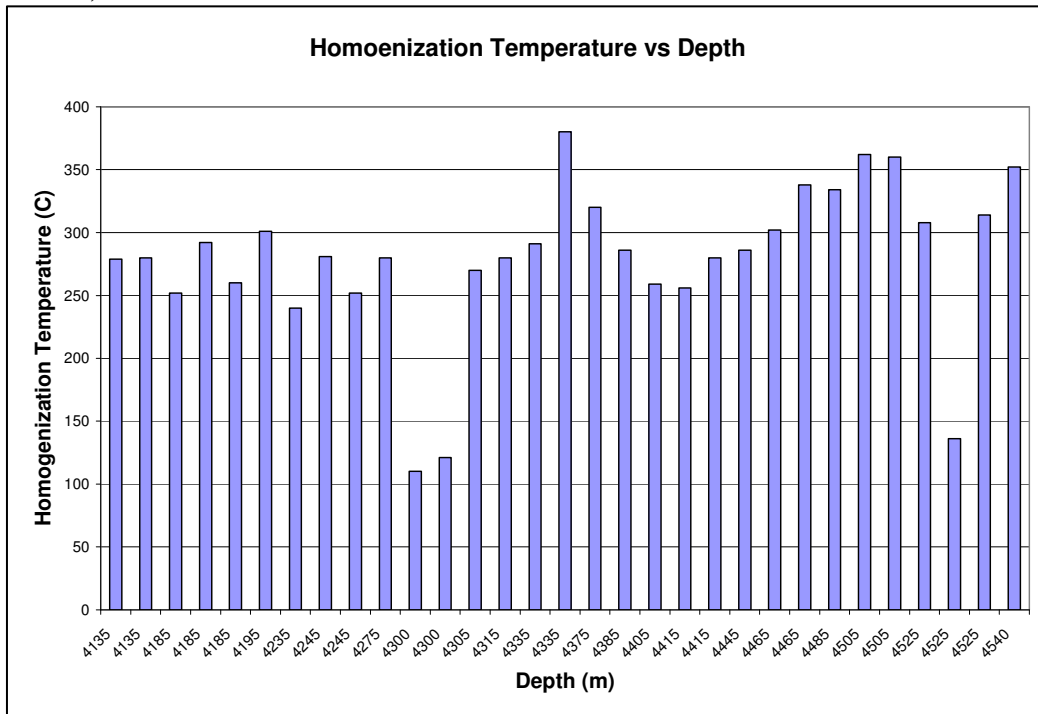


Fig. 40a: Microthermometric behavior of a group of aqueous fluid inclusions showing phase changes during cooling-heating processes (sample G4185)

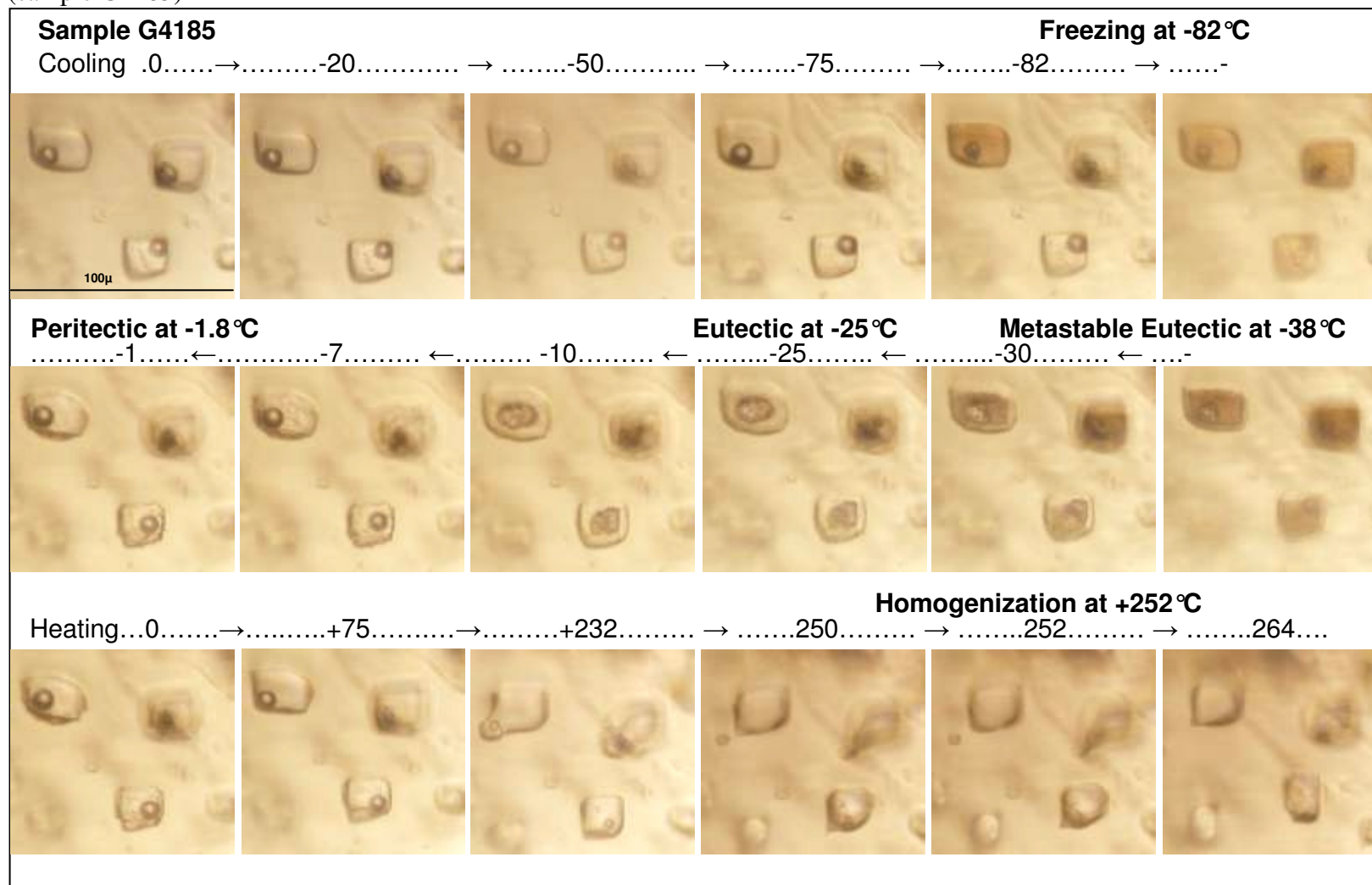


Fig. 40b: Microthermometric behavior of a group of aqueous fluid inclusions showing phase changes during cooling-heating processes (sample G4305)

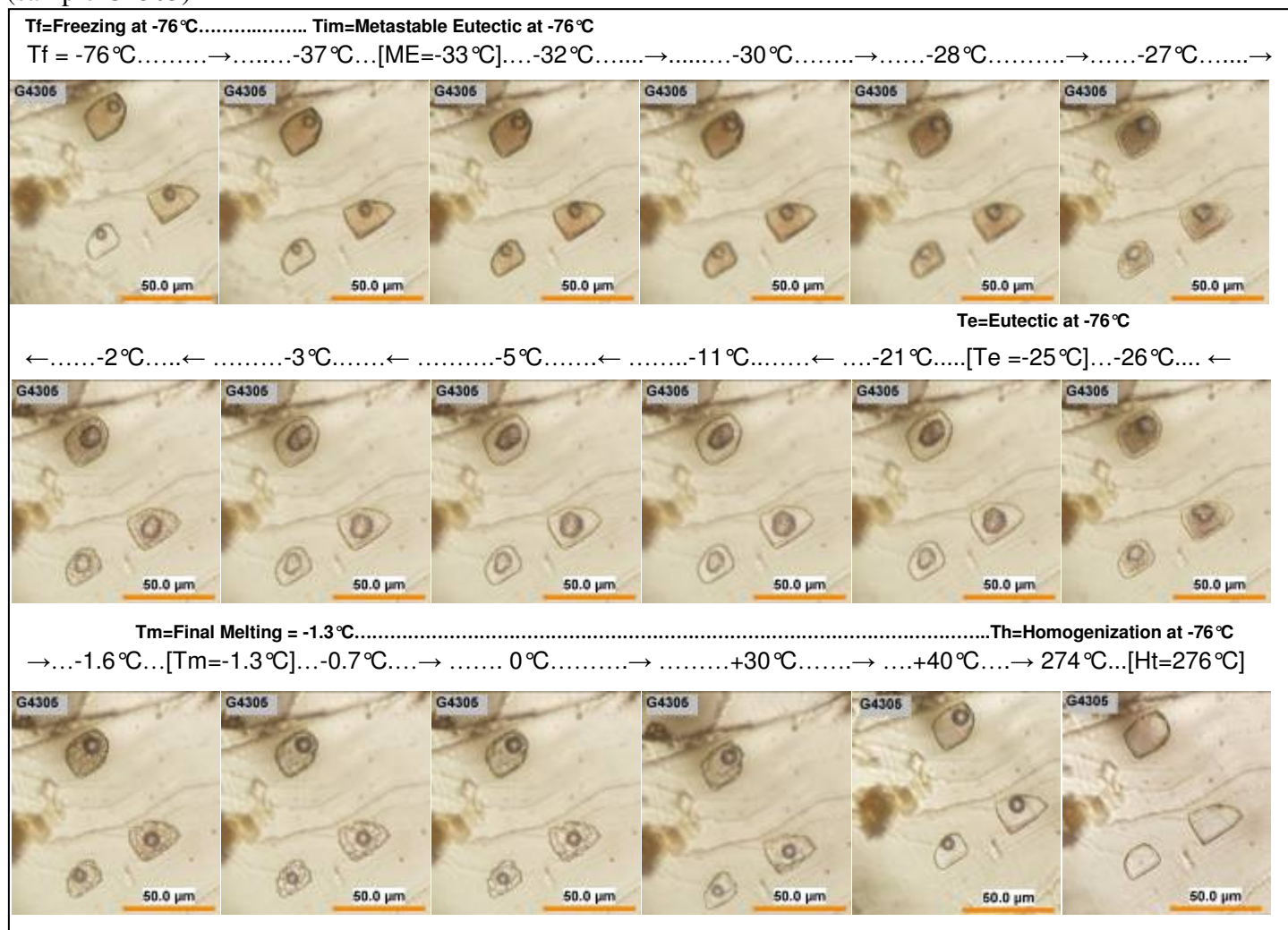


Fig. 40c: Microthermometric behavior of an aqueous fluid inclusion showing phase changes during cooling-heating processes (sample G4525)

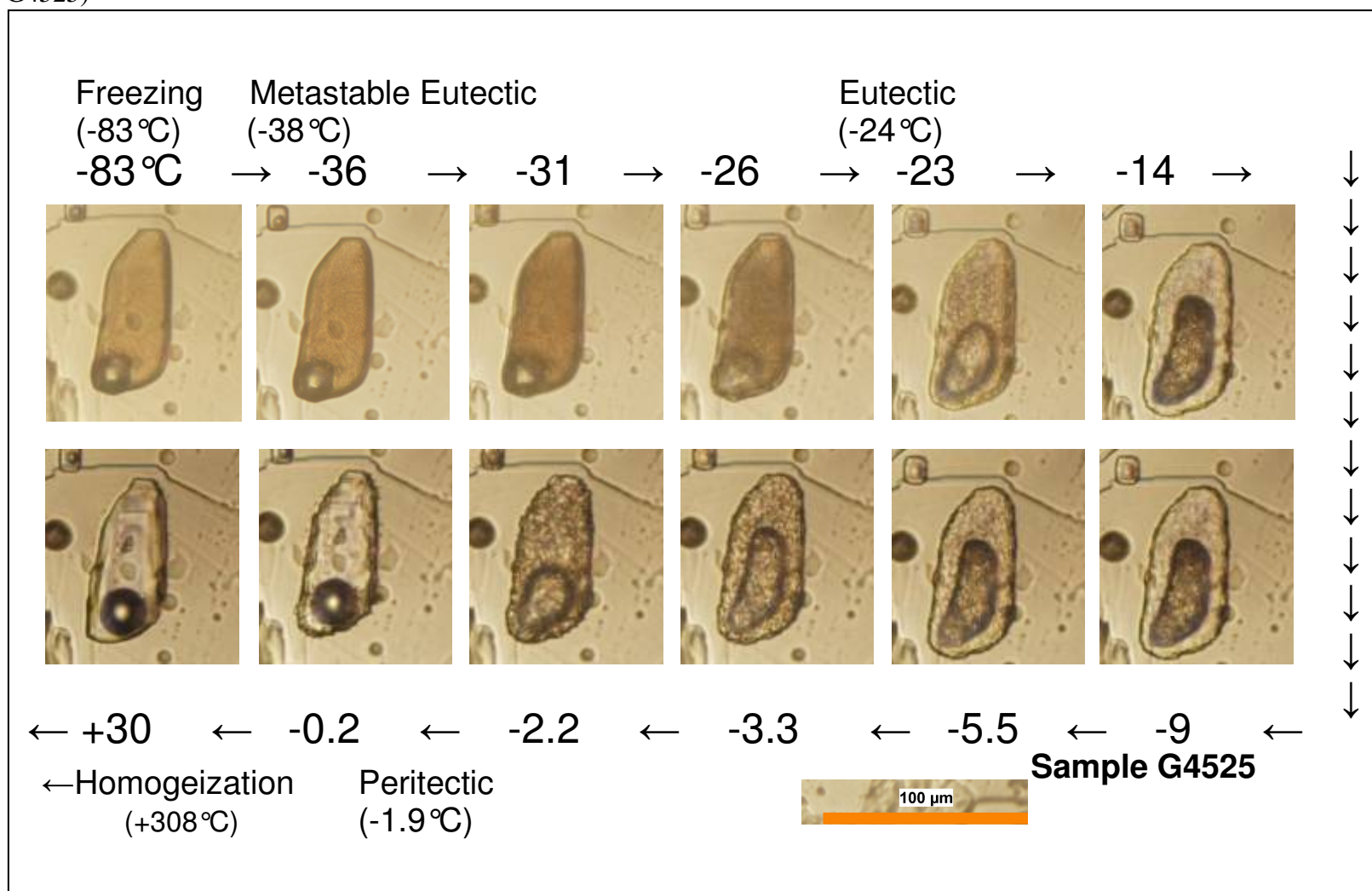


Fig. 40d: Microthermometric behavior of a large accidental aqueous fluid inclusion showing no phase changes during cooling-heating processes other than changes in the bubble size and deformation in the internal structure and external shape until final decrepitation (sample 4300)

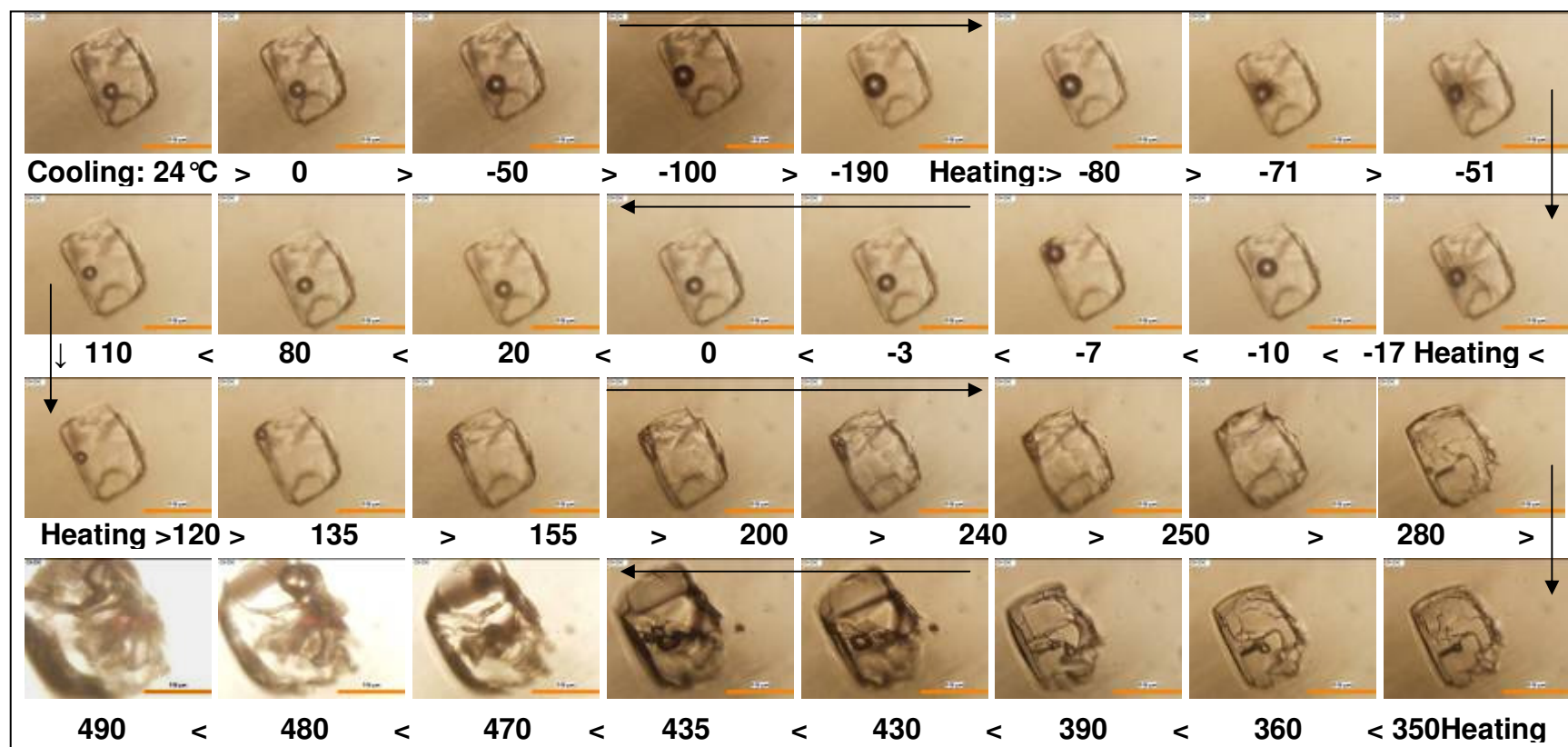
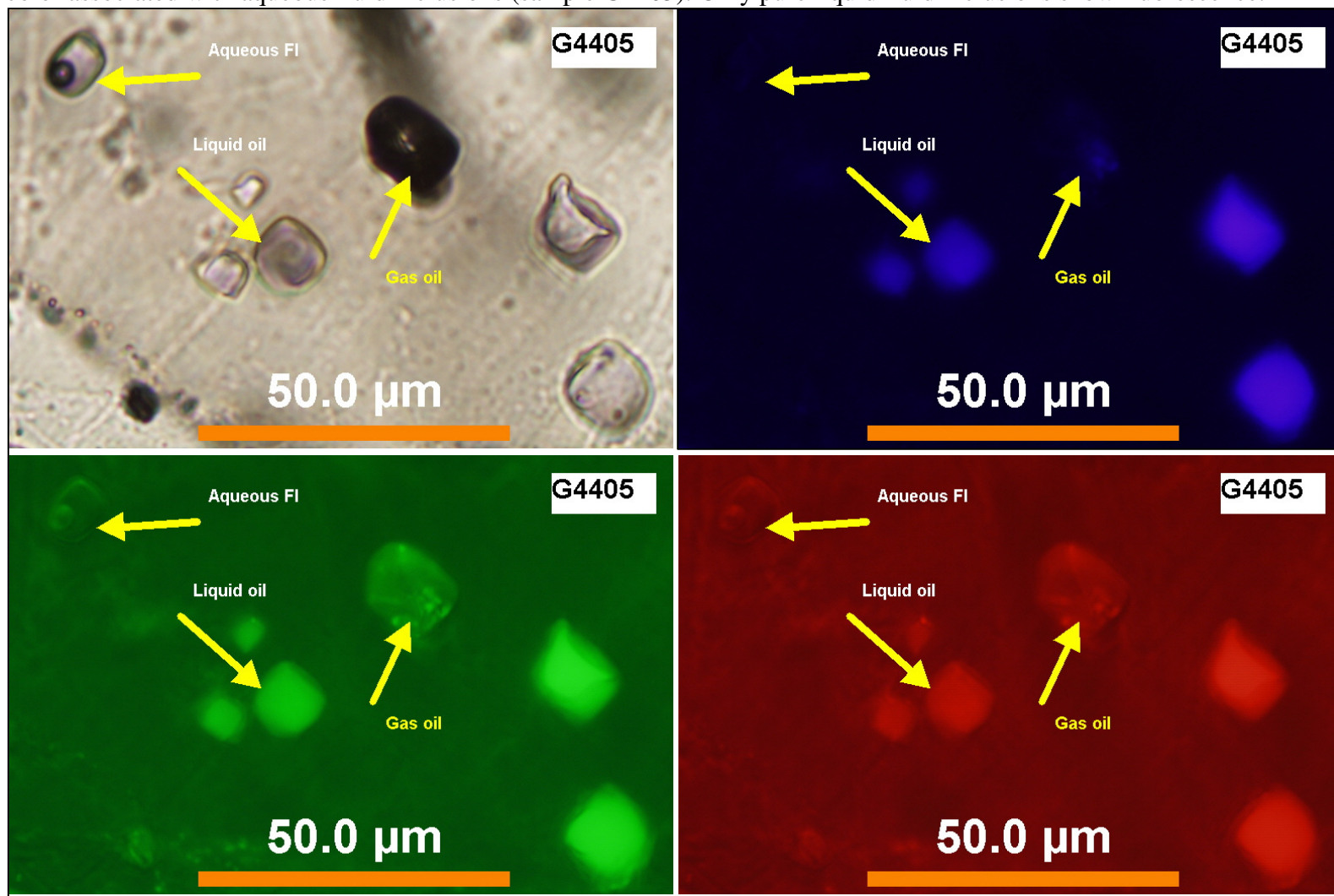


Fig. 41: Pure petroleum fluid inclusions (with no aqueous components) of one-phased type (gas of dark black color and liquid of light color associated with aqueous fluid inclusions (sample G4405). Only pure liquid fluid inclusions show fluorescence.



2. Microthermometry of the fluid inclusions in the salt of Weymouth-A45 well

The salt of Weymouth-A45 well is dominated by secondary fluid inclusions and richer in petroleum fluid inclusions compared to the salt of Glooscap-C63 well. These inclusions are aqueous (AFI), petroleum (PFI) and mixed aqueous-petroleum (AFI-PFI) types. These three types of inclusions coexist together in the same samples suggesting their coeval formation. The aqueous fluids in the AFI and in the PFI-AFI have the same microthermometric characteristics suggesting their formation/reformation as secondary inclusions under burial conditions during the generation of petroleum at a possible depth not much different from the current salt body's depth of ~3-4.5 km. Eighteen samples covering the sampled depth intervals were studied microthermometrically (Tables 6, 8 and 9 and Figures 42 to 45).

The fluid inclusions with lenticular and pin-like shapes, do not show any changes during microthermometric studies and are apparently air-filled only (Fig. 23a). These inclusions were not found in the salt samples of Glooscap-C63 well.

The aqueous fluid inclusions which are not very common have rectangular outlines, small in size, form large numbers as assemblages, and usually do not contain vapor bubbles (Fig. 23b). Although they look like primary inclusions in their shapes and distribution, but their existence side by side with PFI and PFI-AFI as well as similar microthermometric properties suggest their reequilibration or even secondary origin. The microthermometric properties of these inclusions are listed in Tables 8 and 9 and shown in Fig. 42. They freeze at a temperature range of -80°C to -67°C with a median of -71°C and average of -73°C and usually turn brown upon freezing. Their initial melting temperature (metastable eutectic) range of -53°C to -38°C, with a median of -52°C and average of -48°C during which rims form around the inclusions and gradually become clear and grow towards the core to end up at the eutectic point (final ice melting) with a dark spot in the core covering the bubble. The eutectic temperature ranges between -38°C and -27°C with a median of -37°C and an average of -34°C. Their final melting temperature (peritectic) ranges between -3°C and -2.6°C with a median of -2.7°C and average of -2.8°C during which a granular texture appears prior to the final melting and clearance of the bubble and the surrounding liquid. Homogenization takes place at a temperature range of 97°C to 128°C with a median of 122°C and average of 116°C. The

nearest chemical systems to the characteristics of these inclusions are NaCl-MgCl₂-H₂O and NaCl-CaCl₂-H₂O which have stable eutectic temperatures of -35°C and -52°C, respectively (Davis, et al., 1990). The NaCl-MgCl₂-H₂O system is more likely because of the close eutectic value; however the NaCl-CaCl₂-H₂O system which is more common in fluid inclusions in general is also possible based on the description given by Goldstein and Reynolds (1994) and Davis et al (1990). The experimental data given by Davis et al (1990) showed different temperatures between the stable eutectic (ranging between -56°C to -47°C depending on molality) and that of final melt ice (ranging between -50°C and -23°C depending on the molality). It is not possible to distinguish between the eutectic and final ice melting temperature in the studied samples because the two events were possibly taking place at the same or very close temperatures and for this reason the NaCl-CaCl₂-H₂O system is also a possibility; this is also supported by the abundance of relatively large (up to 100µm) anhydrite crystal inclusions within these salts.

The AFI-PFI are of secondary origin and display a wide variety of shapes, sizes and are of multi-phased nature ranging from two to four phases (Fig. 25). They are very common and have been found in most of the studied samples. They range from aqueous phase-dominant to petroleum phase-dominant. During microthermometric treatment the majority show mixed properties between those of aqueous fluid inclusions and those of petroleum fluid inclusions. The aqueous phase within these multi-phased inclusions behaves similar to the AFI by usually turning brown once they freeze (Fig. 43). The brown coloration during freezing mostly covers the aqueous part while in some cases also covers the whole inclusion body including the petroleum part which is usually ring-like. Such brown coloration is helpful to recognize various phase changing stages during treatment unlike the pure petroleum fluid inclusions which remain uncolored and do not show phase changes other than disappearance of the bubble as the sign of homogenization. These inclusions freeze at a temperature range of -84°C to -63°C with a median and average of -75°C. Their metastable temperature ranges between -53°C to -48°C with a median of -52°C and average of -51°C where rims appear around the inclusion and gradually widens towards the core and the brown color fades leading to the eutectic where a burst of ice melting takes place accompanied by the reappearance of the bubble and clearing out of the liquid. The eutectic phase change occurs at a temperature

range of -42°C to -28°C with a median of -38°C and average of -36°C . Final melting (peritectic) happens at a range of -6.5°C to -2°C with a median of -3°C and average of -3.9°C which is preceded by appearing of a granular texture within the inclusion prior to complete final melting (Fig. 43). They homogenize at a range of 17°C to 170°C with a median of 76°C and average of 69°C . It can be noticed that there is similarity in the microthermometric behavior of the aqueous liquid in AFI and those of the mixed PFI-AFI suggesting their common origin. Again like the AFI, the aqueous liquid within the mixed PFI-AFI have the characteristics of $\text{NaCl-MgCl}_2\text{-H}_2\text{O}$ and/or $\text{NaCl-CaCl}_2\text{-H}_2\text{O}$ systems based on the descriptions given for such systems by Davis et al (1991) and Goldstein and Reynolds (1994). The eutectic temperatures are closer to that of $\text{NaCl-MgCl}_2\text{-H}_2\text{O}$ excluding one sample (3910 in Table 8) which has a eutectic of -55 close to that of $\text{NaCl-CaCl}_2\text{-H}_2\text{O}$ system (-52°C).

The petroleum fluid inclusions (PFI) are also common and coexist with the other types of inclusions. Similar to those of Glooscap-C63 salt, these inclusions show very little changes during microthermometric measurements. They do not show those sudden movements of the bubble during supposed freezing below -190°C upon cooling or final melting at -182.5°C during heating (Fig. 44).as suggested by Goldstein and Reynolds (1994) and described in detail in the “background on fluid inclusions” section of this report. They also do not homogenize at the supposed temperature of -82.1°C as the methane fluid inclusions do but instead they homogenized at a temperature range of 17°C to 97°C with a median of 23°C and average of 44°C (Fig. 42 and 44). There is no color change during freezing. The only noticed change is the appearance of a bubble in the inclusions which did not originally contain one at negative temperatures (-10°C and lower) and increase of its size during cooling with gradual deformation (not sudden) at around -100°C or at much higher temperatures (Fig. 44). Such deformation in the bubble is sometimes very distinct as the enlarged dark bubbles form tail-like extension (meniscus) which become longer and longer during continued cooling and its gradual disappearance during heating (Fig. 44b). The reverse happens to the bubbles during heating, i.e., gradual decrease in their size and restoration of the original spherical shape around -100°C or at higher temperatures. The homogenization temperature for these pure liquid PFI is relatively low in most case (median 23°C) which is not unusual for

petroleum fluid inclusions; however such low temperatures needs pressure corrections which will increase the actual trapping temperature few tens of degrees (Bodnar, 2010, pers. email comm.). Such correction can not be done because the final melting temperature could not be noticed during measurements as mentioned above. The reason for these inclusions not showing distinct signs of phase changes are obviously because of stretching effect during treatment which is a common phenomenon in halite that is one of the weakest fluid inclusion-bearing minerals and can not withstand high cooling-heating temperatures (naturally and during treatment and measurement). Because of this fact the microthermometric results did not exactly match the supposed published data and for this reason they should be treated with caution. Many famous fluid inclusion scholars such as Bodnar do not rely on microthermometric results in halite because of stretching problem during cooling-heating measurements (Bodnar, 2010, pers. email. comm.).

The gas-dominated petroleum fluid inclusions are also common. They seem to be pure gas; however during successive heating of gas fluid inclusions initially with no signs of fluorescence turned into liquid-dominated phase at high temperature with distinct fluorescence due to condensation of gas under high temperature and high internal pressure build up within the inclusion (Fig.45).

Table 8: Micrometric results for the fluid inclusions in the salt of Weymouth-A45 well. AFI= Aqueous fluid inclusions; PFI= Petroleum fluid inclusions; AFI-PFI = Aqueous + petroleum phases within the same fluid inclusion; T_f = Freezing Point Temperature; T_{im} = Metastable Eutectic Temperature (initial melting); T_e = Eutectic Melting Temperature; T_m = Peritectic Temperature (final melting); T_h = Homogenization Temperature; n.o.= not observed.*3901 is excluded from statistics due to its much lower T_{im} and T_e .

Sample	Type	Origin	T_f	T_{im}	T_e	T_m	T_h	Notes
2950	AFI-PFI	secondary	-73	-51	-42	-2.6	117	4-phased (oil-water-halite crystal-bubble) FIs; at 97C the bubble homogenized; at 117C the halite crystal melted
	PFI	secondary	n.o.	n.o.	n.o.	n.o.	56	Bubble appeared during cooling
3055	PFI-AFI	secondary	-65	-52	-39	-3	144	The petroleum part did not show any phase changes.
	PFI-AFI	secondary	-70	-52	-28	-2.9	77	Petroleum liquid, did not have bubbles before treatment
	AFI-PFI	secondary	-63	-50	-28	-3	109	
	PFI	secondary	n.o.	n.o.	n.o.	n.o.	97	Liquid PFI. Bubble formed at -27 to -42C) during cooling
3140	PFI-AFI	secondary	-78	-52	-37	-5.5	20	They produced bubble during cooling at -42
3200	PFI	secondary	n.o.	n.o.	n.o.	n.o.	21	Liquid PFI. Bubble formed at (-27 to -42C) during cooling
3260	AFI	primary	-67	-38	-27	-2.6	128	
3350	PFI	secondary	n.o.	n.o.	n.o.	n.o.	75	Pure liquid PFI with bubble before treatment
	PFI	secondary	n.o.	n.o.	n.o.	n.o.	47	with bubble before treatment
	PFI	secondary	n.o.	n.o.	n.o.	n.o.	97	with bubble before treatment
3410	AFI-PFI	secondary	-84	-48	-35	-2	81	
	AFI	primary	-71	-53	-38	-2.7	122	Small rectangular assemblages
	PFI	secondary	n.o.	n.o.	n.o.	n.o.	21	Did not contain bubbles before treatment
	PFI	secondary	n.o.	n.o.	n.o.	n.o.	77	Originally had bubble before treatment
3470	PFI-AFI	secondary	-77	-52	-38	-2.6	18	Bubble formed during cooling
	PFI	secondary	n.o.	n.o.	n.o.	n.o.	21	Pure liquid PFI with no bubbles before treatment
3530	PFI-AFI	secondary	-80	-53	-38	-2.6	18	Bubbles formed at <-30C during cooling.
3620	PFI-AFI	secondary	-84	-50	-38	-3	18	It developed a bubble during cooling at -41C
	AFI	primary	-80	-52	-37	-3	97	
3700	PFI	secondary	n.o.	n.o.	n.o.	n.o.	22	Upon cooling, bubbles formed at ~ (-20°C to -42°C) which gradually deformed at ~ (-100°C) and then retained their sphericity ~ (-100°C) during heating.
	AFI-PFI	secondary	-71	-50	-33	-6.5	17	The AFI-PFI produced bubbles while cooling at ~+10C
	AFI-PFI	secondary	-71	-50	-33	-6.5	74	The AFI-PFI produced bubbles while cooling at ~+10C
3790	PFI	secondary	n.o.	n.o.	n.o.	n.o.	24	
3820	PFI	secondary	n.o.	n.o.	n.o.	n.o.	22	No bubbles before treatment
3880	AFI-PFI	secondary	-81	-52	-39	-6.3	16	

3910*	AFI-PFI	secondary	-84	-65	-55	-5.5	20	
3940	AFI-PFI	secondary	-84	-52	-37	-2	88	
4000	PFI	secondary	n.o.	n.o.	n.o.	n.o.	17	Upon cooling, bubbles formed at -27°C to -37°C which gradually deformed ~-100°C and retained its shape ~-70°C during heating.
4060	PFI	secondary	n.o.	n.o.	n.o.	n.o.	19	
Median	All types of FI together		-73	-52	-37	-3.0	56	
Average			-75	-50	-36	-3.7	62	
Minimum			-84	-53	-42	-6.5	17	
Maximum			-63	-38	-27	-2.0	170	

Table 9: Median, average, minimum and maximum values for freezing, initial melting, eutectic, final melting and homogenization temperatures for the microthermometrically of the analyzed fluid inclusions in the salt of Weymouth-A45 well

Type of FI	Statistical Parameters	Freezing Temperature T_f	Metastable Eutectic Temperature (Initial Melting) T_{im}	Eutectic Temperature T_e	Peritectic Temperature (Final Melting) T_m	Homogenization Temperature T_h	Number of Studied Samples
AFI	Median	-71	-52	-37	-2.7	122	3
	Average	-73	-48	-34	-2.8	116	
	Minimum	-80	-53	-38	-3.0	97	
	Maximum	-67	-38	-27	-2.6	128	
PFI-AFI	Median	-75	-52	-38	-3.0	76	14
	Average	-75	-51	-36	-3.9	69	
	Minimum	-84	-53	-42	-6.5	17	
	Maximum	-63	-48	-28	-2.0	170	
PFI	Median	n.o.	n.o.	n.o.	n.o.	23	14
	Average	n.o.	n.o.	n.o.	n.o.	44	
	Minimum	n.o.	n.o.	n.o.	n.o.	17	
	Maximum	n.o.	n.o.	n.o.	n.o.	97	
All	Median	-73	-52	-37	-3.0	56	31
	Average	-75	-50	-36	-3.7	62	
	Minimum	-84	-53	-42	-6.5	17	
	Maximum	-63	-38	-27	-2.0	170	

Fig. 42a: Histogram of freezing point temperatures (T_f) versus depth of the PFI-AFI, PFI, and AFI in the salt of Weymouth-A45 well. T_f [median = -77°C ; average = -75°C ; minimum = -84°C ; maximum = -63°C]

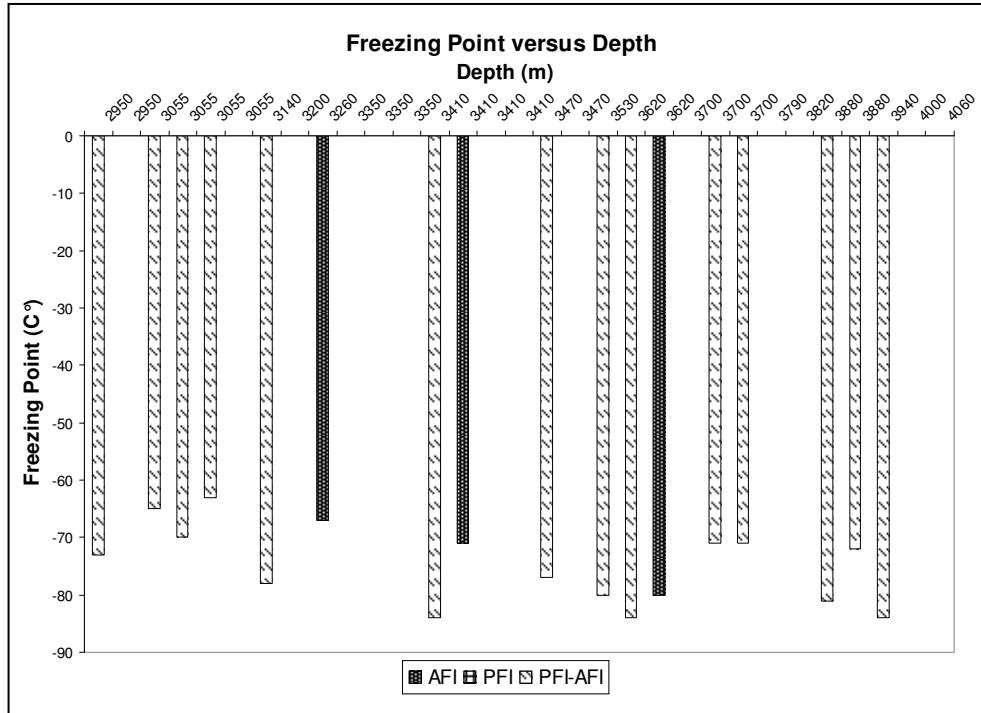


Fig. 42b: Histogram of metastable eutectic temperatures (initial melting- T_{im}) versus depth of the PFI-AFI, PFI, and AFI in the salt of Weymouth-A45 well. T_{im} [median = -52°C ; average = -50°C ; minimum = -53°C ; maximum = -38°C]

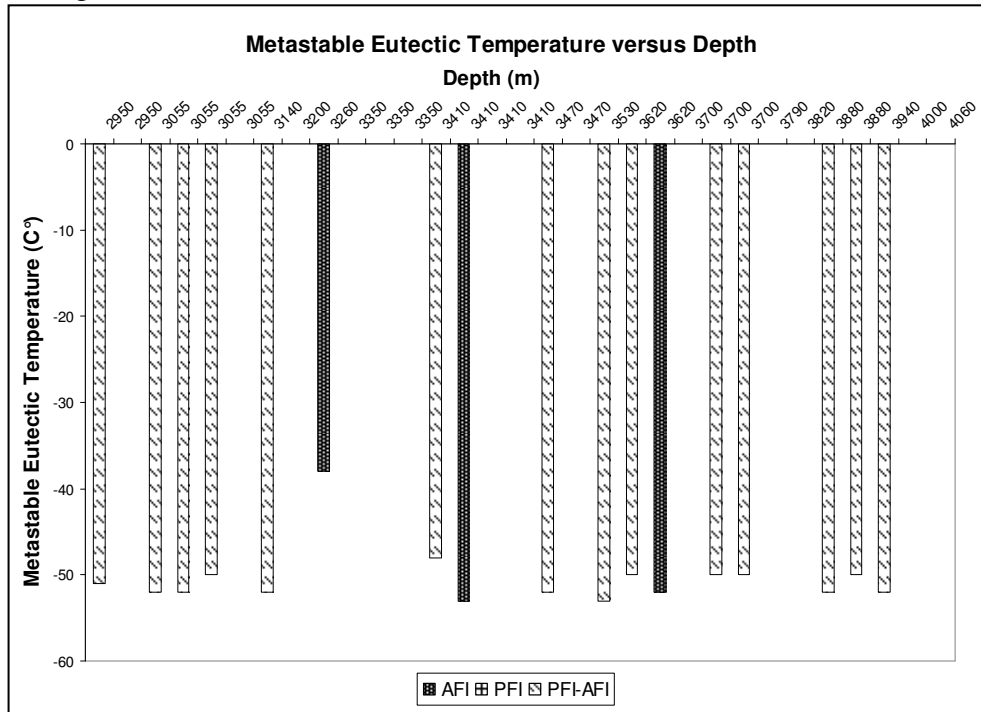


Fig. 42c: Histogram of eutectic temperatures (T_e) versus depth of the AFI-PFI fluid inclusions in the salt of Weymouth-A45 well. T_e [median = -37 °C; average = -36°C; minimum = -42°C; maximum = -27°C]

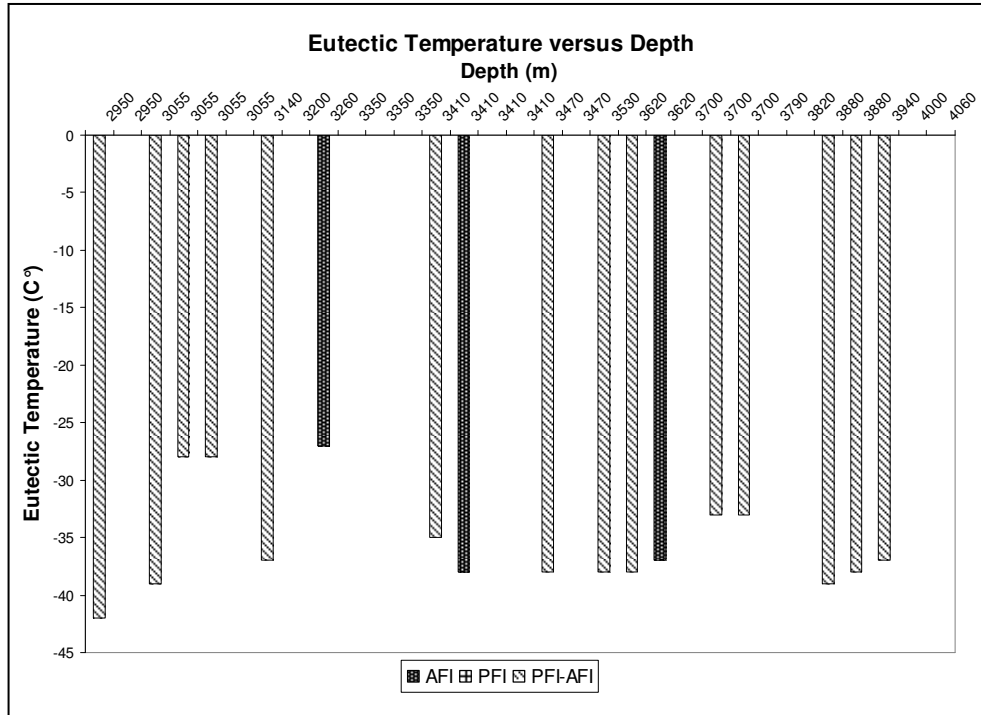


Fig. 42d: Histogram of peritectic temperatures (final melting – T_m) versus depth of the PFI-AFI, PFI, and AFI in the salt of Weymouth-A45 well. T_m [median = -3°C; average = -3.7°C; minimum = -6.5°C; maximum = -2°C]

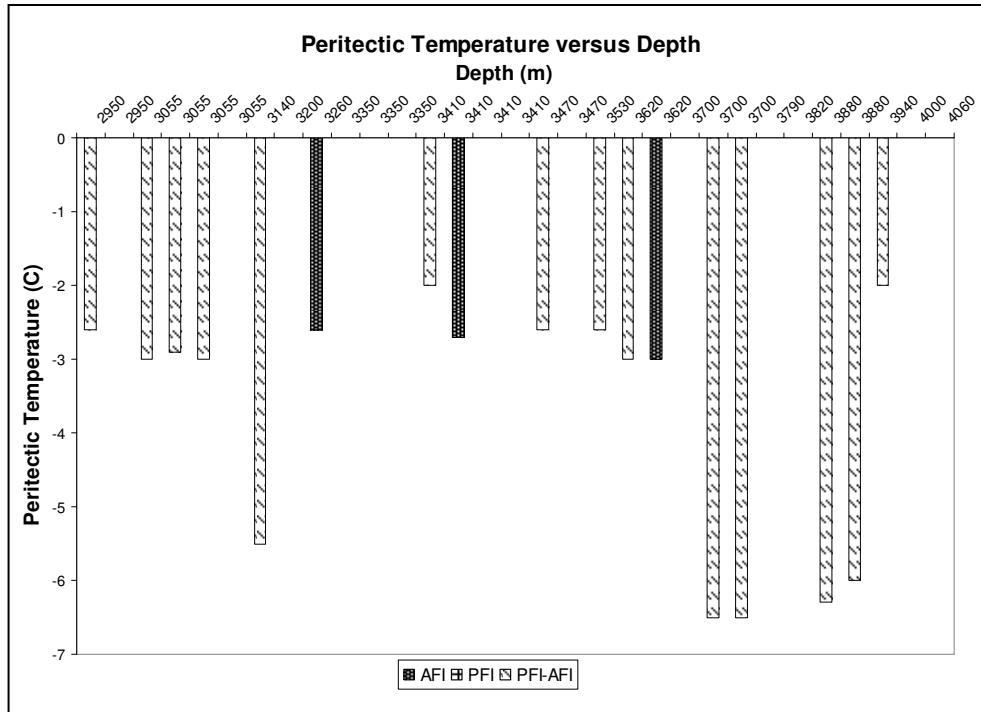


Fig. 42e: Histogram of homogenization temperatures (T_h) versus depth of the PFI-AFI, PFI, and AFI in the salt of Weymouth-A45 well. T_h [median = 56°C; average = 62°C; minimum = 17°C; maximum = 170°C]

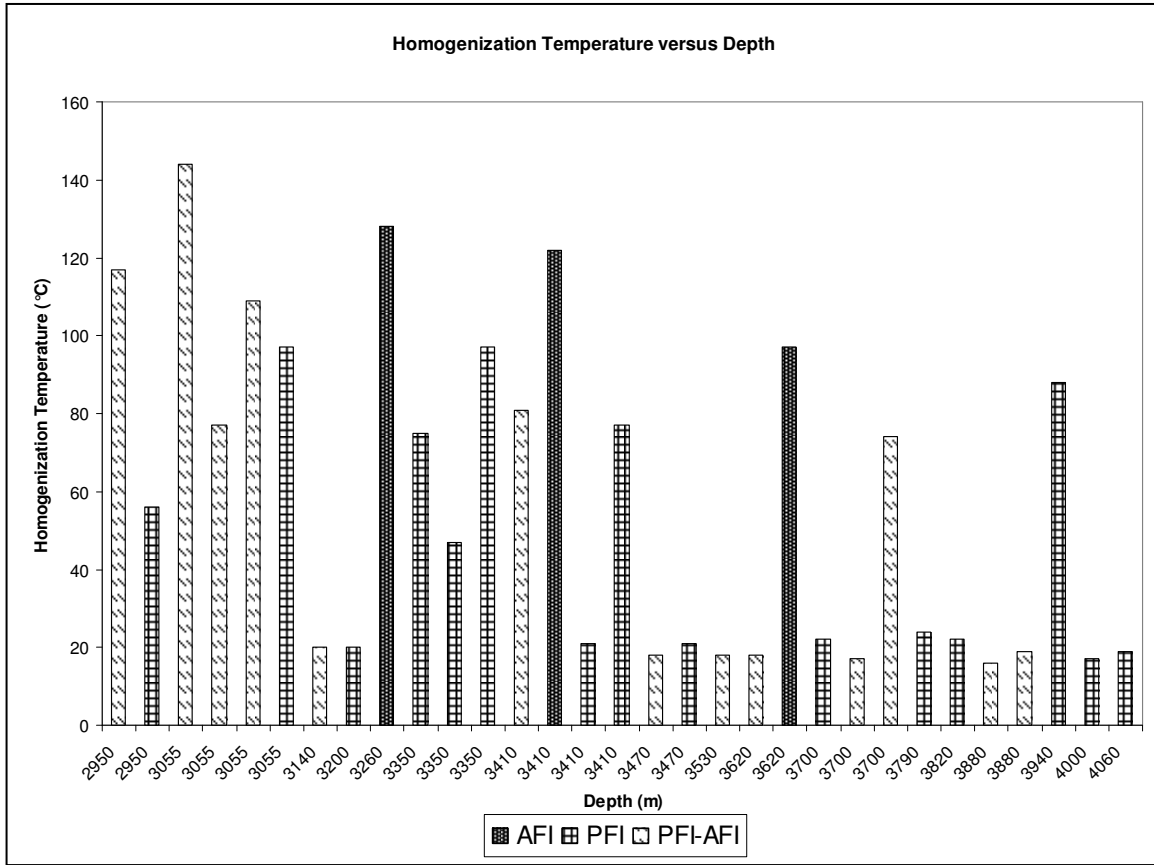


Fig. 43a: Two-phased AFI-PFI showing brown coloration as a sign of freezing during microthermometric treatment

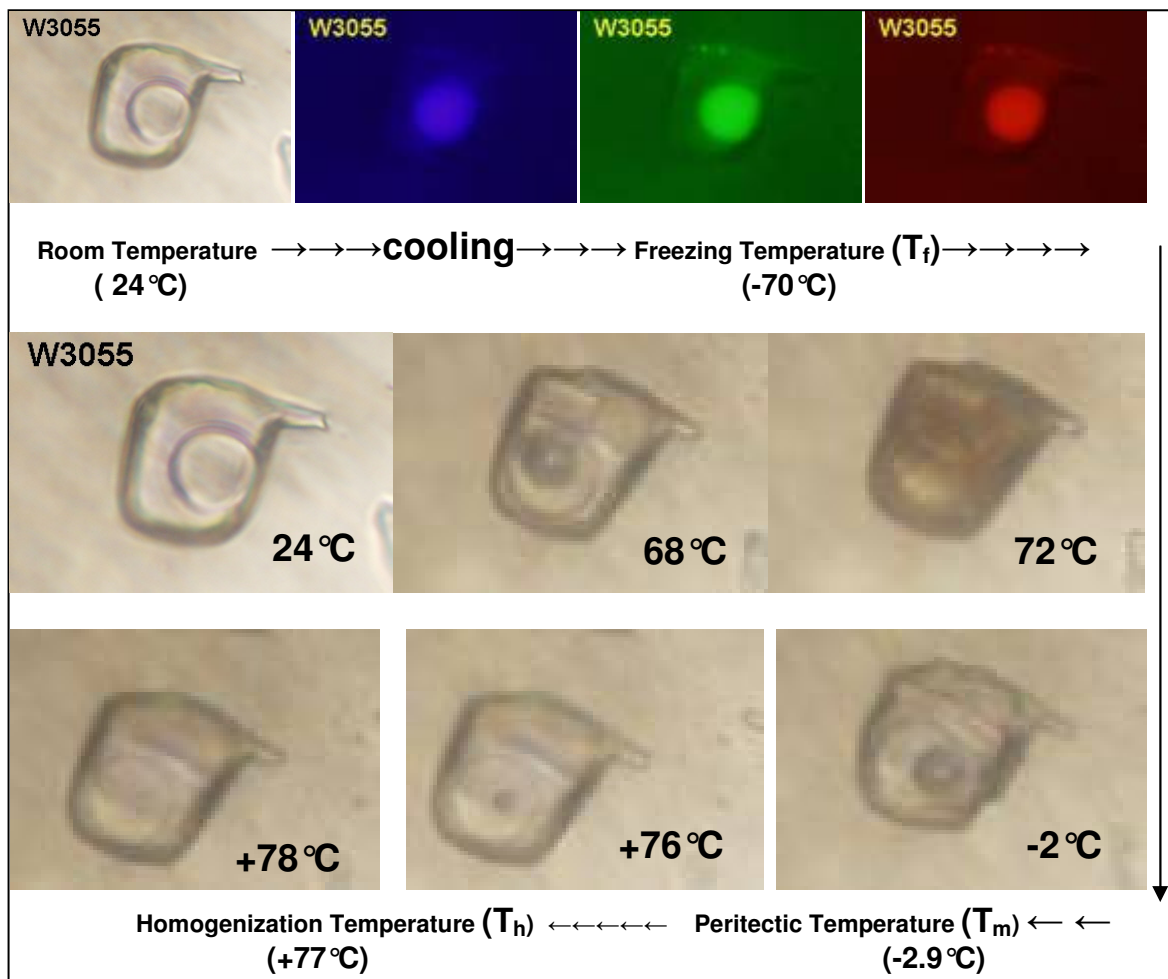


Fig. 43b: Multi-phased AFI-PFI showing no color change during freezing which has produced a bubble during cooling and homogenized by disappearance of the bubble at 22 °C. The ring-like petroleum phase did not mix with the aqueous phase inspite of excessive heating and end up with decrepitation ~ 50°C. The change of shape and size as a result of deformation during treatment is evident.

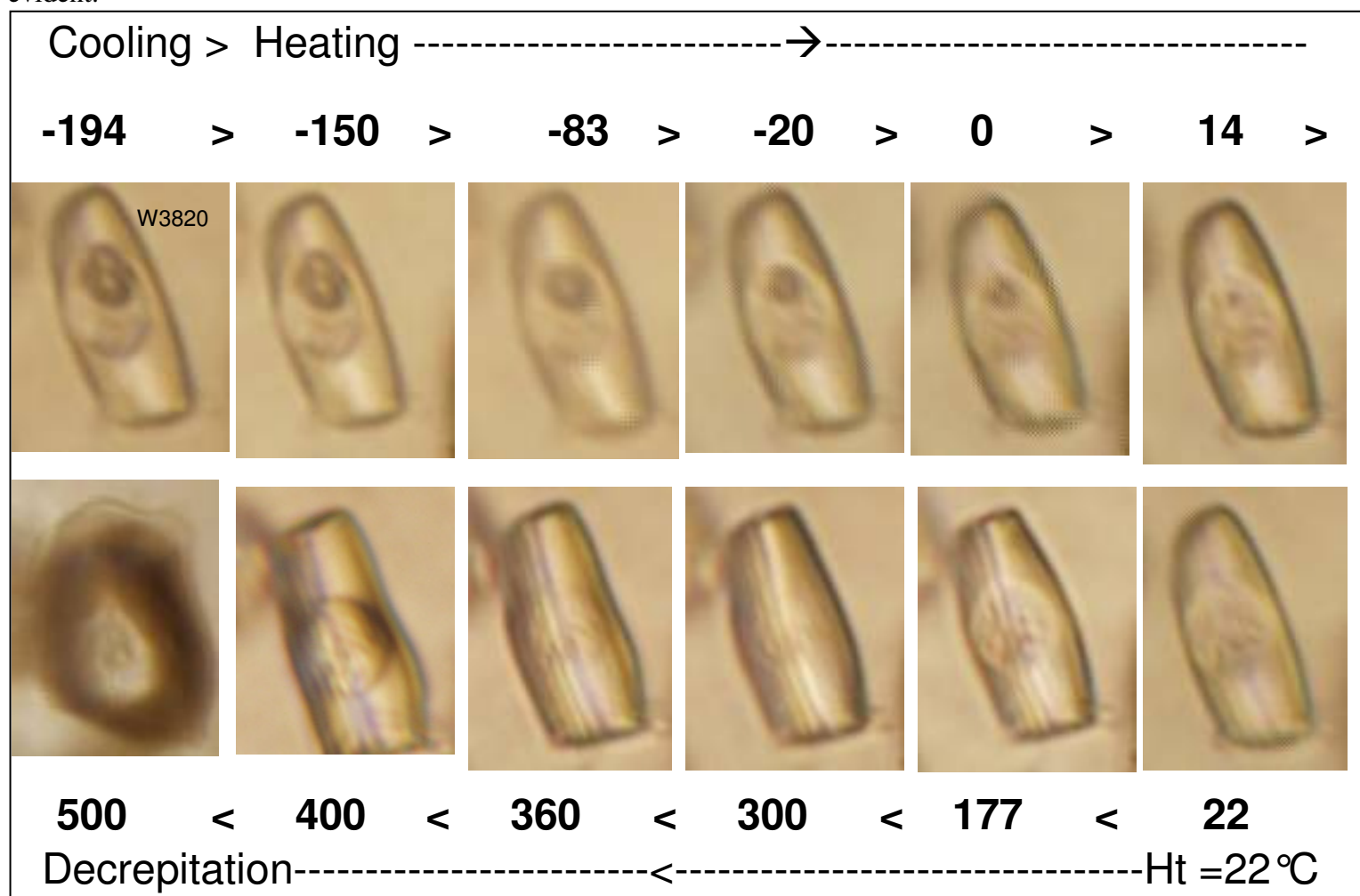


Fig. 43c: Microthermometric behavior of three-phased AFI-PFI in Wymouth-A45 salt (sample W3880). It is aqueous liquid-dominated with a small spot of oil and a large bubble. $T_f = -80^\circ\text{C}$; $T_{im} = -52^\circ\text{C}$; $T_e = -39^\circ\text{C}$; $T_m = -6^\circ\text{C}$; $T_h = +170^\circ\text{C}$.

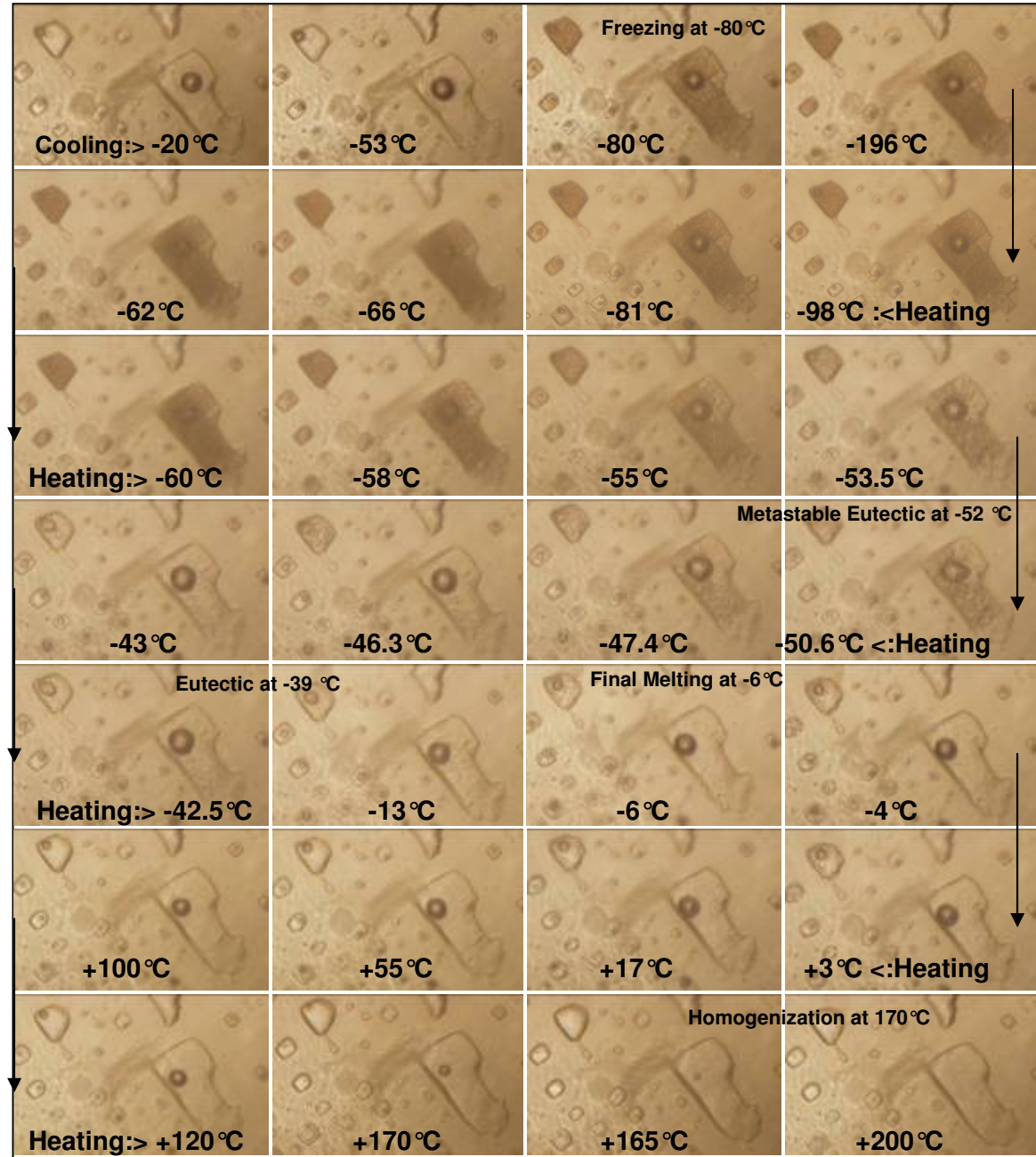


Fig. 44a: Microthermometric treatment of one-phased liquid petroleum which did not show any color changes or distinct signs during phase changes other than gradual deformation of the bubble during cooling ($\sim -100^{\circ}\text{C} \pm \text{few degrees}$) and regaining its original spherical shape approximately at the same range of temperature during heating. For details enlarged views see Figs. 44-a1 and 44-a2.

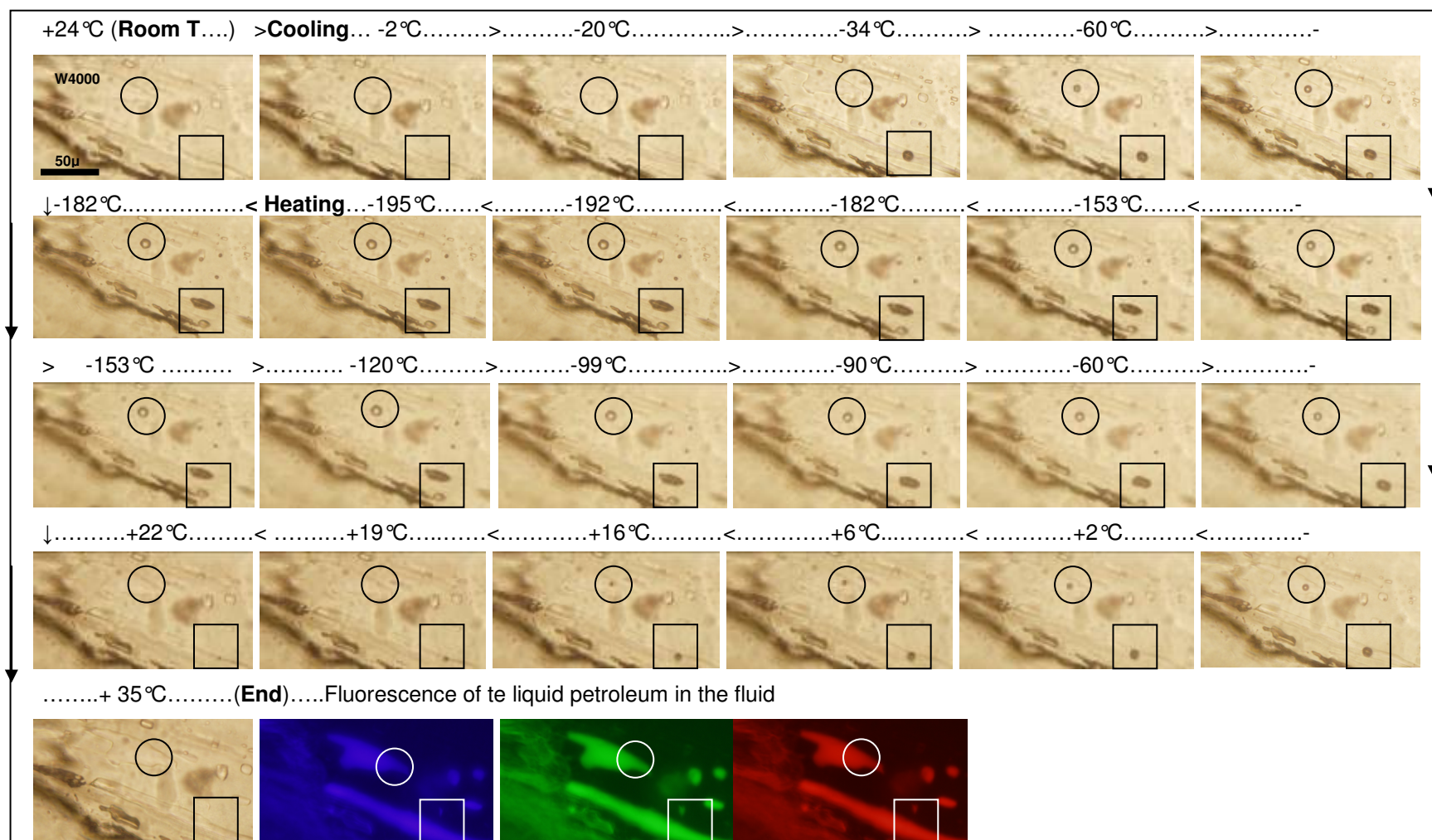


Fig. 44a-1: Microthermometric treatment of one-phased liquid petroleum which did not show any color changes or distinct signs during phase changes other than gradual deformation of the bubble during cooling ($\sim -100^{\circ}\text{C} \pm \text{few degrees}$) and regaining its original spherical shape approximately at the same range of temperature during heating.

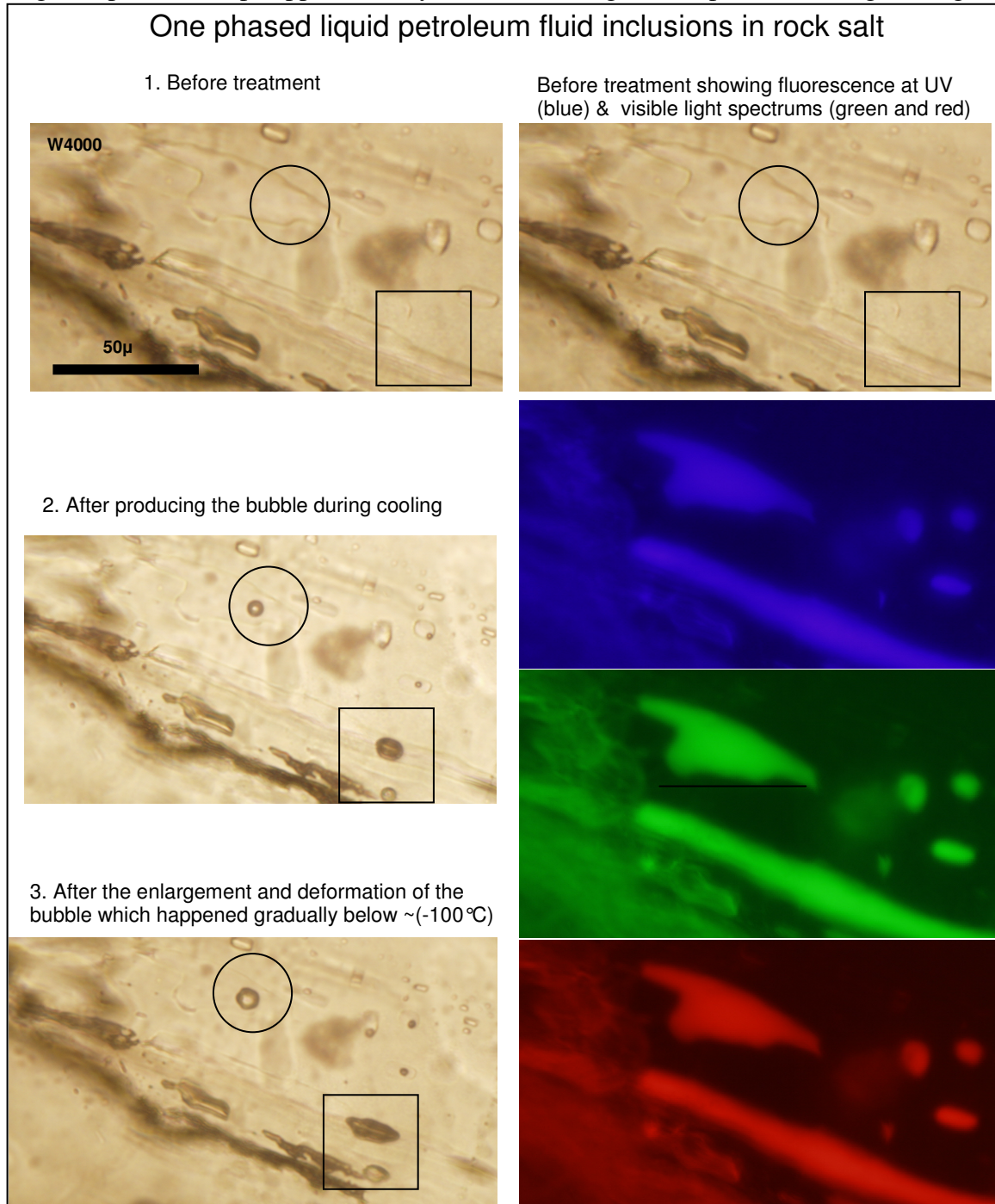


Fig. 44a-2: Microthermometric treatment of one-phased liquid petroleum which did not show any color changes or distinct signs during phase changes other than gradual deformation of the bubble during cooling ($\sim -100^{\circ}\text{C} \pm \text{few degrees}$) and regaining its original spherical shape approximately at the same range of temperature during heating.

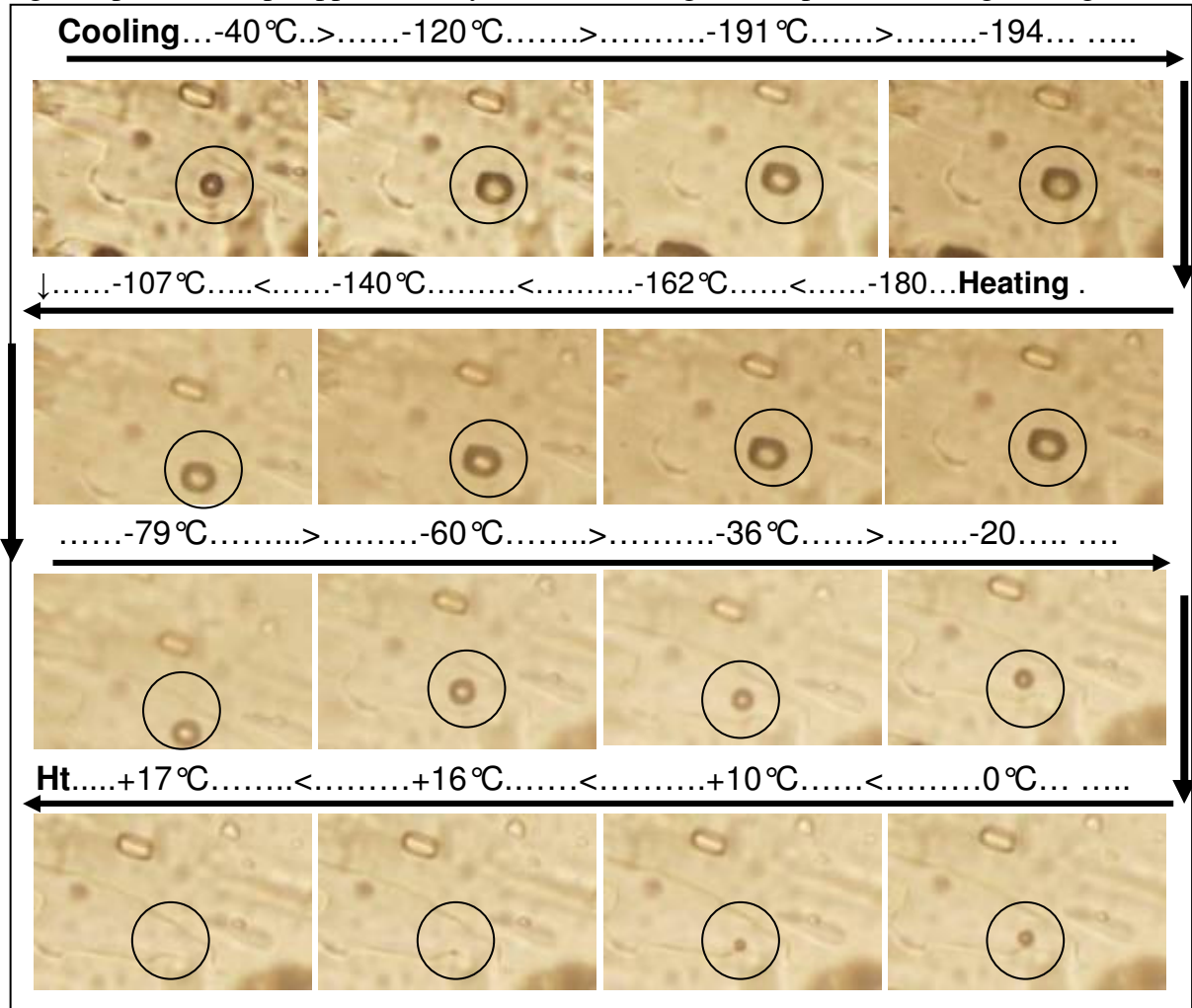
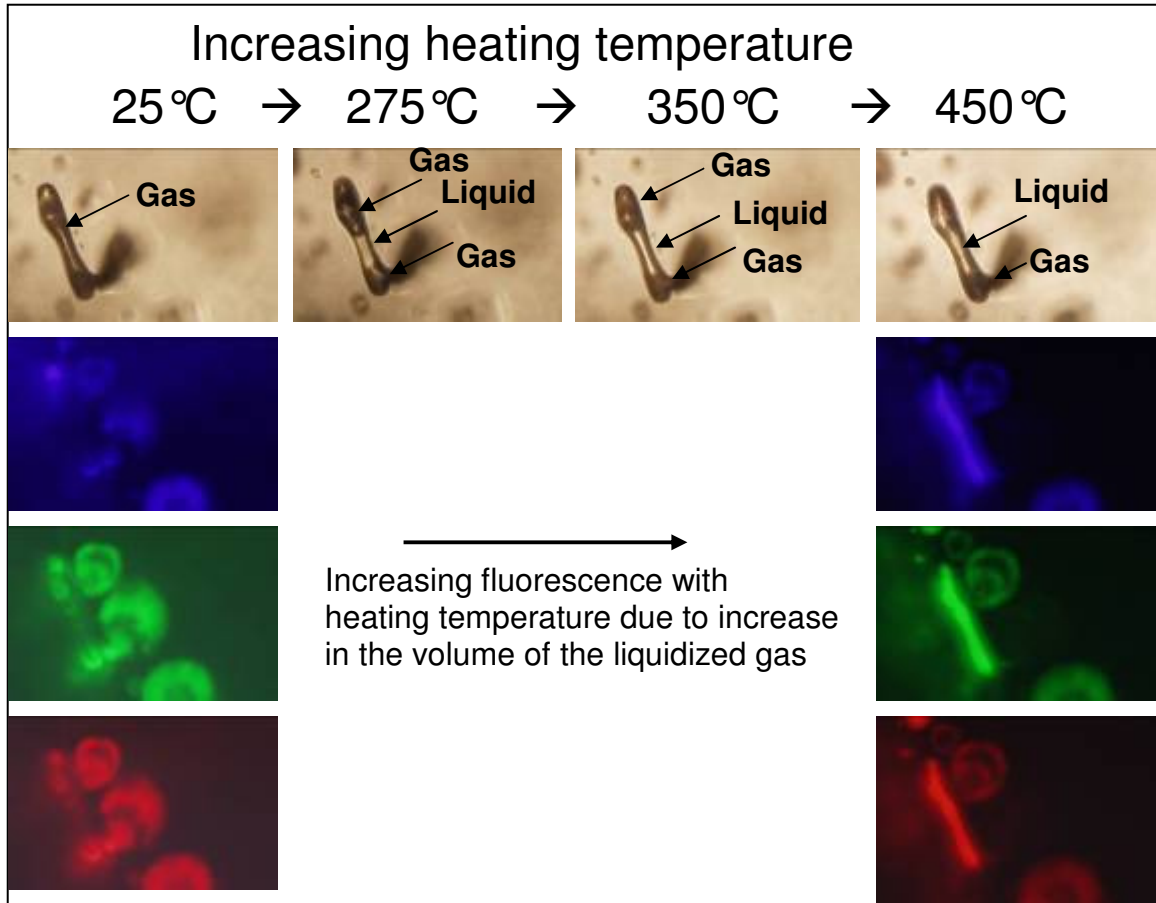


Fig. 44b: Microthermometric treatment of two-phased liquid petroleum inclusions (PFI) which neither showed any color changes nor distinct signs during phase changes other than gradual size increase and deformation of the bubble during cooling ($\sim > -75^{\circ}\text{C} \pm \text{few degrees}$) and regaining its original spherical shape approximately at the same range of temperature during heating.



Fig. 45: A gas dominated petroleum fluid inclusions initially with no signs of fluorescence (left) turns into liquid-dominated phase at excessive temperature (right) with distinct fluorescence due to condensation of the gas under high temperature and high internal pressure build up within the inclusion. The circular fluorescent spots to the right of the gas inclusion are coming from other fluid inclusions which are out of focus.



SUMMARY AND DISCUSSION

The Argo salt in Glooscap-C63 and Weymouth-A45 wells have many differences and some similarities in their properties and fluid inclusion content which are summarized in Table 10. Among the similarities, both contain a variety of aqueous, petroleum and mixed petroleum-aqueous fluid inclusions. In addition to their content of fluid inclusions, both contain crystals of anhydrite, hematite and rarely quartz as solid inclusions as well as containing lubricant-like liquid along cleavage planes and on the surface of the halite crystals. However there are many important differences between them such as the quantity, type and chemical systems of their fluid inclusions as well as distinct difference in their color and transparency of hand specimens. The Weymouth-A45 salt is richer in petroleum fluid inclusions and poorer in aqueous fluid inclusions. The salt of Glooscap-C63 well is always transparent with clear colorless appearance and occasionally brownish due to iron impurities content. The salt of Weymouth-A45 well is always non-transparent, yellowish buff in color with shades of brown due to iron staining and waxy in feeling; the color and non-transparency is probably due to the high content of anhydrite crystals as solid inclusions and also possibly due to high petroleum fluid inclusions content. The Weymouth salt forms an allochthonous canopy/diapir-shaped body of prominent thickness (>1.5km) compared to the autochthonous pillow-shaped body of Glooscap-C63 well with much less thickness (~0.5 km).

The aqueous fluid inclusions (AFIs) in both wells are different. The AFIs of Glooscap-C63 well are common and generally exist in two types, small normal ones and large accidental ones. The small normal ones exist as assemblages in large numbers with relatively large bubbles compared to the size of inclusions; while the large ones are accidental and few in number and are not as common as the smaller ones. Both are possibly of primary origin although this can not be confirmed because their host halite crystals neither show hopper-shaped crystals, nor growth lines parallel to crystal boundaries possibly because of their recrystallization at depth conditions. Their homogenization at very high temperatures (286°C in median value) shows that they were reequilibrated under burial conditions and lost their original depositional characteristics. Their low eutectic and metastable eutectic temperatures -25°C and -38°C as median

values compared to -21.2°C and -28°C values of aqueous fluid inclusions in halite belonging to $\text{H}_2\text{O}-\text{NaCl}$ system can also be attributed to the reequilibration and/or the presence of other cations in solution such as calcium (Bodnar, 2003).

The mixed petroleum-aqueous fluid inclusions of Glooscap-C63 well with no distinct separation between the two phases also behave like the aqueous ones during microthermometric measurements. They belong to $\text{H}_2\text{O}-\text{NaCl} \pm \text{Petroleum} (\text{CH}_4)$ system. This mixed nature of the content of fluid inclusions could also be the reason for the differences in the eutectic and metastable eutectic temperature as compared with the expected corresponding values in $\text{H}_2\text{O}-\text{NaCl}$ systems within fluid inclusions in halite. The salinity of the aqueous and mixed aqueous-petroleum fluid inclusions must be ~ 23.2 wt.% NaCl or more in the case of few samples which contain daughter halite crystals or produce such crystals during cooling process. According to Bodnar (2003) inclusions with salinities more than the peritectic composition (26.3 wt.% NaCl) should show halite as the last solid phase to disappear during heating from low temperatures and practically inclusions with salinities less than 30-35 wt.% NaCl often fail to nucleate a halite daughter crystal even during repeated thermal cycling at temperatures below 0°C .

The aqueous fluid inclusions in Weymouth-A45 salt are different from those of Glooscap-C63 well. They exist in two forms, both as assemblages and again possibly of primary origin which can not be confirmed because of the lack of hopper structures and growth lines in halite crystals due to recrystallization process, and thus their reequilibration. They mostly do not contain bubbles. The rectangular-shaped ones contain the same liquids as in the mixed PFI-AFI group which belongs to $\text{H}_2\text{O}-\text{MgCl}_2-\text{NaCl}$ and/or $\text{H}_2\text{O}-\text{CaCl}_2-\text{NaCl}$ systems. The lens and pin-like fluid inclusions behave very strangely as they do not show any phase changes even at extreme cooling and heating temperature suggesting that they are empty or air-filled.

There are two types of petroleum fluid inclusions in both wells (PFI and PFI-API) although there are important differences between them. These inclusions have been trapped heterogeneously where up to four phases can be seen in a single inclusion (aqueous liquid + petroleum liquid + solid impurities within petroleum + vapor or gas bubble). The PFI in both wells are either one-phased (liquid or gas) or two-phased (liquid + gas). The PFI-AFI group shows a major difference in the two wells. The liquid

petroleum of PFI-AFI in the salt of Weymouth-A45 well, exist in immiscible isolated form, usually containing tiny solid inclusions, surrounded with the aqueous liquid which is similar to that found in AFI, with or without vapor/gas bubble. While the liquid petroleum of PFI-AFI in the salt of Glooscap-C63 well, do not form isolated phase but exist as dispersed or mixed phase within the aqueous liquid and usually contain tiny solid particles similar to those found in their counterparts of Weymouth-A45 salt. However, the one-phased petroleum fluid inclusions in both wells have some similarities as they both look pure, transparent clear in appearance with no solid particles in them and they have similar microthermometric behavior by showing no signs of phase changes other than homogenization within a range of 51°C to 107°C with a median of 79°C in Glooscap-C63 well's salt and ranging between 17°C and 97°C with a median of 23°C in Weymouth-A45 well's salt. Although these homogenization temperatures are reasonable for the depth at which the salt bodies are located (4045.5m - 4542.4m in Glooscap-C63 well and 2840m - 4348m in Weymouth-A45 well) but still they must be interpreted with caution. If we consider a temperature gradient of 25°C/km beneath the Scotian Margin where the studied wells are located; that mean the corresponding temperature will be ~ 100°C to 125°C in Glooscap-C63 well and ~71°C to 109°C in Weymouth-A45 well. However, due to the reequilibration and stretching of fluid inclusions because of burial conditions and during cooling-heating treatment as indicated earlier, such conclusions must be treated cautiously. Such results can only give an approximate idea about the depth at which these fluid inclusions were trapped following the maturation of oil in a nearby source rocks followed by its movement and trapping within the nearby salt bodies of Argo Formation. The homogenization temperatures (T_h) of the aqueous fluid inclusions in Weymouth-A5 well's salt range between 17°C to 170°C with a median of 81°C and that of the Glooscap-C63 well's salt ranges between 110°C to 380°C with a median of 286°C. This means that the T_h of AFIs in Weymouth-A45 are more realistic and overlaps with those with the associated PFI and PFI-AFI while those of Glooscap-C63 are much higher than those of the accompanied PFI. There is no obvious reason for such difference although it can be argued that the burial depth of the autochthonous salt in Glooscap-C63 well is more than that of the allochthonous Weymouth-A45 well's salt which have resulted in greater reequilibration of the fluid inclusions in the former well

due to higher temperature and pressure. Due to the fact that most of the fluid inclusions in the studied wells are either secondary in origin or primary that have suffered from reequilibration under natural burial conditions and also stretched and deformed during microthermometric measurements, it is difficult to make any accurate estimation of the salinity of liquids in the fluid inclusions. However, it can generally be said that the salinity is around that of the solubility of their host halite (~23.2 wt% NaCl), and slightly higher in rare cases where few samples contained daughter halite crystals in their fluid inclusions or appeared during cooling measurements.



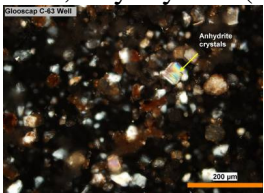


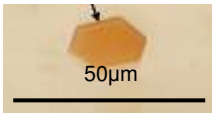

The PFIs in both studied wells showed distinct fluorescence in UV light as well as the visible light spectrums. Only liquid petroleum fluoresces while the one-phased gas inclusions do not fluoresce (Burruss, 2003a). According to Burruss (2003), as the fraction of liquid petroleum phase increases in petroleum fluid inclusions, the intensity of fluorescence increases. This view proved to be true in the studied petroleum fluid inclusions of Glooscap-C63 and Weymouth-A45 well's salts. Petroleum fluorescence at the visible spectrum wavelengths requires the presence of aromatic molecules that have >10 carbon atoms in the petroleum (Burruss, 1991; Stasiuk and Snowden, 1997). According to Burke (2001), fluid inclusions fluoresce when they contain cyclic or aromatic hydrocarbons, or fluorescent daughter minerals. This means that the petroleum in the fluid inclusions of both studied wells contain complex aromatic or cyclic molecules with >10 carbon atoms since they show distinct fluorescence in UV and visible spectrum wavelengths. To accurately identify the hydrocarbon compounds within these inclusions more advanced techniques are required. Gas Chromatography-Mass Spectrometry (GC-MS) is usually used to analyze biomarker compounds which are molecules whose carbon atoms range between 20 to >35 (Burruss, 2003a). On the other hand Raman Microspectroscopy (Microspectrometry) and Infrared (IR) Microspectroscopy are usually used to identify molecular compounds in PFI such as CH₄, CO₂, N₂, H₂O and molecular ions such as HS⁻ or SO₄⁻ (Burruss, 2003b; Wopenka, et al. 1990; Dubessy, et al. 2001; Burke, 2001).

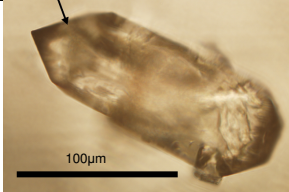

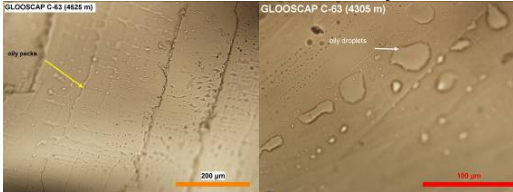
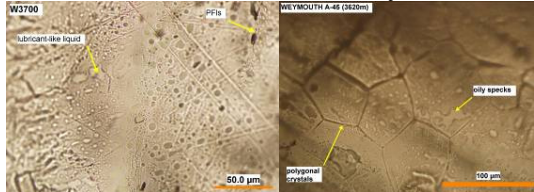
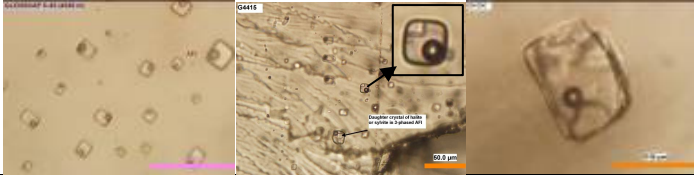
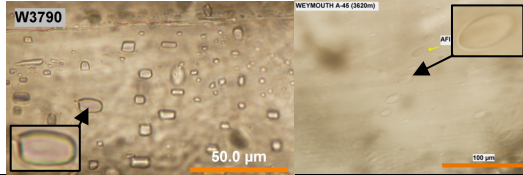
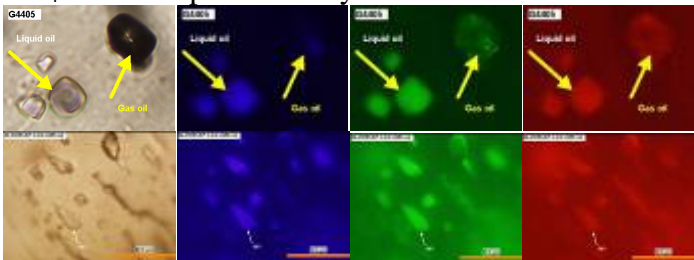
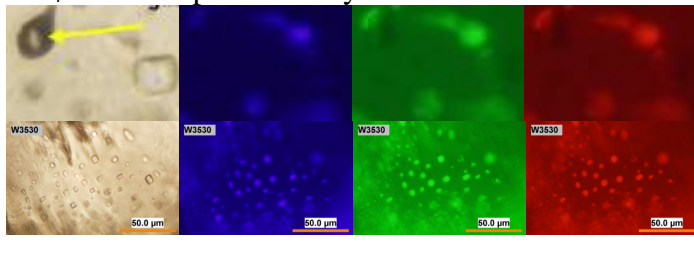
Halite is known to many as non-porous, impermeable rocks acting as cap rock for hydrocarbon reservoirs. However, the presence of secondary aqueous and petroleum-bearing fluid inclusions in rock salt suggests otherwise. Laboratory measurement of

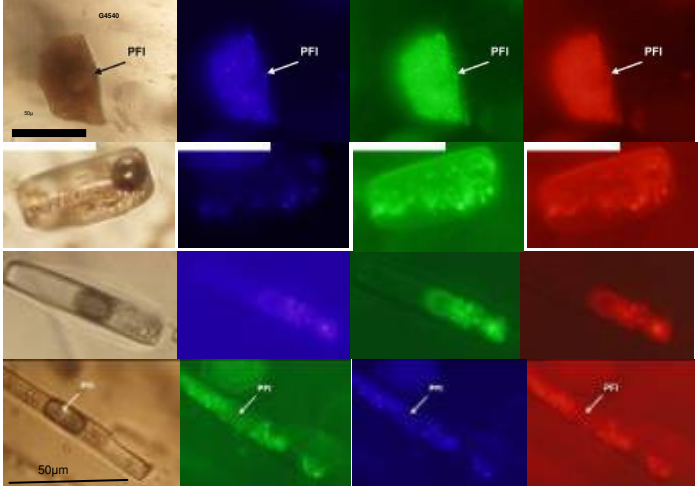
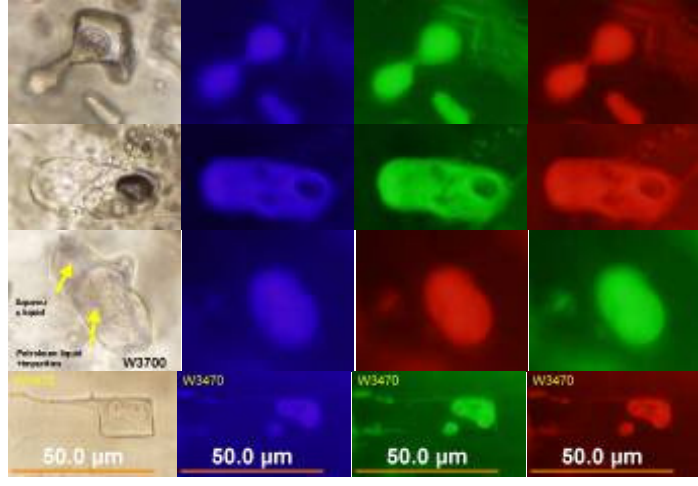
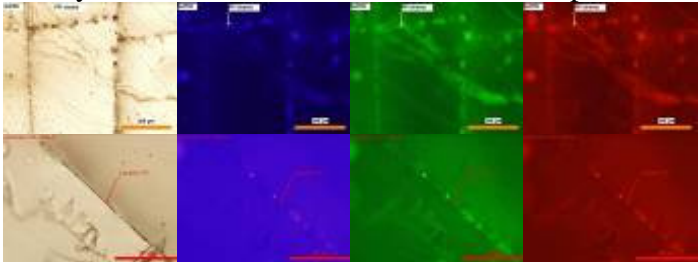
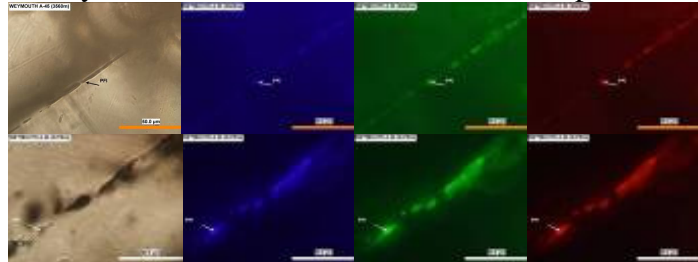
porosity and permeability of halite are in the range 0.1% to 1.4% and 1029 to 1026 D, respectively (Yaramanci, 1994 and Bredehoeft, 1988 in Lewis and Holness, 1996). Experimental work of Lewis and Holness (1996) indicated that the halite-brine dihedral angle, that controls the connectivity of pore-fluid and hence permeability, is a sensitive function of both temperature and pressure. They concluded that within sedimentary basins which have normal geothermal gradients, halite bodies at >3 km depth will contain a stable interconnected brine-filled porosity that results in permeabilities comparable to those of sandstones. According to Lewis and Holness (1996), their experimental results explain recent observations of major salt-fluid interactions at depth, and suggest that deep-rooted salt diapirs may act as conduits for basinal formation water. These results have important implications and explain the reasons for the introduction of fluids into the salt bodies at depth conditions similar to those of the studied Glooscap-C63 and Weymouth-A45 wells to form secondary aqueous and petroleum fluid inclusions. A question which should be asked is how these fluid inclusions survive and remain intact in spite of the movement of the salt laterally and also vertically to form diapirs? If the salt moves as plastic viscous material in a turbulent way, these inclusions can not survive and keep their identity. According to Davison et al. (1996), the viscosity of salt has little to do with the triggering mechanism of diapirism that is primarily dependent on the strength and stress status of the overburden. Salt can be faulted in a brittle way at high strain rate (Davison et al. 1993, Smith, 1996). I have noticed very tight folding in the salt diapir of Pugwash Salt Mine in Nova Scotia, Canada (Fig. 46) indicating that the salt, like many other sedimentary rocks can be folded in a brittle manner. Shear zones have been noticed developed parallel to bedding in potassic horizons (Sans et al. 1996), where the salt attained gneissose structure in Zechstein salt (Smith, 1996) and Red Sea diapirs (Davison et al. 1993). Relatively undeformed layers of halite have been carried laterally (Smith, 1996) and upward as rafts between shear zones into diapirs (Burliga, 1996) and undeformed halite rafts are often transported in a highly sheared sylvinite matrix (Sans et al. 1996) (quoted from Davison et al. 1996). Occurrence of long range methane gas migration have been documented in salt in many basins such as Algarve in Portugal (Terrinha et al. 1994) and Sergipe-Alagoas in Brazil (Davison et al. 1996).

The origin of hydrocarbons within the petroleum-bearing fluid inclusions in Argo salt intersected in Weymouth-A45 and Glooscap-C63 wells is arguable. The salt body in Glooscap-C63 well is autochthonous and has a pillow shape while it is of allochthonous nature and is a diapir with a canopy top in Weymouth-A45 well. The thickness of salt in Weymouth is ~3 times that of Glooscap-C63. The salt in Glooscap-C63 well is interbedded with many thick shale interlayers and is underlain by the older, shale/claystone-dominated Eurydice Formation (Late Triassic-Early Jurassic); for this reason the shale dominated lithology of both sources could have acted as the source of petroleum which has migrated after its formation along faults and partially trapped in the planes of weakness (cleavage and fractures) within the adjacent Argo salt. The Argo salt in the Weymouth-A45 well has no shale interbeds and is currently underlain by the shale-dominated lithological units of Cretaceous-aged formations (Naskapi, Logan Canyon and Missisauga formations). It can be suggested that the petroleum was generated in any of these Cretaceous formations (particularly in the Early Cretaceous Missisauga Formation) and migrated and partially trapped within cleavage/fracture planes of Argo salt as PFI and PFI-AFI during its movement through these Cretaceous formations. However, it can equally be argued that the source of petroleum was originally from the formations older than the Argo salt (Eurydice Formation of Late Triassic/Early Jurassic age) which moved into the overlying Argo Formation and trapped as PFIs and survived as intact identities in spite of the movement of the salt to the currently observed position as a diapir with a canopy top. Taking the situation of Argo salt in both studied wells into consideration, it is more probable that the source of petroleum in the PFIs is the Late Triassic/Early Jurassic Eurydice or older underlying formations in the area. Eurydice Formation underlies Argo salt in most parts of the Scotian Continental Margin which strengthens this conclusion.

Table 10: Summary comparison between the properties of rock salt in Glooscap-C3 and Weymouth-A45 wells.

Properties	Glooscap-C63 salt	Weymouth-A45 salt
Salt body shape, lithology, depth and thickness	Pillow (autochthonous); salt interbedded with thick shale layers; 4045m – 4542m depth (497m thick)	Canopy/diapir (allochthonous); Salt with no shale interbeds; 2840m – 4348m depth (1508m thick)
Location	Continental shelf	continental slope
Salt color & Transparency	clear colorless or brownish due to iron stain; transparent 	Buff yellowish or brownish due to iron stain; non-transparent 
Salt transparency	Transparent	Non-transparent
Anhydrite inclusions	little; tiny crystals (can be seen in insoluble residue) 	Abundant; up to few 100µm long crystals  
Hematite inclusions	Common euhedral hematite crystals and iron stain 	Common euhedral hematite crystals and iron stain 
Quartz inclusions	Rare perfect crystals	Rare perfect crystals

		
Lubricant-like liquids in halite crystals	<p>Lubricant-like liquid is found along cleavage planes and on the surface of halite crystals</p> 	<p>Lubricant-like liquid is found along cleavage planes and on the surface of halite crystals</p> 
Aqueous fluid inclusions (AFI)	<p>Abundant; different from Weymouth-A45</p> <ol style="list-style-type: none"> (1) H_2O-NaCl system (2) Rarely H_2O-NaCl-KCl system (3) Large accidental FI 	<p>Less abundant, different from Glooscap-C63</p> <ol style="list-style-type: none"> (1) H_2O-CaCl_2-NaCl and/or H_2O-MgCl_2-NaCl (3) Air-filled? FI 
Petroleum fluid inclusions (PFI)	<p>Common: pure liquid or gas phases or together CH_4? or other petroleum system</p> 	<p>Abundant: pure liquid or gas phases or together CH_4? or other petroleum system</p> 

<p>Mixed petroleum and aqueous fluid inclusions (PFI-AFI)</p>	<p>Common: dispersed in each other as 2,3 & 4 phases Behave as the aqueous FI in microthermometry (H₂O-NaCl system)</p> 	<p>Very abundant: immiscible 2,3,& 4 phases The aqueous part behave similar to the aqueous systems (H₂O-CaCl₂-NaCl and/or H₂O-MgCl₂-NaCl); the petroleum part behave like the petroleum systems (CH₄? or other petroleum systems)</p> 
<p>Occurrence of fluid inclusions</p>	<p>Mostly along planes of weaknesses (cleavage, fracture, crystal boundary); and in many cases within the crystal with no obvious relation to these planes</p> 	<p>Mostly along planes of weaknesses (cleavage, fracture, crystal boundary); and in many cases within the crystal with no obvious relation to these planes</p> 

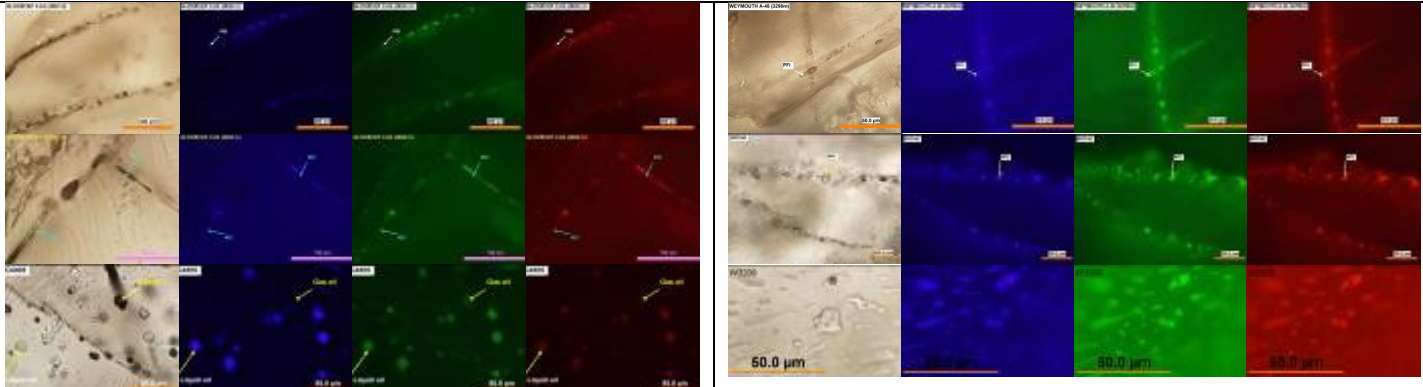
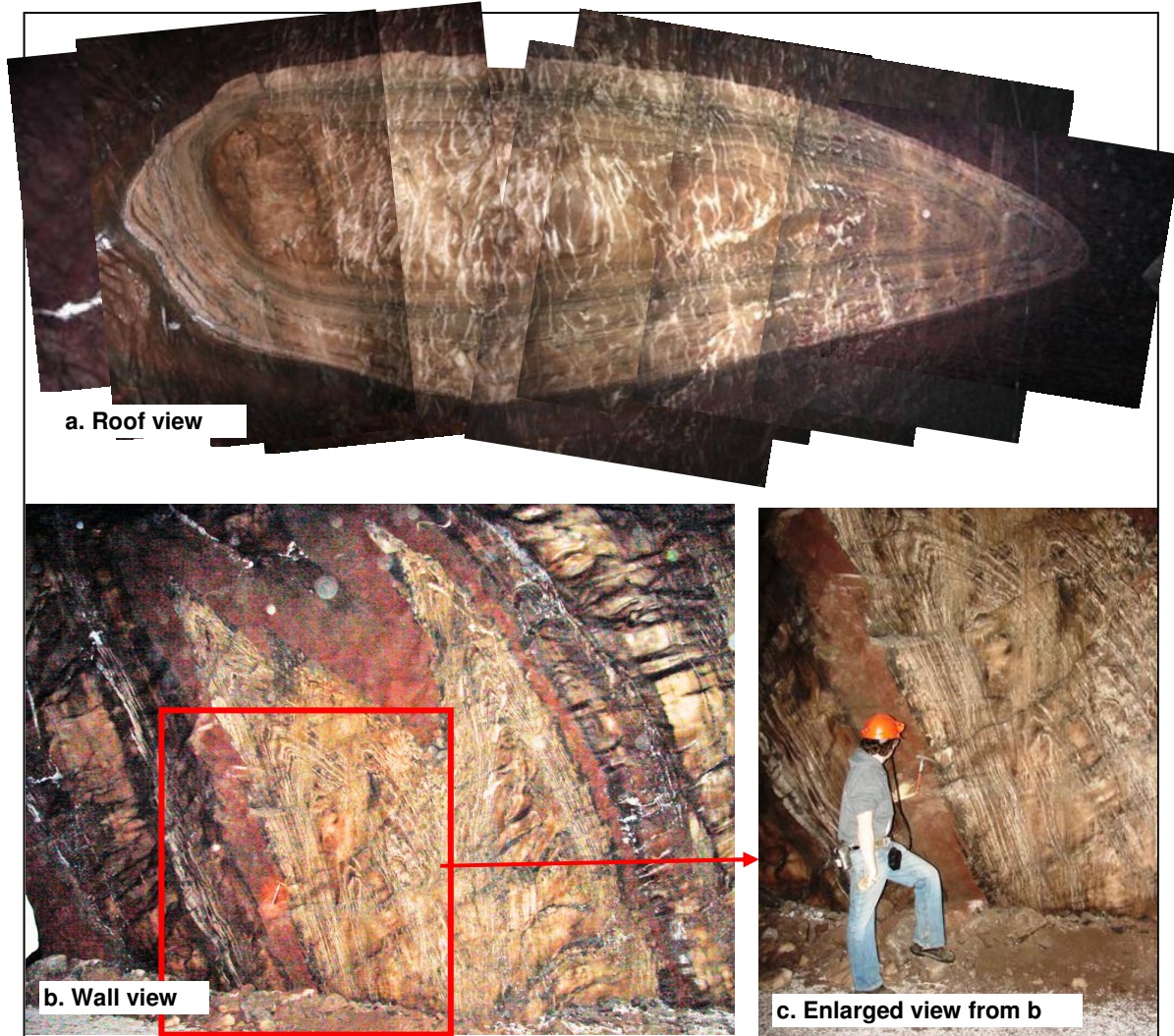
																															
Microthermometry of the AFI and the mixed PFI-AFI	<p>Both the AFI and the mixed PFI-AFI behave similarly:</p> <table><tr><td></td><td>T_f</td><td>T_{im}</td><td>T_e</td><td>T_m</td><td>T_h</td></tr><tr><td>Median</td><td>-81</td><td>-38</td><td>-25</td><td>-1.8</td><td>286</td></tr><tr><td>Average</td><td>-82</td><td>-40</td><td>-26</td><td>-2</td><td>282</td></tr><tr><td>Minimum</td><td>-119</td><td>-51</td><td>-38</td><td>-6.8</td><td>110</td></tr><tr><td>Maximum</td><td>-64</td><td>-34</td><td>-22</td><td>0</td><td>380</td></tr></table>		T_f	T_{im}	T_e	T_m	T_h	Median	-81	-38	-25	-1.8	286	Average	-82	-40	-26	-2	282	Minimum	-119	-51	-38	-6.8	110	Maximum	-64	-34	-22	0	380
	T_f	T_{im}	T_e	T_m	T_h																										
Median	-81	-38	-25	-1.8	286																										
Average	-82	-40	-26	-2	282																										
Minimum	-119	-51	-38	-6.8	110																										
Maximum	-64	-34	-22	0	380																										
Microthermometry of pure liquid PFI	<p>Both the AFI and the AFI part within the mixed PFI-AFI behave similarly:</p> <table><tr><td></td><td>T_f</td><td>T_{im}</td><td>T_e</td><td>T_m</td><td>T_h</td></tr><tr><td>Median</td><td>n.o.</td><td>n.o.</td><td>n.o.</td><td>n.o.</td><td>79</td></tr><tr><td>Average</td><td>n.o.</td><td>n.o.</td><td>n.o.</td><td>n.o.</td><td>79</td></tr><tr><td>Minimum</td><td>n.o.</td><td>n.o.</td><td>n.o.</td><td>n.o.</td><td>51</td></tr><tr><td>Maximum</td><td>n.o.</td><td>n.o.</td><td>n.o.</td><td>n.o.</td><td>107</td></tr></table>		T_f	T_{im}	T_e	T_m	T_h	Median	n.o.	n.o.	n.o.	n.o.	79	Average	n.o.	n.o.	n.o.	n.o.	79	Minimum	n.o.	n.o.	n.o.	n.o.	51	Maximum	n.o.	n.o.	n.o.	n.o.	107
	T_f	T_{im}	T_e	T_m	T_h																										
Median	n.o.	n.o.	n.o.	n.o.	79																										
Average	n.o.	n.o.	n.o.	n.o.	79																										
Minimum	n.o.	n.o.	n.o.	n.o.	51																										
Maximum	n.o.	n.o.	n.o.	n.o.	107																										

Fig. 46: Tight folds in the salt of Pugwash Mine diapir as an indication of brittle style deformation: (a) a composite roof view showing a domal structure (b) wall view (c) enlarged view from b. The yellowish-brownish salt is halite; the reddish brown salt is sylvite horizons; the white spots are anhydrite filling cracks in salt.



CONCLUSIONS

1. The salt of both Glooscap-C63 and Weymouth-A45 wells contain a variety of fluid inclusions, solid crystal inclusions and lubricant-like liquid. They have similarities and dissimilarities.
2. The fluid inclusions in the studied salts include aqueous (AFI), petroleum (PFI), and heterogeneously trapped mixed petroleum-aqueous (PFI-AFI) types. The petroleum-bearing fluid inclusions are common in both studied wells but they are richer in the salt of Weymouth-A45 well compared to that of Glooscap-C63 well.
3. The AFI of Glooscap-C63 well are either one-phased (liquid), two-phased (liquid + vapor) and rarely three-phased (liquid + vapor + daughter crystal of halite or sylvite); they belong to $\text{H}_2\text{O-NaCl}$ and rarely to $\text{H}_2\text{O-NaCl-KCl}$ systems; while those of Weymouth-A45 well are one-phased (liquid) and two-phased (liquid + vapor) and belong to $\text{H}_2\text{O-CaCl}_2\text{-NaCl}$ and/or $\text{H}_2\text{O-MgCl}_2\text{-NaCl}$ systems and some others are air-filled. The median temperatures of freezing (T_f), metastable eutectic (T_{im}), eutectic (T_e), peritectic (T_m) and homogenization (T_h) in the AFI + PFI-AFI of Glooscap-C63 well's salt are -81°C , -38°C , -25°C , -1.8°C and 286°C respectively; the corresponding values for Weymouth-A-45 well's salt are -73°C , -52°C , -37°C , -3°C and 81°C respectively. The eutectic temperatures do not exactly match the expected values for corresponding systems which are either due to the stretching effect (naturally or during measurements). The homogenization temperatures are too high for the Glooscap-C63 salt and more reasonable for the Weymouth-A45 salt due to above mentioned reasons. If the T_h for Weymouth-A45 well is dependable, it mean that trapping has taken place ≥ 3 km depth.
4. The mixed PFI-AFI are common in both studied wells. They exist as 2-, 3-, and 4-phase (aqueous + petroleum \pm solid impurities \pm vapor or gas bubble). The solid impurities exist within petroleum part of the inclusions; they could be degraded petroleum or some sort of dead oil-generating bacteria or algae. The petroleum (+solid impurities) in the fluid inclusions of Weymouth-A45 well always exist as distinct separate phase in the form of one or more immiscible spots within the aqueous liquid, while that of Glooscap-C63 always exist as dispersed or mixed

- phase with no distinct boundaries. Obviously these phases must have been trapped within the salt as mixed inclusions heterogeneously soon after the generation of petroleum at the appropriate depth conditions. The temperatures at which phase changes takes place for AFI and mixed PFI-AFI are overlapping and their combined median and ranges are given in conclusion 3 above.
5. The PFI in both wells are pure liquid and pure gas. The identity of the fluids in these inclusions could not be confirmed because of the stretching (deformation) of halite during cooling-heating microthermometric studies. According to the literature ~80% of PFI are CH₄-type which has a freezing point below -190°C, eutectic at -182.5°C and homogenization temperature at -82.1°C. The PFI in both wells did not show any of these phase changing temperatures; the expected reasons are the stretching of halite which was taking place during microthermometric measurement or they could be containing some other more complex hydrocarbon compounds other than methane as their fluorescence behavior suggests. The median homogenization temperature for PFI of Glooscap-C63 is 79°C with a range of 51°C to 107°C, while that of Weymouth-A45 is 23°C with a range of 17°C to 97°C; however these data must be looked at cautiously because of the stretching behavior of their host halite which is one of the weakest and softest minerals.
 6. The petroleum-bearing fluid inclusions (PFI and PFI-AFI) in both studied wells showed distinct fluorescence in UV and visible spectrum wavelengths which suggest that they contain complex, high-molecular weight, aromatic or cyclic hydrocarbon compounds higher than CH₄.
 7. The salinity of AFI and PFI-AFI is about the same as the eutectic composition of halite (23.2wt.% NaCl) or higher in rare case where daughter crystals of halite exist in fluid inclusions.
 8. The solid (crystal) inclusions in the studied salt of both wells are anhydrite, hematite, and quartz. Both salts also contain a loose lubricant-like liquid which seeps along cleavage planes.
 9. The origin of hydrocarbon within the petroleum-bearing fluid inclusions in Argo salt intersected in Weymouth-A45 and Glooscap-C63 wells is probably the

shale/clay dominated, Late Triassic/Early Jurassic Eurydice formations which is widely distributed at depth in the Scotian Margin underlying the salt and other younger formations. The other possibility for Glooscap-C63 well is the thick shale layers interbedded with the Argo salt; while in the case of Weymouth-A45 well, the shale-dominated Cretaceous Formations (Naskapi, Logan Canyon and Missisauga) underlying the salt canopy are additional possible sources.

10. The hydrocarbons which were generated in the above mentioned possible sources must have moved along faults and spread along planes of weaknesses (fractures, cleavage and crystal boundaries) to be trapped within salt which become porous and permeable at >3km depth that was overlying the source rocks. The salt was probably acting as brittle material in the Glooscap-C63 well area which was either not moving or laterally moving indicated by its pillow shape (autochthonous), and in the case of Weymouth-A45 well area was vertically moving to form a diapir capped by a canopy.

RECOMMENDATIONS

Petroleum fluid inclusions have been found in almost all studied salt samples in both Glooscap-C63 and Weymouth-A45 wells. The limitations of the fluorescence microscopic and microthermometric studies, requires further studies to accurately identify the biomarker and molecular compounds in the studied salts. The recommended studies are:

1. Gas Chromatography-Mass Spectrometry (GC-MS) on the bulk samples to analyze biomarkers.
2. Raman Microspectroscopy and infrared (IR) Microspectroscopy on individual fluid inclusions to analyze molecular compounds.

ACKNOWLEDGMENTS

I am thankful to all who have helped in adopting, supporting, following up and executing this project. They are:

1. Dr. Wayne St-Amour and Mrs. Jennifer Matthews from the Offshore Energy Technical Research Associations (OETR-A) for adopting, following up and financially supporting the project, and Mrs. Wanda Barrett for following up the financial issues
2. Dr. Matt Luheshi from PARAS Consulting (RPS), Mr. Tony LaPierre and Dr. Hamish Wilson from RPS Energy for adopting, following up and continuously supporting the project.
3. Dr. Frederic Monnier from Beicip-Franlab for adopting and following up the project.
4. Mary Jean Verrall and Nancy White from the Canada-Nova Scotia Offshore Petroleum Board (CNSOPB) for providing the samples and their help during sampling
5. Ms. Crystal Winters for her help in sampling
6. Dr. Grant Wach from Dalhousie University – Department of Earth Sciences for leasing his microscope for the study.
7. Mr. Gordan Brown from University – Department of Earth Sciences for preparing part of the samples for study.

REFERENCES

- Barss, M.S., Bujak, J.P. and Williams, G.L., 1979. Palynological zonation and correlation of sixty-seven wells, eastern Canada: Geological Survey of Canada, Paper 78-24, 118p.
- Bodnar, R.J., 2003. Introduction to Fluid Inclusions. In I. Samson, A. Anderson, and D. Marshall, eds. Fluid Inclusions: Analysis and Interpretation. Mineral. Assoc. Can., Short Course Ser. 32, 1-8.
- Bodnar, R.J., 2010. Personal email communication.
- Bujak, J.P. and Williams, G.L., 1977. Jurassic paleostratigraphy of offshore eastern Canada, pp.321-339: in F.M. Swain (ed.), Stratigraphic Micropaleontology of Atlantic Basin and Borderlands; Elsevier Scientific Publishing Company, New York, 603p.
- Burke, E.A.J., 2001. Raman microspectrometry of fluid inclusions. *Lithos*, 55, 139-158.
- Burliga, S., 1996. Kinematics within the Klodawa salt diapir, central Poland. Geological Society, London, Special Publications 100: 11-21.
- Burruss, R.C., 1991. Practical aspects of fluorescence microscopy of petroleum fluid inclusions, In Luminescence microscopy: Qualitative and quantitative applications, Vol. Short Course 25. Barker, C.E. and Kopp, O. (eds), pp.1-7. SEPM (Society for Sedimentary Geology).
- Burruss, R.C., 2003a. Petroleum Fluid Inclusions, an Introduction. In I. Samson, A. Anderson, and D. Marshall, eds. Fluid Inclusions: Analysis and Interpretation. Mineral. Assoc. Can., Short Course Ser. 32, 159-174.
- Burruss, R.C., 2003b. Raman spectroscopy of fluid inclusions. In I. Samson, A. Anderson, and D. Marshall, eds. Fluid Inclusions: Analysis and Interpretation. Mineral. Assoc. Can., Short Course Ser. 32, 279-289..
- Burruss, R.C., Cercone, K.R. and Harris, P.M. (1985). Timing of hydrocarbon migration: evidence from fluid inclusions in calcite cements, tectonics, and burial history. In Schneidermann, N. and Harris, P.M., eds. Carbonate Cements: SEPM Special Publ. 26, 277-289.
- Datalog Canada Ltd, 2004. EnCana - End of well report. EnCana Shell et al: Weymouth A-45 Main & A-45 ST.
- Davis, D.W., Lowenstein, T.K. and Spencer, R.J. (1990). Melting behavior of fluid inclusions in laboratory-grown halite crystals in the systems NaCl-H₂O, NaCl-KCl-H₂O, NaCl-MgCl₂-H₂O, NaCl-CaCl₂-H₂O. *Geochimica et Cosmochimica Acta*, 54, 591-601.

Davison, I., 2009. Faulting and fluid flow through salt. *Journal of the Geological Society*, London, Vol. 166, 205-216.

Davison, I., Alsop, I. and Blundell, D., 1996. Salt tectonics: some aspects of deformation mechanics. Alsop, G.I., Blundell, D.J. and Davison, I. (eds.), 1996, *Salt Tectonics*. Geological Society Special Publication No. 100, pp. 1-10.

Davison, I., Insley, M., Harper, M., Weston, P., Blundell, D., McClay, K. and Quallington, A., 1993. Physical modeling of overburden deformation around salt diapirs. *Tectonophysics*, 228, 255-274.

Dubessy, J., Buschaert, S., Lamb, W., Pironon, J., and Thiery, R., 2001. Methane-bearing aqueous fluid inclusions: Raman analysis, thermodynamic modeling and application to petroleum basins. *Chemical Geology*, 173, 193-205.

Goldstein, R.H. and Reynolds, T.J., 1994. Systematics of fluid inclusions in diagenetic minerals: SEPM short course 31. SEPM Society for Sedimentary Geology, 199p.

Holloway, K.A., 1973. Behavior of fluid inclusions in salt during heating and irradiation. Fourth Salt Symposium Proceeding, Houston, 303-312.

Jansa, L.F., Gradstein, F.M., Jenkins, W.A.M. and Williams, G.L., 1977. Geology of the Amoco Imp. Skelly A-1 Osprey H-84 well, Grand Banks, Newfoundland: Geological Survey of Canada, Paper 77-21, 17p.

Jansa, L.F. and Wade, J.A., 1975. Geology of the continental margin of Nova Scotia and Newfoundland, pp. 51-105: in W.J.M. Van der Linden and J.A. Wade (eds.), *Offshore Geology of Eastern Canada*, geological Survey of Canada, Paper 74-30, vol.2, 258p.

Kidston, A.G., Brown, D.E., Smith B.M. and Altheim, B., 2002, *Hydrocarbon Potential of the Deep-Water Scotian Slope*. Canada-Nova Scotia Offshore Petroleum Board, Halifax, 111p.

McIver, N.L., 1972. Cenozoic and Mesozoic stratigraphy of the Nova Scotia Shelf. *Canadian Journal of Earth Sciences*, vol.9, pp.54-70.

Roedder, E., 1984. Fluid Inclusions. Mineralogical Society of America, *Reviews in Mineralogy* 12, 644p.

Samson, I., Anderson, A., and Marshall, D. (eds.), 2003. Fluid inclusions: Analysis and interpretation. Mineralogical Association of Canada, short course series volume 32, Vancouver, 374p.

Sans, M., Sánchez, A.L. and Santanach, P., 1996. Internal structure of a detachment horizon in the most external part of the Pyrenean fold and thrust belt (northern Spain) *Geological Society, London, Special Publications* 100: 65-76.

Selley, R.C., 1998. Elements of Petroleum Geology. San Diego, Academic Press, 470p.
Smith, D.B., 1996. Deformation in the late Permian Boulby Halite (EZ3Na) in Teesside, NE England, Geological Society, London, Special Publications 100: 77-87.

Stasiuk, L.D. and Snowden, L.R., 1997. Fluorescence micro-spectrometry of synthetic and natural fluid inclusions: crude oil chemistry, density and application to petroleum migration. Applied Geochemistry, 12, 229-241.

Terrinha, P., Ribeiro, A. and Coward, M.P., 1994. Mesoscopic structures in a salt wall. The Loule salt wall diapir, Algarve Basin, south Portugal. Salt Tectonics meeting, Geological Society, London, 14-15th September 1994, abstract

Wade, J.A., 1981. Geology of the Canadian Atlantic margin from Georges Bank to the Grand Banks, pp. 447-460: in J.W. Kerr and A.J. Fergusson (eds.), Geology of the North Atlantic Borderlands; Canadian Society of Petroleum Geologists, Memoir 7, 743p.

Williams, G.L., Fyffe, L.R., Wardle, R.J., Colman-Sadd, S.P. and Boenner, R.C. (eds.), 1985. Lexicon of Canadian Stratigraphy Volume VI Atlantic Region. Canadian Society of Petroleum Geologist, Calgary, Canada, 572p

Wopenka, B., Pasteris, J.D., and Freeman, J.J., 1990. Analysis of individual fluid inclusions by Fourier transform infrared and Raman microspectroscopy. Geochimica et Cosmochimica Acta, 54, 519-633.

<http://basin.gdr.nrcan.gc.ca/wells>

END
